FUSION TECHNOLOGY

Annual Report of the Association EURATOM/CEA 1999

Compiled by : Ph. MAGAUD

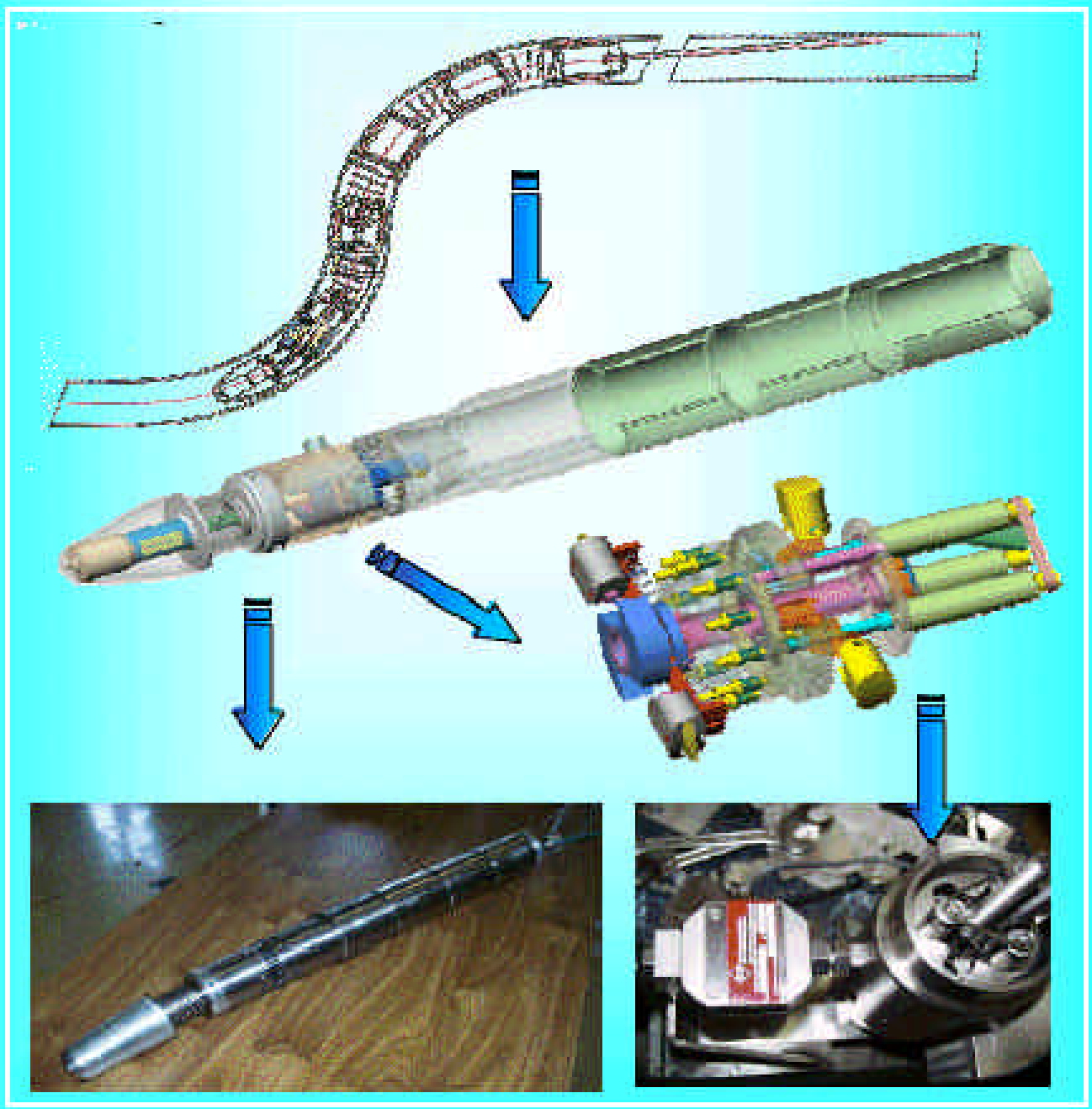

ASSOCIATION CEA/EURATOM
DSM/DRFC

SM 1-1

Task Title : IMPROVEMENT OF RAFM STEEL FOR DBTT & IRRADIATION HARDENING

INTRODUCTION

The main objective of this proposal is to study the sensitivity to hardening/embrittlement of RAFM steels in relation to compositional effects at irradiation temperatures relevant for EBP structural materials. In the period 95-98 several heats of RAFM steels have been irradiated and some PI mechanical testing have been performed. To complete data it is proposed for the period 1999-2002 to irradiate the precursor EU heat EUROFER97 and other RAFM steels (like JLF-1) in Osiris reactor at 325°C up to a dose of about 4-5 dpa. These results will be compared to mechanical testing data of several RAFM steels previously obtained (HFR, irradiation temperatures ranging from 250 to 450°C, 2.4 dpa ; Osiris, 325°C, several doses from 1 to 8 dpa) and will contribute to the final specification for the industrial heat of EU RAFM steel.

1999 ACTIVITIES

As the plates of EUROFER steel were delivered on December 1999 the machining of specimens and the preparation of the irradiation was delayed on 2000.

Consequently, the activities during this year were oriented to the treatment and analysis of data obtained on other RAFM steels irradiated in previous experiments, that is, in Osiris reactor at 325°C for various dose levels and HFR reactor at different irradiation temperatures ranging from 250 to 450°C.

The main objective was is to examine the susceptibility to hardening and embrittlement of Fe7.5/11CrWTaV Reduced Activation (RA) compared to conventional 9/12Cr-Mo martensitic steels as a function of :

- the fluence level up to 3.4 dpa for the irradiation temperature of 325°C.
- the irradiation temperature in the range of 250-450°C for a constant dose of 2.4 dpa.

MATERIALS

Chemical compositions of RA and conventional martensitic steels investigated are summarised in table 1. F82H RA-steel (7.5Cr-2W-0.1C) was supplied by JAERI as plates in the N&T condition. Experimental RA heats (referenced as LA...) were produced in the N&T-CW, that is normalisation and tempering followed by a final cold-working of 10% [1].

Two heats 9Cr-0.7W-0.1C with different Ta contents (LA12TaLC, 0.1%Ta and LA12LC, 0.01%Ta) are investigated as well others with higher Cr (LA4Ta, 11Cr-0.7W-0.1Ta) and W (LA13Ta, 9Cr-3W-0.1Ta) concentrations.

Conventional martensitic steels examined here are commercial alloys with different contents of Cr (9 to 12%), Mo and stabilising elements (V, Nb). In general, these materials were produced as plates in the normalised and tempered condition (N&T), except for 9Cr-1Mo and mod. 9Cr-1MoVNb, which were also obtained in the N&T-CW condition.

Table 1 : Chemical composition of RA and conventional martensitic steels (in wt%)

	C	Si	Mn	Cr	V	W	Mo	N	Ta	Nb
RA steels										
F82H	0.087	0.10	0.21	**7.46**	0.15	1.96	-	0.0066	0.023	-
LA12TaLC	0.090	0.03	1.13	8.80	0.30	0.73	-	0.0190	**0.100**	
LA12LC	0.089	0.03	1.13	8.92	0.30	0.73	-	0.0350	**0.010**	-
LA4Ta	0.142	0.03	0.78	**11.08**	0.23	0.72	-	0.0410	0.070	-
LA13Ta	0.179	0.04	0.79	8.39	0.24	**2.79**	-	0.0480	0.090	-
Conv. steels										
9Cr-1Mo	0.105	0.37	0.52	8.39	-	-	1.05	0.0175	-	-
9Cr-1MoNbV	0.105	0.43	0.38	8.26	0.20	-	0.95	0.0055	-	0.08
Manet II	0.10	0.18	0.76	10.37	0.21	-	0.58	0.0320	-	0.16
HT9	0.21	0.37	0.50	11.80	0.29	0.51	0.99	-	-	

EXPERIMENTAL

Materials were irradiated in Osiris reactor at 325°C as plate tensile specimens of 2 mm wide, 1 mm thick and 8 mm of gauge length. Tensile tests were performed at the irradiation temperature with a strain rate of 3.10^{-4} s^{-1}.

Irradiation in HFR reactor have been performed at five irradiation temperatures, that is 250, 300, 350, 400 and 450°C. Two tensile and seven Charpy specimens of each RA-material were irradiated at each irradiation temperature. Tensile tests were conducted at the irradiation temperature on cylindrical specimens of 3 mm in diameter and 18 mm of gauge length, using a strain rate of $1.8\ 10^{-4}$ s^{-1}.

Impact properties were determined with Charpy V subsize specimens of 3 x 4 x 27 mm^3 with a notch depth of 1 mm obtained along the rolling direction of plates (L-T orientation). The Ductile-Brittle Transition Temperature (DBTT) was determined as the midway level between the upper and the lower shelf energies.

EFFECTS OF THE DOSE

Effects of the fluence level are studied from the irradiation experiment performed in Osiris reactor at 325°C [2]. Table 2 compares the tensile properties of RA and conventional steels before and after irradiation at 325°C with a dose of 3.4 dpa available up to now.

In all the cases, an increase of tensile strength with the fluence is observed, which ranges from 150 to 450 MPa depending on the chemical composition and the metallurgical condition of steels. Ductility values decrease simultaneously with the increasing strength.

RA steels exhibit the lower amount of irradiation-induced hardening at 325°C for both N&T and N&T-CW metallurgical conditions as shown in figure 1a and 1b. In particular, cold-worked RA-steels display a lower increase of strength compared to the normalized-tempered F82H.

A saturation of hardening is observed for N&T-CW RA-steels and 9Cr-1Mo beyond 2 dpa. In contrast, the conventional steels HT9 and Manet II steels display a continuous strength increase up to 3.4 dpa and the most important irradiation-induced hardening. They also present the stronger decrease of reduction in area values, which goes down to 25-35% after 3.4 dpa .

Normalized-tempered 9Cr-1Mo steel shows at 3.4 dpa a high level of all ductility parameters, i.e., total/uniform elongations and reduction in area. F82H presents comparable values of tensile strength and area reduction to 9Cr-1Mo steel, but exhibit a loss of strain hardening capacity as shown in table 1 and previous work [3].

Correlation of the irradiation hardening with the chemical composition is not easy to establish. As shown in figure 1, for N&T-steels the increasing sensitivity to hardening could be related to Cr-content (F82H (7.5Cr), 9Cr-1Mo, Manet II (10.4Cr), HT9 (12Cr)).

But, in the case of N&T-CW steels, 9Cr-1Mo hardens much faster than LA12LC (9Cr-0.7W) and the same strength increase is detected for LA4Ta (11Cr-0.7W) and LA13Ta (9Cr-3W). Consequently, hardening seems to be determined not only by the chemical composition but also by the initial metallurgical condition.

On the other hand, it is important to remark that materials which present such as low values of reduction in area (< 50%) like HT9, Manet II and 9Cr-1MoVNb, should exhibit poor impact properties.

Such behavior can be anticipated according to previous CEA works, where a linear relation was established between the Upper Shelf Energy (USE) of transition curves and the reduction in area determined from tensile tests for several CrW RA-steels [4] (see tasks SM2.1/SM2.2) and Cr-Mo [2] conventional ferritic/martensitic steels including different metallurgical conditions (N&T, N&T-CW, unaged and thermal aged).

Table 2 : Tensile properties at 325°C of RA and conventional martensitic steels determined before and after irradiation (3.4 dpa) in Osiris reactor

	Metallurg. Condition	0.2% Yield Stress (MPa)		UTS (MPa)		Total Elong. (%)		Uniform Elong. (%)		Reduction in Area (%)	
RA steels		Unirr.	Irrad	Unirr.	Irrad	Unirr.	Irrad	Unirr.	Irrad	Unirr.	Irrad
F82H	N&T	456	734	513	734	15.0	8.3	2.9	0.2	73	59
LA12LC	N&T-CW	541	700	559	701	13.5	7.6	0.7	0.1	71	61
LA4Ta	N&T-CW	645	807	646	809	12.0	6.3	0.8	0.3	63	51
LA13Ta	N&T-CW	690	819	691	832	9.9	6.4	1.1	0.7	60	47
Conv. steels											
9Cr-1Mo	N&T	462	741	584	783	17.0	12.1	7.7	4.2	64	58
9Cr-1Mo	N&T-CW	612	938	623	955	12.5	7.9	1.1	1.1	66	52
9Cr1MoVNb	N&T-CW	667	941	688	943	11.0	6.4	0.7	0.3	59	45
Manet II	N&T	591	990	677	1005	13.5	5.5	2.7	0.7	65	36
HT9	N&T	485	932	691	1013	17.0	8.6	9.0	5.0	51	25

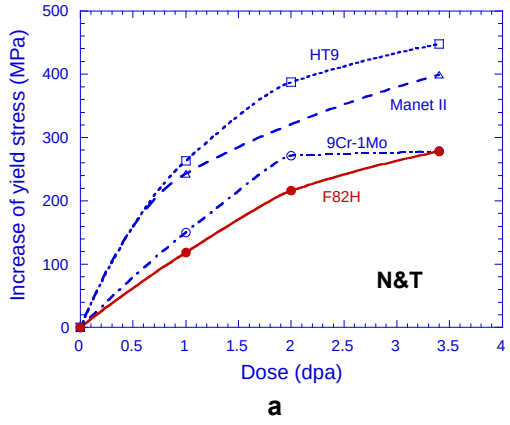

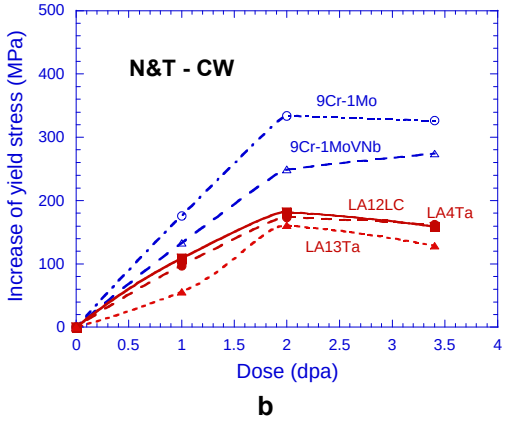

Figure 1 : Increase of yield stress with the dose for reduced-activation and conventional steels in (a) normalized-tempered (N&T) and (b) normalized-tempered-cold worked (N&T-CW) conditions. Irradiation experiment performed in Osiris reactor. $T_{test} = T_{irr} = 325°C$

EFFECTS OF THE IRRADIATION TEMPERATURE

The irradiation experiments performed in HFR reactor in the range 250-450°C allow to put forward the influence of the irradiation temperature (T_{irr}). Figure 2 present the evolution of the yield stress with T_{irr} for LA12TaLC and LA12LC RA-steels and 9Cr-1Mo (N&T) conventional steel. The dose level reached 2.4 dpa for RA-steels and 0.8 dpa for 9Cr-1Mo alloy.

In the case of RA-steels, both materials present the same behavior. The irradiation-induced hardening reaches the higher values at 250 and 300°C. In the range 350-450°C, the tensile strength of irradiated specimens is very close to the level obtained on thermal controls. Note that the same behavior was observed for UTS values and that no important effects of T_{irr} are detected on the total elongation and reduction in area.

As shown in figure 2, the conventional steel 9Cr-1Mo exhibit nearly the same qualitative behavior as a function of T_{irr}. But, the main difference is related to the fact that the irradiation-induced hardening is produced over a wide range from 250 to 400-450°C.

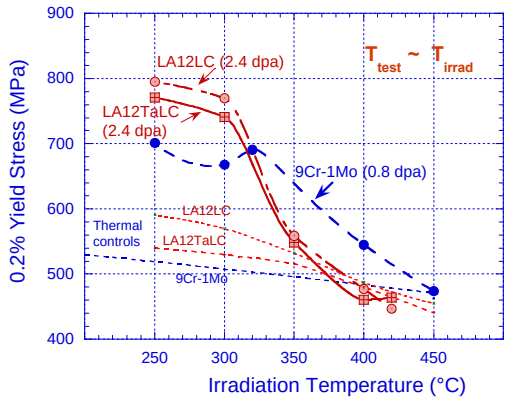

Figure 2 : Evolution of yield stress with the irradiation temperature for LA12LC and LA12TaLC reduced-activation steels irradiated at 2.4 dpa and 9Cr-1Mo conventional steel irradiated at 0.8 dpa. Irradiation experiment performed in HFR reactor

The hardening induced by the irradiation, measured by the increase in yield stress, is reported in figure 3 for materials investigated here and compared with data obtained from the literature for F82H [5] and 9Cr-1Mo irradiated in Phenix reactor at high doses [6] for the same metallurgical condition (N&T).

F82H and 9Cr-1Mo irradiated in the same conditions and dose (HFR-0.8 dpa) show the same dependence with T_{irr} and equivalent hardening as also observed in Osiris experiment. Their maximum hardening seems to be extended up to 320°C-350°C. Consequently, the dependence of the increasing strength with the dose determined in the Osiris experiment should approximately correspond to the evolution of the maximum hardening of both materials. So, an important increase of strength is expected for higher doses as shown in figure 3.

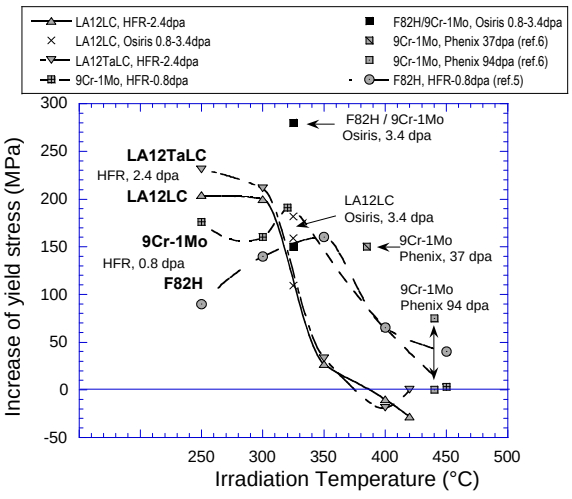

Figure 3 : Increase of the yield stress as a function of the irradiation temperature for LA12LC, LA12TaLC, F82H [9] reduced-activation and 9Cr-1Mo conventional steels. Comparison of data obtained from HFR, Osiris and Phenix [10] irradiation experiments. $T_{test} = T_{irr}$

In the case of LA12LC and LA12TaLC, the maximum of hardening occurs at 250-300°C. The low increase of strength for LA12LC detected at 325°C in Osiris, corresponds in fact to the temperature where hardening decreases significantly with T_{irr}. These results suggest that materials in the cold-worked condition harden in a lower temperature range than materials in the N&T condition. To explain these results, it could be argued that the higher dislocation density of cold-worked steels should act as effective sinks for defect annihilation resulting in a recovery of irradiation damage at lower T_{irr} compared to N&T materials.

Impact properties as a function of the irradiation temperature were determined only for LA12LC and LA12TaLC RA-steels for a dose of 2.4 dpa. The evolution of their DBTT is presented in figure 4. In contrast to tensile properties, a different evolution of the DBTT-shift (ΔDBTT) with the irradiation temperature is found for both materials.

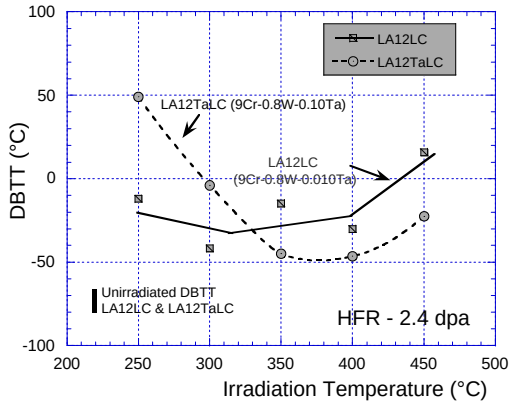

Figure 4 : Evolution of the DBTT with the irradiation temperature corresponding to LA12LC and LA12TaLC reduced-activation steels irradiated in HFR reactor.

In the case of LA12TaLC alloy, the highest increase of DBTT occurs at 250°C, where the maximum hardening is observed. The lower DBTT values are found at 350-400°C and DBTT increases again at 450°C as observed for other RA-steels irradiated in the same conditions [7, 8]. For LA12LC steel, the most important shift is detected at 450°C as shown in figure 4 and no correlation was found between hardening and ΔDBTT.

The main difference between LA12LC and LA12TaLC steels is given by Ta-content, which induces also a difference on prior austenite grain size. At 450°C, the lower embrittlement is obtained for the material with the higher Ta-content. This one seems to increase the resistance to embrittlement at T_{irr} > 400°C, as proposed in [8]. However, this assumption can not be applied for T_{irr} = 250°C, where the minimum DBTT-shift is observed for the material having the lower Ta-content. A great deal of work is still necessary to explain compositional and microstructural effects on embrittlement mechanisms occurring in martensitic steels.

CONCLUSION

Several FeCrW reduced-activation and FeCrMo conventional martensitic steels have been irradiated at different doses from 0.8 to 3.4 dpa and various irradiation temperatures in the range 250-450°C. The main results enable to set the following conclusions :

- For dose levels and irradiation temperatures used in the present work, 9Cr and in particular the reduced-activation variants present a better resistance to irradiation-hardening compared with conventional high Cr steels.

- In the range 250-450°C, the hardening/embrittlement is strongly determined by the irradiation temperature and their magnitude seems to vary with the chemical composition and the metallurgical condition of steels.

- The irradiation-induced hardening is shown to decrease rapidly with increasing irradiation temperature and disappears at $T_{irr.}$= 350°C for cold-worked RA-steels and at $T_{irr.}$= 450°C for normalized-tempered alloys.

- Different behavior of impact properties were found for 9Cr-0.7W-0.1C(Ta) RA-steels after irradiation at 2.4 dpa. The lower DBTT shift is observed at 250°C for the steel with the lower Ta-content, while at 450°C the higher Ta-content steels present the higher resistance to embrittlement.

REPORTS AND PUBLICATIONS

[1] A. Alamo, J.C. Brachet, A. Castaing, C. Lepottevin, F. Barcelo, J. Nucl. Mater. 258-263 (1998) 1228.

[2] X. Averty, J.C. Brachet, J.P. Pizzanelli, A. Castaing, Proc. Int. Symposium Fontevraud IV : Contribution of materials investigation to the resolution of problems encountered in PWR, Sept. 1998, France , vol. 1, A74.

[3] A.F. Rowcliffe, J.P. Robertson, R.L. Klueh, K. Shiba, D.J. Alexander, M.L. Grossbeck, S. Jitsukawa, J Nucl. Mater. 258-263 (1998) 1275.

[4] Y. de Carlan, A. Alamo, M.H. Mathon, G. Geoffroy, A. Castaing, communication to ICFRM 9, USA, 11-15 Oct. 99, CEA report NT SRMA 99-2345, Dec 99; to be published in J. Nucl. Materials.

[5] E.I. Materna-Morris, M. Rieth, K. Ehrlich, Effects of radiation on Materials : 19th Int. Symposium, ASTM STP 1366 (1999)

[6] J.L. Séran, A. Alamo, A. Maillard, H. Touron, J.C. Brachet, P ; Dubuisson, O. Rabouille, J. Nucl. Mater. 212-215 (1994) 588.

[7] M. Rieth, B. Dafferner, H.D. Röhrig, J Nucl. Mater. 258-263 (1998) 1147.

[8] R.L. Klueh, D.J. Alexander, M. Rieth, J Nucl. Mater. 273 (1999) 146.

A. Alamo, M. Horsten, X. Averty, E.I. Materna-Morris, M. Rieth, J.C. Brachet, ***"Mechanical behaviour of reduced activation and conventional martensitic steels after neutron irradiation in the range 250-450°C"***, communication to ICFRM 9, USA, 11-15 Oct. 99, CEA report NT SRMA 99-2344, Dec 99; to be published in J. Nucl. Materials.

TASK LEADER

A. ALAMO

DTA/DECM/SRMA
CEA Saclay
91191 Gif-sur-Yvette Cedex

Tél. : 33 1 69 08 67 26
Fax : 33 1 69 08 71 30

E-mail : ana.alamo@cea.fr

SM 2-1
SM 2-2

Task Title : METALLURGICAL AND MECHANICAL CHARACTERISATION OF REDUCED ACTIVATION FERRITIC-MARTENSITIC (RAFM) STEELS

INTRODUCTION

The main objective of these tasks is to characterise the microstructure (task SM2.1) and the metallurgical behaviour (task SM2.2) of RAFM steels after different thermal cycles, normalisation and tempering treatments, thermal ageing.

Activities are oriented in particular to the characterisation of the new EU heat EUROFER97 and the comparison with F82H and other RAFM experimental CrWTaV steels.

Special effort will be devoted to the study of the stability of microstructure during thermal ageing in relation to the mechanical behaviour examined in task SM2.2.

1999 ACTIVITIES

The plates of EUROFER steel were delivered on December 1999. So, the activities during this year were focalised on the treatment and analysis of data obtained on other RAFM steels (F82H, JLF-1, LA12LC .....). The evolution of the microstructure studied by Transmission Electron Microscopy (TEM) and Small Angle Neutron Scattering (SANS) was correlated to the modifications of tensile and impact properties of several RAFM steels, specially in the thermal aged condition.

MATERIALS AND EXPERIMENTAL PROCEDURES

In this work, a series of six experimental alloys supplied by AEA-Culham (named LA...) and also F82H and JLF-1 steels from respectively JAERI and Tokyo University were characterised. LA… steels supplied in the as-cast condition, were subsequently produced in our lab. as plates of 3.5 mm thick in the normalised (40 min.-1030°C) and tempered (1h-750°C/795°C) condition followed by a final cold-working of 10%. This initial condition is identified as N&T-CW. The F82H and JLF-1 steels have been supplied as plates of 7.5 mm and 15 mm thick in the Normalised and Tempered conditions (N&T), that is normalisation at 1040/1050°C and tempering at 750°C (F82H) and 780°C (JLF-1) for 1 h. Chemical composition, prior austenite grain size and metallurgical conditions of the steels are given in Table 1. Thermal ageing was performed in the range 250-450°C for 5000 hours for LA12LC and LA12TaLC steels, 10 000 hours for LA12TaLN, LA12Ta, LA13Ta and LA4Ta steels and 13 500 hours for F82H and JLF-1 steels.

Cylindrical tensile specimens of 2 mm in diameter and 12 mm gauge length were machined parallel to the rolling direction. The strain rate was 3.10-4 s-1 and the test temperatures ranged from 20 up to 650 °C.

Impact specimens were machined along the rolling direction (LT orientation according to ASTM standard). They were Charpy V-notch subsize specimens (27 mm long, 4 mm wide and 3 mm thick) for LA12LC and LA12TaLC and quasi standard Charpy V-notch samples of 55 mm long, 10 mm wide and 3.5 mm thick for the other steels. Charpy V tests were conducted over the temperature range -200 °C +400°C, in order to produce full transition curves for each material. The Ductile-Brittle Transition Temperature (DBTT), corresponding to 50% ductile and 50 % cleavage fracture mode, was deduced from the half-value of the Upper Shelf Energy (USE) or from force-time curves. The accuracy of DBTT values is about ± 10°C. Energy values were normalised to the initial cross-section area (3 X 3 mm^2 for the subsize specimens and 8 X 3.5 mm^2 for the quasi-standard specimens).

MICROSTRUCTURAL CHARACTERISATION

The microstructure of RAM steels consists of laths of tempered martensite within prior austenite grains. Only in F82H steel, partially recristallised zones are observed. For each alloy, different kinds of precipitates were identified on carbon extraction replica (LA12LC, LA12TaLC and LA12TaLN steels were not characterised by TEM). For all the steels, the main precipitation consists of fine or coarse $M_{23}C_6$ precipitates, with a typical chemical composition (at%) 60Cr-30Fe-5V-5W. These carbides are located along grain and lath/subgrain boundaries. Depending on the alloys (in F82H steel only $M_{23}C_6$ were identified), other carbonitrides were observed in the As-Received (AR) condition :

- M_2X : Cr-rich in LA4Ta steel,
- MX or M_6X : Ta-rich in LA4Ta, LA12Ta, LA13Ta and JLF-1 steels,
- M_4X_3 :V-rich particles in LA4Ta, LA12Ta, LA13Ta and JLF-1 steels.

After thermal ageing, no significant evolution of the precipitation was observed by TEM except for LA4Ta steel, where M_2X particles disappeared whatever the ageing temperature was, and for LA13Ta steel where Fe_2W Laves phase was observed after ageing at 550°C for 10 000 hours.

Table 1 : Chemical composition of RAM steels (wt%)

Alloy	C	Si	Mn	Cr	V	W	N	Ta	Grain Size (μm)	Metallurgical Condition
LA12TaLN	0.165	0.02	0.84	9.04	0.24	0.75	**0.0048**	0.10	20	N&T+CW
LA12Ta	0.155	0.03	0.88	9.86	0.28	0.84	0.0430	0.10	20	N&T+CW
LA13Ta	0.179	0.04	0.79	8.39	0.24	**2.79**	0.0480	0.09	25	N&T+CW
LA4Ta	0.142	0.03	0.78	**11.08**	0.23	0.72	0.0410	0.07	7	N&T+CW
LA12LC	**0.089**	0.03	1.13	8.92	0.30	0.73	0.035	0.01	40	N&T+CW
LA12TaLC	**0.090**	0.03	1.13	8.80	0.30	0.73	0.019	0.10	25	N&T+CW
F82H	0.087	0.10	0.21	**7.46**	0.15	**1.96**	**0.0066**	0.023	100	N&T
JLF-1	0.106	0.05	0.52	8.70	0.18	**1.91**	0.028	0.08	25	N&T

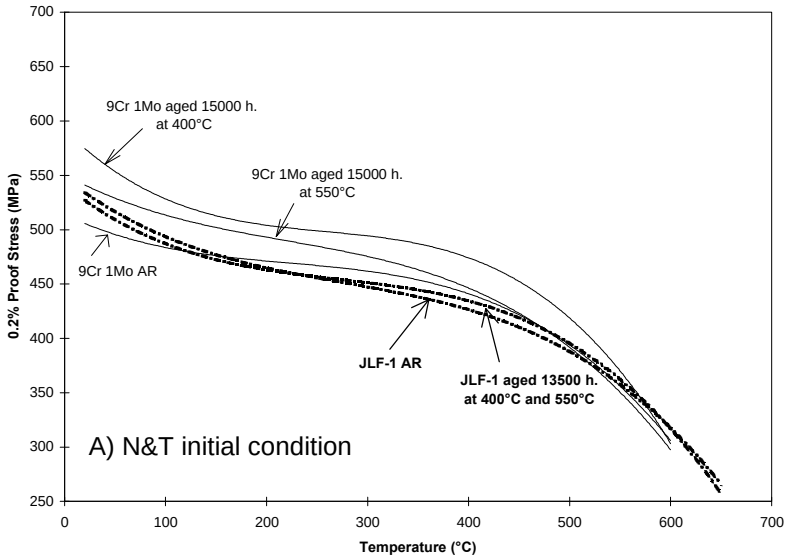

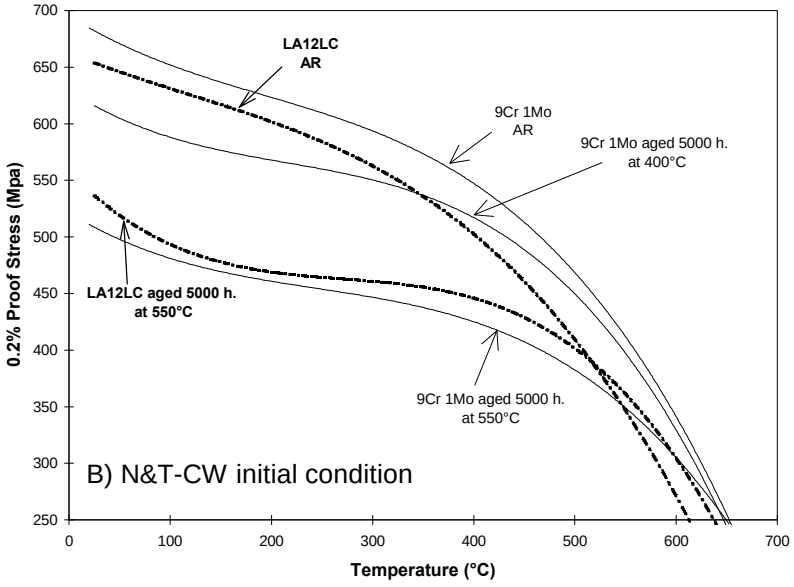

Figure 1 : Evolution of the 0.2% proof stress with thermal ageing of steels having different initial metallurgical conditions

This last phase appears as a thin film that engulfs carbides along grain and lath/subgrain boundaries. The chemical composition of this Laves phase film obtained by XEDS was typically (in at %) : 49Fe-24Cr-2V-25W.

MECHANICAL BEHAVIOUR

Before ageing, strength values of all the materials were similar to those of the conventional 9Cr-1Mo steels obtained in the same metallurgical condition. As shown in figure 1 for LA12LC steel and JLF-1 steel, the evolution of tensile properties after thermal ageing depends on metallurgical conditions.

Cold-Worked steels exhibit a decrease of the proof stress because of the recovery of the structure and no significant change of Ultimate Tensile Strength (UTS) and ductility is observed. N&T steels display very stable strength values and just a slight decrease of the reduction in area is detected specially after ageing at 550°C.

Table 2 gives the impact properties of all the studied steels. Impact properties are not very sensitive to the initial metallurgical conditions but depend on chemical composition and on ageing temperature. The main modifications are observed after ageing at 400°C in the case of high Cr-content (LA4Ta) and at 550°C for high W-concentration (LA13Ta).

Table 2 : Upper Shelf Energy (USE) and Ductile to Brittle Transition Temperature (DBTT) of RAFM steels before and after ageing

	USE (J/cm^2)						DBTT (°C)					
	AR	250°C	350°C	400°C	450°C	550°C	AR	250°C	350°C	400°C	450°C	550°C
LA12TaLN*	170		150	155	155	160	-65		-75	-55	-70	-70
LA12Ta*	190		180	145	155	180	-60		-70	-70	-65	-70
LA13Ta*	145		135	135	135	110	-70		-50	-45	-65	**- 20**
LA4Ta*	155		130	130	140	140	-65		-65	**- 45**	-65	-65
LA12LC‡	100	105	105	110	100	110	-75	-85	-75	-75	-75	-90
LA12TaLC‡	100		100	110	105	110	-70		-75	-80	-70	-85
F82H¤	195	200	205	190	200	175	-75	-65	-50	-55	-55	**-30**
JLF-1¤	190	190	180	190	185	160	-75	-65	-60	-70	-60	**- 45**

* 10000 hours aged, quasi standard Charpy V-notch specimens
‡ 5000 hours aged, Charpy V-notch subsize specimens
¤ 13500 hours aged, quasi standard Charpy V-notch specimens

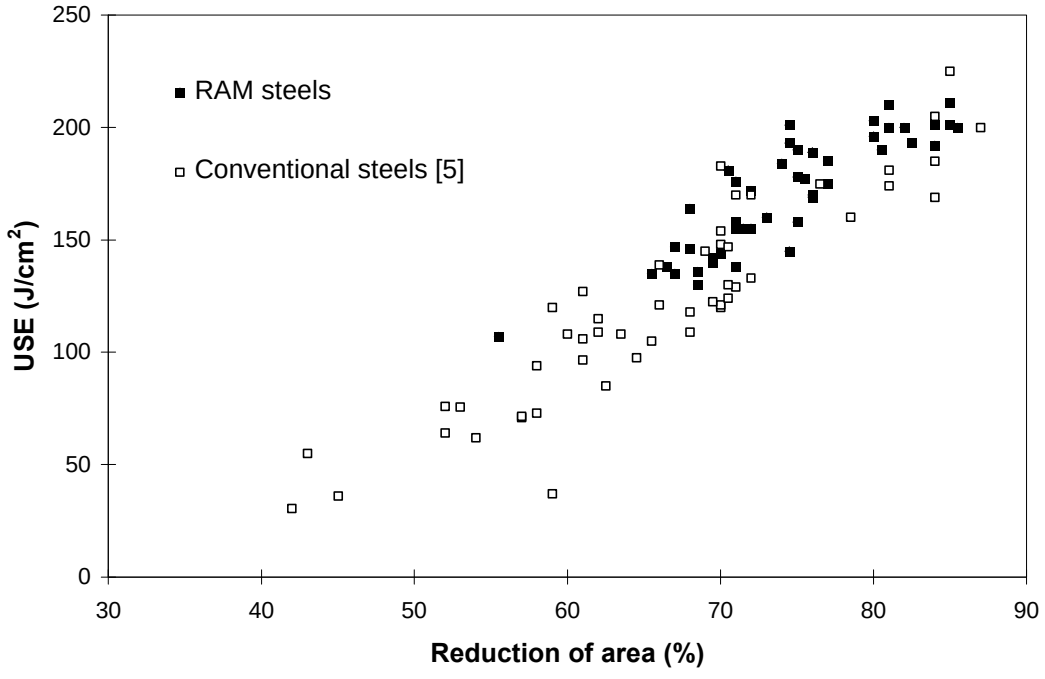

Figure 2 : Correlation between the reduction of area to failure (determined from tensile tests at 20°C) and USE (determined from Charpy tests)

An empirical correlation between Reduction in Area (RA) values and USE values was found (see figure 2). In fact, RA values measured from tensile tests at 20°C and 450°C show, for a given Charpy-V specimens geometry, a linear dependence with experimental USE values.

All materials and metallurgical conditions are included : as-received, N&T, N&T-CW, aged at different temperatures and times. This correlation allows to obtain, from the measurement of the RA after a tensile test at 20°C, a good estimation of the USE value.

The same correlation was already determined for CrMo conventional steels with the same Charpy-V specimens geometry [1].

After ageing at 400°C, in the case of steels with the highest Cr content (11 %), a degradation of impact properties is observed (Delta DBTT = +20°C and Delta USE = - 25 J/cm^2). TEM observations in LA4Ta (11Cr-WVTa) steel show that thermal ageing between 400°C and 550°C seems to induce the dissolution of M_2X particles (which were located initially between $M_{23}C_6$ carbides).

This evolution could not explain the embrittlement observed in that steel. On the other hand, SANS (Small Angle Neutron Scattering) experiments carried out on LA4Ta aged at 400°C show the occurrence of Cr-rich alpha prime particles all over the matrix which could explain this behaviour [2] (see task UT-SM&C-LAM3).

The fact that an increase in Cr-content induces a detrimental effect on impact properties after thermal ageing in the temperature range 400°C-450°C was already observed in conventional 12Cr-MoWVNb martensitic steels [1, 3] and also related to the presence of alpha prime precipitates in the matrix [3].

Concerning the ageing at higher temperature (550°C), the behaviour depends on the W content in the alloy. No degradation of impact properties is observed for materials with 0.7% W aged at 550°C. For a W content above or equal to 2 % (F82H and JLF-1), the USE decreases and the DBTT increases.

For the steel with 3% of W (LA13Ta), a clear embrittlement is observed : decrease of 20% of the USE, increase of 50°C of the DBTT associated to indications of intergranular fracture mode.

This behaviour, due to the precipitation of Laves phase as an intergranular brittle film, has already been observed in conventional 9/12Cr-MoW martensitic steels [1] and especially in 12Cr1Mo0.5Mo(V)-HT9 steel. According to Tamura et al. [4] and Abe et al. [5], the faster kinetics for Laves phase precipitation is found at about 650°C in 9Cr-4W and in 7.5Cr-2W steel and is slightly higher compared to Laves phase in 9/12Cr1Mo steels (T91 and HT9) [4].

At this temperature, Laves phases are more or less globular and probably induce a less detrimental effect on impact properties.

In F82H and JLF-1 steels (7.5/9 Cr-2WVTa), a degradation of impact properties (increase of the DBTT of almost 35 °C) was detected after ageing at 550°C.

On the other hand, at this ageing temperature, the precipitation of Laves phase was not observed by TEM and neither by SANS [2] even though it was observed in these steels after thermal ageing at 650°C [4], fatigue tests at 600°C [6] and neutron irradiation at 460 °C, 600°C and 750°C [7, 8, 9].

Before the precipitation of Laves phase at grain/lath boundaries, one could assume the presence of some segregation of W at interfaces that induces the embrittlement observed after thermal ageing at 550°C.

Further Auger electron microscopy or high resolution TEM observations should allow to confirm this assumption.

CONCLUSIONS

Experimental Fe-7.5/11CrWVTa RAM steels were characterised by mechanical tests and by TEM before and after thermal ageing. Mechanical behaviour depends on the chemical and metallurgical conditions (N&T-CW or N&T).

Significant embrittlement was observed in steels with W ≥ 2% after thermal ageing at 550°C and at 400°C for materials with a Cr-concentrations higher than 10%.

REPORTS AND PUBLICATIONS

[1] J.C. Brachet, A. Castaing, C. Foucher, Proceeding of Int. Symposium on Materials Ageing and Component Life Extension, Milan, Italy, 10-13 Oct. 1995, Engineering Materials Advisory Services Ltd. (UK), p.75-87.

[2] M. H. Mathon et al., submitted to the 20th. ASTM Symposium on Effects of Radiation on Materials, June 6-8 2000, Williamsburg, Va.

[3] T. Angeliu, E.L. Hall, M. Larsen, A. Linsebigler, C. Mukira, Proc. On Advanced heat resistant steels for power generation San Sebastien, Spain, Edited by R. Viswanathan and J. Nutting, 27-29 April 1998.

[4] M. Tamura, H. Hayakawa, A. Yoshitake, A. Hishinuma, T. Kondo, J. Nucl. Materials, 155-157, p 620-625, 1998.

[5] F. Abe, H. Araki, T. Noda, Metallurgical Transactions A, Volume 22A, p 2227, october 1991.

[6] T. Ishii, K. Fukaya, Y. Nishiyama, M. Susuki, M. Eto, J. Nucl. Materials 258-263 pt. B, p 1183-1186, 1998.

[7] T. Shibayama, A. Kimura, H. Kayano, Journal of Nuclear Science and Technology, vol. 33, N°. 9, p 721-727, September 1996.

[8] A. Kimura, M. Narui, H. Kayano, J. Nucl. Materials 191-194, p 879-884, 1992.

[9] Y. Kohno, A. Kohyama, D. S. Gelles, K. Asakura, Materials Transactions, JIM, Vol. 34, No. 11, p 1018-1026, 1993.

- "Effect of thermal ageing on the microstructure and mechanical properties of 7-11CrW RAFM steels", by Y. de Carlan, A. Alamo, MH. Mathon, G. Geoffroy, A. Castaing, communication to ICFRM 9, USA, 11-15 Oct.99, CEA report NT SRMA 99-2345, Dec 1999; to be published in J. Nucl. Materials.

TASK LEADER

A. ALAMO

SRMA
CEA Saclay
91191 Gif-sur-Yvette Cedex

Tél. : 33 1 69 08 67 26
Fax : 33 1 69 08 61 75

E-mail : ana.alamo@cea.fr

SM 2-3

Task Title : MECHANICAL PROPERTIES OF DIFFUSION BONDED WELDS (RAFM/RAFM HIP Joint)

INTRODUCTION

For DEMO fusion reactor, reduced activation ferritic martensitic steel (RAFM) is the candidate material for the first wall and breeding blanket. Today, there are two possible concepts, WCLL (Water Cooled Lithium Lead) and HCPB (helium Cooled Pebble Bed). Each concept contains several welds, realized by GTAW or EBW and or HIP process. Different welds must be tested to evaluate their properties for designers and manufacturers.

1999 ACTIVITIES

Mechanical properties of RAFM/RAFM junction and bulk material affected by the different thermals treatments have been determined : tensile tests from room temperature to 600°C and impact toughness from –196°C to 400°C.

MATERIAL

Böhler has elaborated the reduced activation ferritic martensitic steel or Eurofer 97. The forged material was supplied after the following heat treatment :

- Hardening : 979 °C – 1H 51, air cooled
- Tempering : 739°C – 3 H42, air cooled

The chemical composition (Heat N° E83699) is given in table 1.

Chemical composition

wt %	Value	wt %	Value
C	0.12	**Ti**	0.008
Si	**0.06**	**Al**	0.008
Mn	0.42	**Nb**	<0.001
P	0.004	**B**	<0.0005
S	0.003	**N**	0.018
Cr	8.87	***Ta***	***0.14***
Mo	<0.001	**O**	0.0013
Ni	***0.0075***	**As**	<0.005
V	0.19	**Sn**	<0.005
W	1.10	**Sb**	<0.005
Cu	***0.021***	**Zr**	<0.005
Co	0.005		

Table 1 : Eurofer 97 composition

Some minor deviations are observed for Si, Ni, Cu and Ta. The grain size is G = 10 or d = 11 µm (specification G > 6), and there is no ferrite content (specification < 3%).

Manufacturing of junction

The conditions of manufacturing have been optimised in task SM 4-5, and details are given in **[1]**. The fabrication route is composed of three main steps :

- Preparation of the assembly
- HIP Cycle
- Post-Bond Heat Treatment (PBHT)

Preparation of the assembly

The assembly is composed of slices which surfaces are carefully prepared before the bonding process. This step is important since the mechanical properties of a joint are strongly correlated to the cleanness of the interface. Any contamination of the surface by oil or dirt should be avoided. Slices were machined up to Ra 0.8µm. Both slices and container were degreased with a mixture of alcohol, ether and acetone in an ultrasonic bath. The surface were then widely rinsed with alcohol and dried. The slices were introduced in a container. They were then degassed at 60°C for 15h before to be sealed under argon.

HIP Cycle

The HIP cycle has been the following : 1100 °C 2h/2h/2h – 100 Mpa

These conditions have been chosen with people working on HIP cycle optimisation (task SM 4-5). They have shown that a minimal HIP temperature of 1050 °C must be applied to obtain a good quality of Eurofer / Eurofer joint.

During the dwell the grain size increased because all carbides are dissolved at this high temperature. To restore the properties (microstructure and mechanical) of Eurofer we had to apply a post-bond heat treatment.

Post bond heat treatment (PBHT)

This treatment comprised a tempering treatment (1hr 750°C) to precipitate carbides in material to limit austenite grain size growth during austenitisation.

This has been followed by an austenitisation treatment (1 hr 950°C, air quenching) and a tempering treatment (1hr 750°C) (see figure 1).

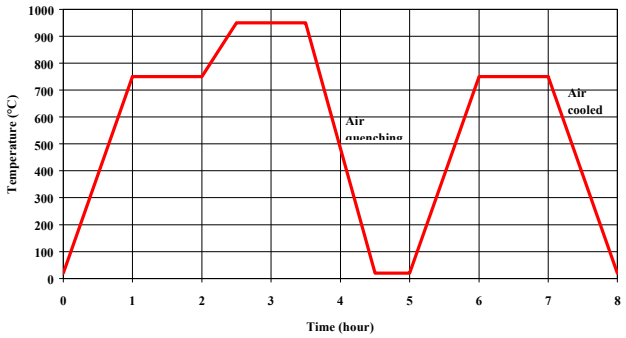

Figure 1 : Post bond heat treatment condition used

To determine properties of the bulk material, this thermal treatment has been applied to a block of Eurofer of the same size to reproduced the same cooling rate

PROPERTIES OF JUNCTION

The influence of the HIP and PBHT cycles on microstructure and mechanical properties is studied in this part.

Metallurgical examination

The microstructure of the bond is reported on figure 2. The metallographic examination at high magnification shows few precipitates along the joint. The junction appears very clean with some recrystallisation through the interface. The initial interface is difficult to detect.

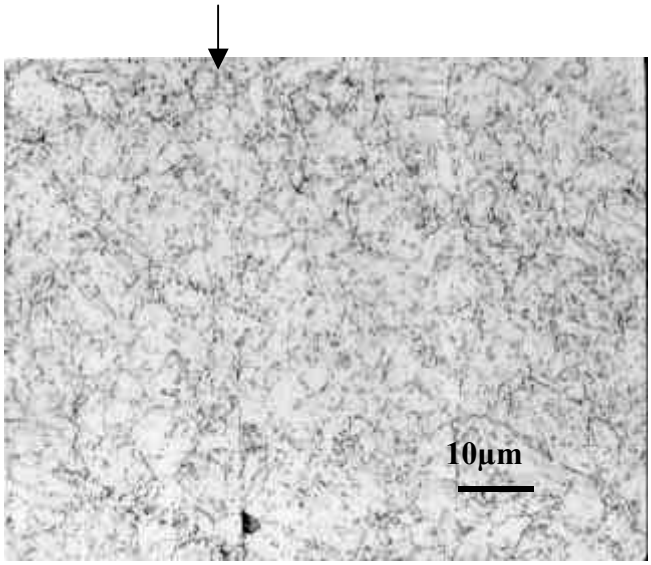

Figure 2 : Metallographic examination of the joint

Evolution of grain size and microstructure

The microstructure after the different cycles has been observed. It is very similar to the initial material. The grain size (G = 10 or d = 11 µm) is the same as in the as-received. There is no ferrite content. The average hardness has been measured at 248 Hv 30

Mechanical characterization

Tensile properties

Tensile tests have been carried out between room temperature and 600°C (RT, 300, 500, 600°C). All the specimens were machined in the longitudinal bar direction. Each condition has been tested twice.

The results of tensile tests are summarized in figure 3. As the failure has never occurred at the interface the behaviour of the specimens with a joint is relevant of the behaviour of the bulk material. This assumption has been checked at room temperature.

The variation of the yield stress and ultimate tensile stress versus the temperature is drawn on figure 4. The value of yield stress, ultimate tensile stress and the total elongation are higher than the minimum required within the specification. The complete HIP-PBHT cycle has lead to a hardening of the material accompanied by a decrease of ductility on comparison with the initial state. The ductility is just above the minimum required and some optimisation is still needed to limit the loss of ductility, for example : increase the time of the tempering treatment.

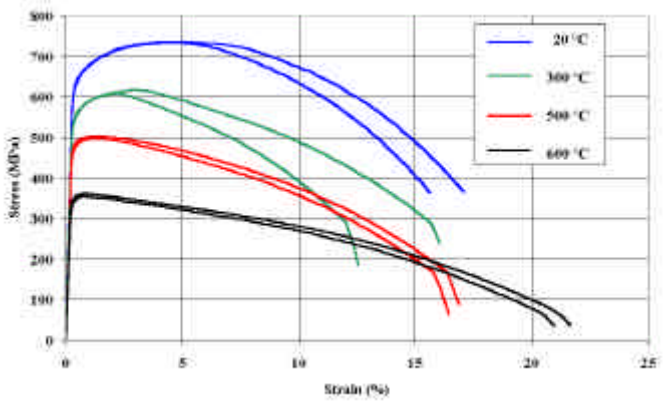

Figure 3 : Tensile properties of junction

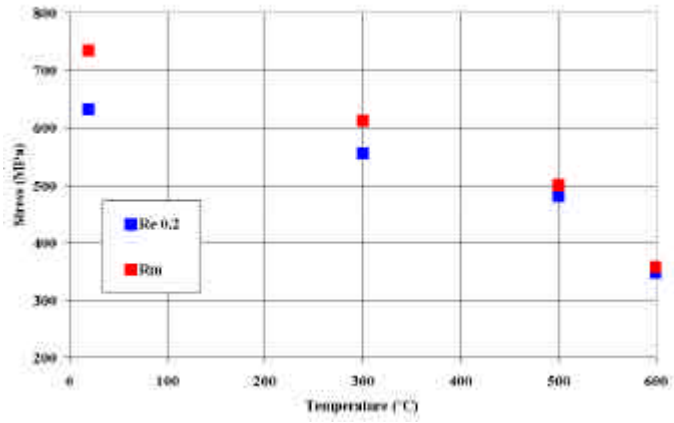

Figure 4 : Re $_{0.2}$ and Rm versus temperature

Impact properties

This test is very severe for a joint. Charpy U tests have been carried out on Eurofer specimens and on Eurofer / Eurofer specimens between –196°C and 400°C.

The ductile-brittle transition curves of both bulk material and junction are drawn on figure 5.

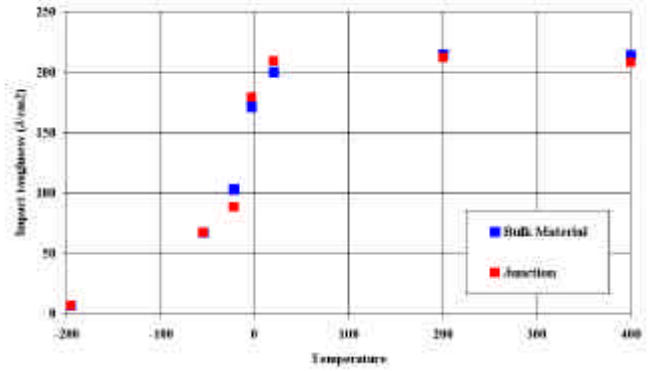

Figure 5 : Impact properties versus temperature of bulk material and junction

The impact properties of the joint are satisfactory : no debonding has been observed of the fracture surface of the specimen. The impact properties of the bulk material and of the joint are similar.

CONCLUSIONS

The work performed has been focused on the mechanical properties of RAFM/RAFM junction under tensile and impact tests. Influence of HIP and PBHT (Post Bond Heat Treatment) on mechanical properties of the bulk material has also been analysed.

A HIP cycle 1100°C – 2 hours has been applied. The PBHT has allowed to restore the microstructure and the mechanical properties of the RAFM. The treatment at 750°C, before the austenitisation, has permitted to limit grains size growth during austenitisation by precipitating carbides in material.

Metallographic examinations have shown a good cleanness and a recrystallisation through the interface.

The mechanical properties of the joints are excellent, the failure has never occurred at the interface but it is always located in the bulk material.

REPORTS AND PUBLICATIONS

[1] E. Rigal, L. Bedel
Development of martensitic steel / martensitic steel HIP joint with improve mechanical properties.
Task SM 4-5. Note Technique DEM 99-91, Décembre 1999

[R1] L. Bedel; E. Rigal, P. Lemoine
Mechanical properties of A RAFM/RAFM HIP Joint
Task SM 2-3. Note Technique DEM 99-87, Décembre 1999

TASK LEADER

Laurent BEDEL

DTA/DEM/SGM/L3M
CEA Grenoble
17, rue des martyrs
38054 Grenoble Cedex 9

Tél. : 33 4 76 88 57 20
Fax : 33 4 76 88 58 91

E-mail : bedel@cea.fr

SM 2-3.1

Task Title : MECHANICAL PROPERTIES OF FUSION WELDMENTS

INTRODUCTION

Concerning the innermost parts of DEMO reactor, the low activation martensitic (LAM) steels and reduced-activation ferritic/martensitic (RAFM) steels are primary candidate alloys as first wall and breeder blanket structural materials. Tungsten Inert Gas welding (GTAW), Electron Beam (EB) welding, laser welding and hot isostatic pressing (HIP) processes are envisaged for the fabrication of structural parts of DEMO. In the frame of weldability studies (TTMS-004), welded joints will be processed by GTAW with or without filler metal and by EBW. The present study aims to characterise the mechanical properties of both EB and GTAW weldments since the designers require data on the weldments mechanical behaviour to ensure the integrity of the whole blanket structure. The weldments to be tested are homogeneous joints of Eurofer and dissimilar joints Eurofer/316. In parallel, welded joints of F82H are tested as references.

1999 ACTIVITIES

TEST MATRIX

The test matrix and the specimen design have been defined with people working on HIP joining with a view to provide a good consistency between the mechanical testing of fusion welded joints and HIP joints. Further, results obtained on Eurofer HIP joints by the end of 1999 [1] are planned to be considered as references for comparison. The reference tensile tests have been planned at room temperature and at 300, 500 and 600°C with tensile specimens of cylindrical shape (2 or 4 mm of diameter). The reference impact tests have been planned between -200 and 300°C with standard V-notch Charpy specimen (55 x 10 x 10 mm3) and subsize specimen of "CEA shape" (55 x 10 x 2,5 mm3).

The mechanical tests on 2-mm thick samples are planned to be carried out using specific 2-mm thick tensile specimen. No impact test is planned in this particular case.

PRODUCTION OF WELDED JOINTS FOR CHARACTERISATION

In order to process F82H TIG welded joints without filler metal intended for mechanical testing, 1 plate of 24 mm of thickness has been hot rolled at 1000°C down to 2 mm of thickness. The plate thickness has been limited to 2 mm since higher thicknesses may not be fully penetrated if not considering a chamfer shaped joint that would involve the use of a filler metal. Heat treatments have been carried out on the hot-rolled plates in order to reproduce the microstructure of the delivery state.

Welding butt joint specimen have been sampled from the 2-mm thick plates. The processing of the welding joints is now in progress following the operating conditions defined previously in the SM4-3.1 action (1998) :

Voltage (V)	Current intensity (A)	Welding speed (cm/min)	Wire speed (m/min)	Wire scanning amplitude (mm)	Shielding gas (l/min)
9,5	85	10	none	none	10

The mechanical tests on 2-mm thick samples are planned to be carried out using specific 2-mm thick tensile specimen. No impact test is planned in this particular case.

CONCLUSIONS

The test matrix for mechanical characterisation consists in carrying out longitudinal and transverse tensile tests on both EB and TIG weldments and impact tests of the melted zones and (in the case of TIG weldments) of the heat affected zone. The processing of welded joints on F82H 2 mm-thick plates (butt joint) is in progress. The sampling of test specimen will be machined in keeping with the drawings selected for the mechanical testing of the F82H weldments processed by JAERI (97-98) and, as far as possible, in keeping with the work done on HIP joins.

REPORTS AND PUBLICATIONS

[1] Bedel L., Rigal E., Lemoine P., Mechanical properties of a RAFM/RAFM HIP joint, CEA internal report n°DEM-99/87, December 1999

TASK LEADER

André FONTES

DTA/CEREM/DPSA/STA/LMS
CEA Saclay
91191 Gif-sur-Yvette Cedex

Tél. : 33 1 69 08 37 21
Fax : 33 1 69 08 75 97

E-mail : andre.fontes@cea.fr

SM 3-3

Task Title : CORROSION IN WATER WITH ADDITIVES Corrosion studies on specimens from task A 4.2.1

INTRODUCTION

The main objective this subtask is to perform screening tests on various Low Activation Ferritic (LAFs) materials in order to access their susceptibility to various forms of water corrosion in fusion representative water conditions.

The proposed programme can be summarised as follows :

SPECIMENS PREPARATION

A maximum of twenty specimens will be tested in the corrosion loop of task A 4.2.1. Depending on material availability, four grades of LAFs could be tested in this programme. The specimens will be prepared from coupons 50 x 20 x 2 mm.

In the case of four grades of LAFs to be tested, the specimens matrix and type of corrosion addressed for each grade of alloy can be summarized as follows:

Table 1 : Specimens matrix and types of corrosion tests

	Nb of test specimens per corrosion type		
Specimens number	General and pitting corrosion	Stress Corrosion	Total nb of coupons
Of each Alloy	3	2	5
For each Test type	12	8	20

GENERAL CORROSION IN WATER AT 320°C

The test will be carried out 3 samples of each grade (Table 1) in the autoclave fitted on the loop of the Task A 4.2.1 for a maximum duration of 5 000 hours. The exact water chemistry will be defined in the Task a 4.2.1. The kinetic of general corrosion will be evaluated by mass variation measurements after removal of adherent corrosion products, and on micrograpghic cuts at the end of the test. The autoclave will be periodically opened for mass variation measurements. These test duration could vary according to the requirements of Task A 4.2.1.

PITTING CORROSION IN WATER AT 320°C

The test conditions will be similar to the ones described before. The general corrosion specimens will be used for this task (Table 1).

Pitting susceptibility will be evaluated by surface examination for non destructive examination and at the end of the test on the micrographic cuts of the specimens.

STRESS CORROSION CRACKING IN WATER AT 320°C

The SCC specimens will consist in U-bend or four point load specimens prepared from coupons.

The SCC susceptibility will be assessed by non destructive microscopic examination of the specimens at the periodic openings of the autoclave. At the end of the tests, the specimens will be cut, resin mounted and polished for destructive examination.

A maximum number of 8 samples will be used in this task , for instance 4 grades x 1 condition x 2 specimens (Table 1).

1999 ACTIVITIES

The first material available is the F82H steel (heat 9741). Two thermal treatments were performed by ENEA:

- normalised at 1040°C x 0.5 hour (air coaled) and,
- normalised at 1040°C x 0.5 hour (air coaled) then tempered at 625°C x 1 hour (air coaled).

The micostructures obtained after these two thermal treatments were characterized and Vikers microhardness imprints were performed at CEA.

For the material normalised at 1040°C, the results obtained show that the superficial microstructure is different from the microstructure in the depth of the coupon (bulk metal). The microhardness imprints, carried out on a section plane of the coupon, show that the superficial microhardness is lower than the one of the bulk metal, respectively 354 HV(1.96N) and 448 HV(1.96N).

For the material normalised at 1040°C then tempered at 625°C, this microstuctural heterogeneity is not observed. The microhardness at the surface of the coupon and the one in the depth of the coupon are 288 HV(1.96N).

The installation of the loop used for the corrosion tests was finished in June 1999. During the second half of 1999, preliminary tests were performed and the loop was improved [1]. The loop consists of an autoclave linked to a water circuit allowing to insure a continuous water flow and to control the water chemistry (Figure 1).

The corrosion specimens will be placed in the autoclave. In this autoclave, there is a martensitic steel permeation membrane, which can be filled with some Pb-17Li and linked to a gas circuit to dissolve hydrogen in PB-17Li by bubbling.

This loop allows to perform the corrosion tests of this task and the hydrogen permeation measurements from Pb-17Li towards water of the task A4-2.1.

Figure 1 : View of the corrosion and permeation loop

CONCLUSION

The susceptibility of four grades of LAFs to various forms of water corrosion in fusion representative water conditions will be investigated in this task in 2000.

In 1999, the first material available was characterized and the loop for theses corrosion tests and the permeation measurements was improved.

This corrosion task could then be followed by a more thorough assessment of specific forms of corrosion on the selected materials, in particular those that could be induced by faulted conditions.

REPORTS AND PUBLICATIONS

[1] "Tritium permeation from Pb-17Li towards water and corrosion loop", T. Dufrenoy, A. Terlain, RT-SCECF 513 (December 1999)

TASK LEADER

O. RAQUET

DTA/DECM/SCECF/LECA
CEA Saclay
91191 Gif-sur-Yvette Cedex

Tél. : 33 1 69 08 15 92
Fax : 33 1 69 08 15 86

E-mail : olivier.raquet@cea.fr

SM 3-7

Task Title : CORROSION IN MAGNETIC FIELD

INTRODUCTION

In the liquid metal blanket, corrosion of structural materials exposed to the Pb-17Li alloy may be affected by the magnetic field. It is known that the presence of a magnetic field can change the flow configuration of an electroconducting fluid and thus the transport of solute from the solid to the liquid phase may also be modified. In order to study such an effect, corrosion experiments in Pb-17Li with flows generated in a cylindrical cavity by a rotating disk are planned. The objective of this task is to determine the velocity distribution in such a geometry in order to have a good knowledge of hydrodynamics.

1999 ACTIVITIES

A numerical analysis has been proposed to determine the velocity distribution in a cylindrical cavity with a rotating end wall under axial magnetic field. Results are obtained without and in presence of magnetic field as a function of the electrical conductivity of walls (cavity and rotating disk).

FORMULATION OF THE PROBLEM

The global geometry of the simulation is described in Fig. 1. It presents a cylindrical cavity which contains the fluid (Pb-17Li alloy): the top end wall of the box is the rotating disk i.e., the sample (steel material) used for corrosion test, the lateral walls of the cavity are fixed.

Assuming low magnetic Reynolds number (i.e., the applied magnetic field is not modified by the induced electric current), the three parameters which control the velocity are: the Hartmann number (Ha), the interaction parameter (N) in which is introduced the angular velocity Ω of the disk and the conductance ratio (K). The choice of the dimensions is in agreement with the future experiment.

Thus, the height (H) of the cavity is three times greater than its radius (R) and the vertical magnetic field, Bo (0, 0, -Bo), is parallel to the oz axis. The problem is assumed to be axisymmetric and only the stationary conditions are considered. It is possible to write the momentum equations in cylindrical coordinates in nondimensional form (u_r u_θ and u_z are the three components of the velocity: radial, swirl and axial, respectively).

The numerical tool used to solve the problem is the commercial code FLUENT. The SIMPLE algorithm is used to solve the equations.

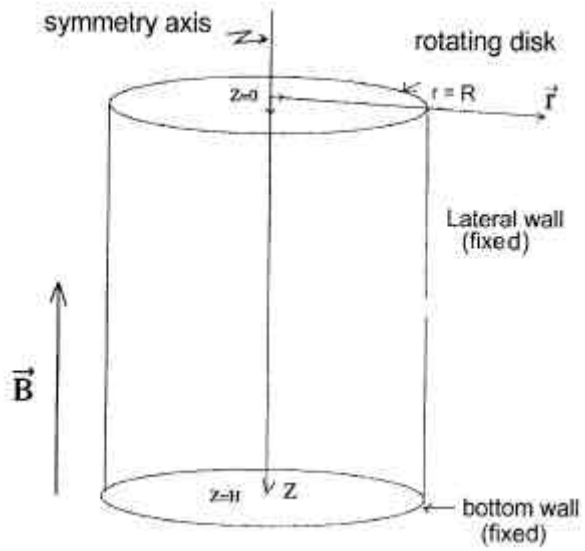

Figure 1 : Geometry of the flow (H/R = 3)

SOLUTION WITHOUT MAGNETIC FIELD

Without magnetic field (Ha = 0), the problem is described by the solution of the Navier-Stokes equations (Re is the Reynolds number). The solutions have only been found for an aspect ratio (H/R) equal to 3 corresponding to the dimension of experimental cavity which will be used. In this context, it is useful to decompose the flow in two parts: the swirl component u_θ and the two components in the meridian plane (u_r, 0, u_z). In the meridian plane, the stream lines can be calculated to visualize the flow. The configuration of the boundary layer (the Ekman layer) at the interface between the disk and the liquid results from an equilibrium between the centrifugal force and the radial pressure gradient which generates a high pressure zone at the periphery of the rotating disk.

This high pressure zone drains flow in the cavity which closes on the axis corresponding to a low pressure zone. This phenomenon is well known as the Ekman pumping. The order of magnitude of both the depth of the layer and the velocity inside the layer can be calculated.

By considering the phenomenological approach which consists in expressing, at the first order, that the depth of the Ekman layer is only function of the kinematic viscosity and the angular rotation of the disk, we obtain: $u_r \approx u_\theta \approx 1$, $u_z \approx Re^{-1/2}$. The curves presented in Fig. 2 are in agreement with this order of magnitude.

SOLUTION IN PRESENCE OF MAGNETIC FIELD

The equations are solved for maximum values of the interaction parameter equal to 10^2. Such values are lower than those corresponding to the fusion reactor but nevertheless they are representative of the asymptotic cases. In the following, the results are presented as a function of the electrical conductivity of the wall i.e., as a function of the conductance coefficient (K).

Case of electrically insulating walls (K = 0)

Such a situation corresponds to the case of walls (including the rotating disk) which are electrically non-conducting (perfect insulating medium). In this case, the electric lines do not penetrate inside the walls and have to close inside the liquid alloy. The Ekman layer is replaced by the Hartmann layer.

For high value of the interaction parameter, the Hartmann layer occurs at the vicinity of the rotating disk and at the bottom wall of the cavity. It is characterized by an equilibrium between the viscous forces and the electromagnetic forces. Concerning the electric condition, this situation corresponds to a conductance ratio equal to zero (K=0).

The effect of the magnetic field can be shown by comparing Figs. 2 and 3. In Fig. 3, the variation of the swirl velocity along a vertical line located at a dimensionless distance from the axis r= 0.7 is presented. The position z=0 corresponds to the interface with the rotating disk and the position z = 3 corresponds to the interface with the bottom wall (fixed wall). It can be observed that when the Harmann number increases, the velocity gradient at the wall also increases.

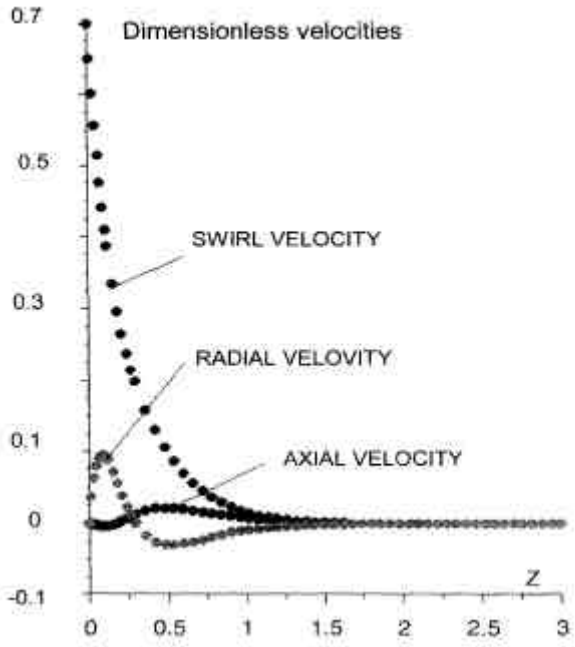

Figure 2 : Distribution of radial, swirl and axial velocities along the vertical axis without magnetic field (at r = 0.7, Re = 100)

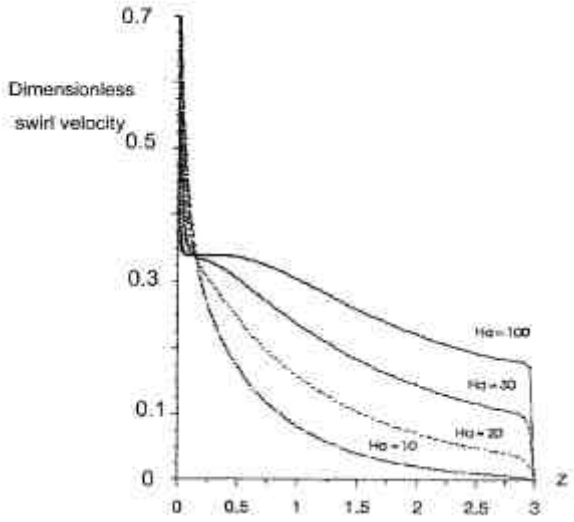

Figure 3 : Variation of the swirl velocity in presence of magnetic field as a function of Ha: Case of electrically insulating walls K = 0 (at r = 0.7, Re = 100).

Case of electrically conducting walls (K ® ¥)

In that case, it is assumed that all the walls are perfectly conducting, which corresponds to an infinite value of the conductance ratio K ($K \rightarrow \infty$).

In this situation, it can be demonstrated that the tangential component of the current density in the fluid vanishes at the wall. Fig. 4 confirms the analysis and exhibits nearly a linear variation of the swirl velocity from the top (z=0) to the bottom (z=3) of the cavity. The effect of the wall conductivity on the velocity distribution is clearly shown by comparing Figs. 3 and 4.

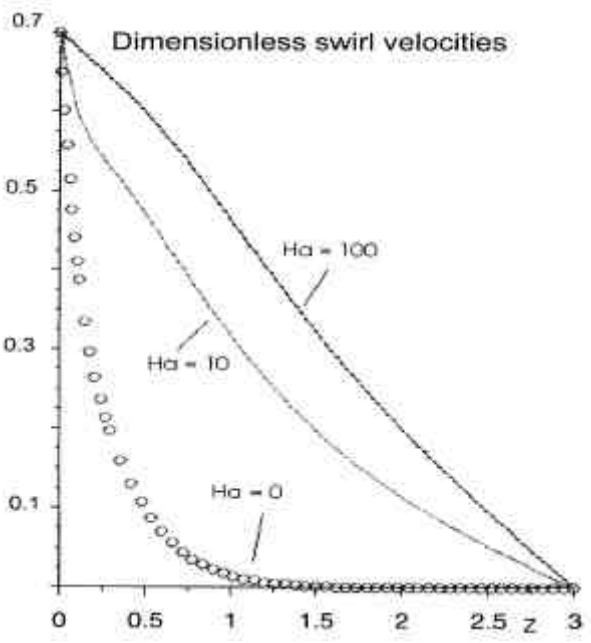

Figure 4 : Variation of the swirl velocity in presence of magnetic field as a function of Ha: Case of electrically conducting walls K ® ¥ (at r = 0.7, Re = 100).

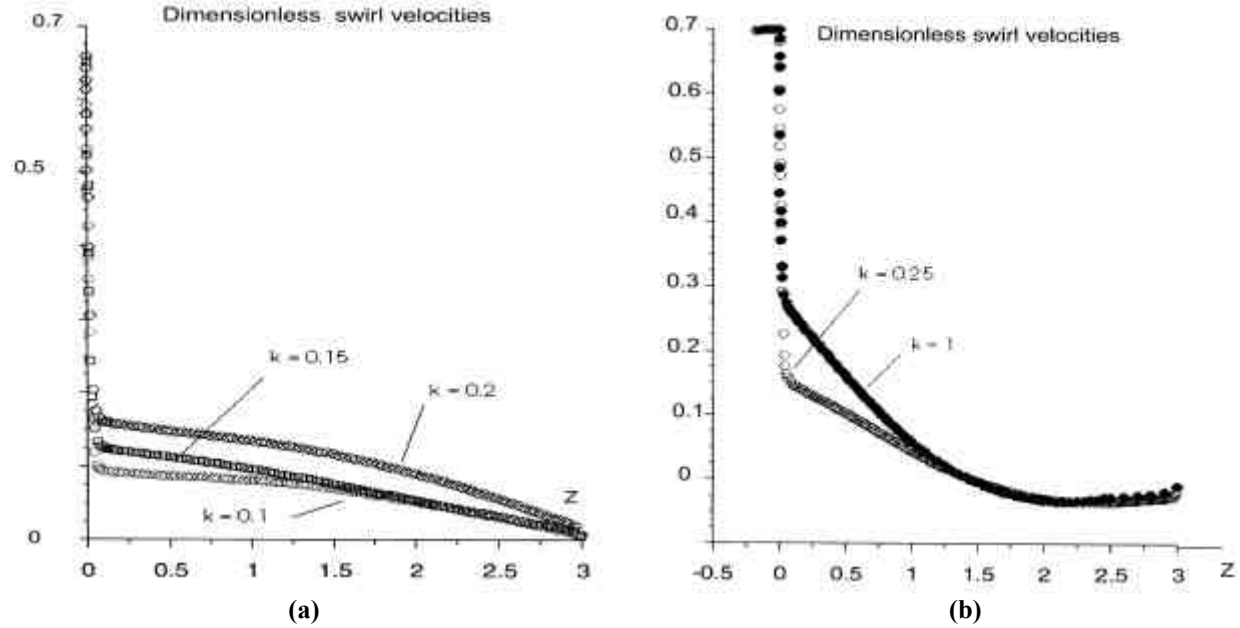

Figure 5 : Variation of the swirl velocity in presence of magnetic field as a function of Ha: (a) Case of electrically conducting walls K < 0.25 - (b) Case of electrically conducting walls K = 0.25 and K = 1 (at r = 0.7, Re = 100)

Case of walls with finite depth and conductivity (0.1 £ K £ 1)

In this case, the conductance coefficient takes finite values. We consider that all the walls (rotating and fixed walls) are identical materials and have the same depth. The main difference with the previous cases is that the electric current circulates inside the liquid alloy and in other parts of the walls. The cases corresponding to different values of the conductance ratio have been tested: K = 0.1, 0.15, 0.25, 0.5. All these situations are analyzed for constant values of both the Reynolds number and the Hartmann number (Re = 100 and Ha = 100).

The results exhibit an unexpected phenomenon. It seems that two different hydrodynamic regimes exist, separated by a critical value of the conductance ratio K_c=0.25. For K < K_c, the situation is roughly similar to the non-conducting case. For K > K_c, it appears a region where the flow has a swirl component opposite to the swirl component of the rotating disk. This means the presence of a reverse flow. This flow is located at the vicinity of the lateral wall and in the lower part of the cavity tangential velocity.

Fig. 5 shows the swirl velocity distribution along a vertical line located at r = 0.7: Fig. 5a corresponds to cases with K < 0.25 whereas Fig. 5b exhibits cases with larger values. It seems that in both cases the velocity gradient at the wall are fixed and that the improvement of the conductance ratio corresponds to an increase of the core velocity.

The difference between the two figures concerns the velocity distribution in the core of the cavity. In the cases corresponding to K < 0.25, it can be noticed that the sign of the velocity does not change.

On the contrary, when K > 0.25, the presence of negative values for the velocity distribution appears clearly in the second half part of the cavity. The amplitude of the negative velocity and the region covered by this reverse flow seems to decrease when K increases. The infinite values of K corresponding to a linear distribution of the velocity from the top to the bottom of the cavity are in agreement with the perfectly conducting case.

CONCLUSION

Corrosion experiments in liquid Pb-17Li under magnetic field are planned with flows generated in a cylindrical cavity by a rotating disk. In order to correlate mass transfer with hydrodynamics in such a geometrical configuration, the velocity distribution has to be known. A numerical analysis has been carried out to predict the flow.

The influence of magnetic field on velocities is clearly shown. When the Hartmann number increases, the velocity gradient at the wall increases. The wall electrical conductivity is also found to be an important parameter. The calculations made for various values of conductance ratio (K = 0, K $\rightarrow\infty$, 0.1 $\leq$ K $\leq$ 1) indicate that hydrodynamics is largely controlled by this factor.

REPORTS AND PUBLICATIONS

[1] F. BARBIER, A. ALEMANY and A. KHARICHA, "Corrosion in moving liquid Pb-17Li under magnetic field: Hydrodynamic modeling in rotating flows", RT SCECF 510 (December 1999)

TASK LEADER

Françoise BARBIER

DTA/DECM/SCECF/LECNA
CEA Saclay
91191 Gif-sur-Yvette Cedex

Tél. : 33 1 69 08 16 13
Fax : 33 1 69 08 15 86

E-mail : francoise.barbier@cea.fr

SM 4-1

Task Title : QUALIFICATION AND FABRICATION PROCESSES Powder HIP development and characterization

INTRODUCTION

For DEMO Blankets, Ferritic/Martensitic (RAF_M) steels have been selected in EU as reference structural materials. In addition the powder HIP techniques have been identified as promising as they assume to overcome drawbacks associated with cast products (poor metallurgical quality, alloying limitations....), to enhance the properties of foundry parts and to lower the cost fabrication through a strong reduction of the machining and the number of welds.

To demonstrate the potential and the availability of such techniques, material development, blanket mock-ups fabrication and numerical modeling for the production of near-net shape component are currently studied by CEA/CEREM.

1999 ACTIVITIES

PRODUCTION OF EUROFER 97 POWDERS

Material

A first heat of Eurofer has been produced and atomized. The chemical composition of this one is shown in table 1. For comparison, compositions of the Eurofer specification and a special Anval heat materials before and after powder atomization are also given.

Table 1 : Comparison of the chemical composition of RAF_M steels before and after powder atomization

Element	Eurofer Specification	Eurofer			ANVAL D87595
		D83334 heat	powder (µm)		powder (µm) +50-250
			>45	**45-250**	
Carbon	0.090-0.120	0.11	0.091	0.86	0.11
Manganese	0.20-0.60	0.37	0.38	0.37	0.58
Phosphorus	<0.005	0.006	0.005	0.002	0.023
Sulphur	<0.005	0.004	0.005	0.005	0.013
Silicon	<0.05	0.08	0.091	0.086	0.32
Chromium	8.5-9.5	8.84	8.88	8.99	8.92
Vanadium	0.15-0.25	0.19	0.19	0.19	0.20
Tantalum	0.05-0.09	0.08-0.13	0.086	0.10	
Tungsten	1-1.2	1.06	1.14	1.16	1.25
Nitrogen	0.015-0.045	0.003	0.024	0.024	0.095
Oxygen	<0.01	0.001	0.055	0.0088	0.006
Nickel	<0.005	0.050	0.14	0.087	

Atomization

To avoid contamination, the steel is remelt in an induction furnace. The powder is produced using a gas atomization technique. O content in argon is a main concern and has to be as low as possible to limit the powder particle oxidation. Large grains (>250µm) are scrapped to eliminate major contaminants. Smaller particles (<45µm) are also eliminated for a better control of the powder filling.

Powder composition

As shown in Table 1 the chemical compositions of the powders are comparable with those of the cast material, except for the O and N nitrogen content that is probably due to the elaboration. Effect of the O contamination results in a decrease of the impact properties. In the range of +45 - 250µm, Eurofer powder looks not so much spherical and presents some porosities. Figure 1 reveals the presence of fine inclusions and carbides mainly for the bigger particles probably due to an insufficient cooling rate during the atomization. By comparison, the powder in the range - 45µm, for which a higher cooling rate is expected, presents much less carbides. Natural sintering of the Eurofer powder begins at 990°C which is similar with the F82H. Grain growth remains low up to 1050°C.

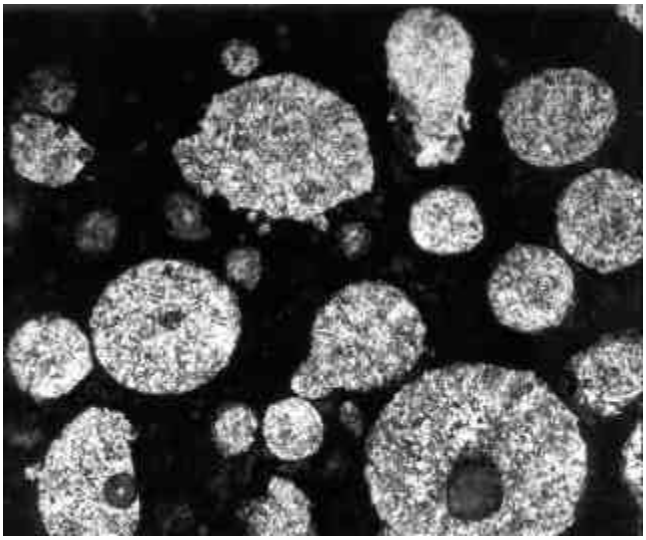

Figure 1 : Metallography of the Eurofer powder +45 -250 mm. (x200)

MECHANICAL CHARACTERIZATION OF THE HIP'ED MATERIAL

After HIP'ing at 950°C, the material is fully dense, as given by density measurement and micrography analysis.

The HIP Eurofer 97 microstructure is characterized by a very small grain size, ranging between 7 and 9 µm after 1h HIP and 9 to 11 after 10h. For 1hour HIP'ing, the Prior Particle Boundary (PPB) draw up a continuous line when after 10hours, only a much less visible dotted line can be observed.

The Vickers hardness data (table 2) of the 1 hour HIP'ed material are very similar to those of the cast material For the lower hardness obtained after 10 hours this is probably due to the PPB coalescence.

Table 2 : HV1 measurements on Eurofer

	As delivred	**HIP'ed 1 hour**	**HIP'ed 1 hour**
N : 950°C	420	420	410
N + T : (750°C)	225	225	210

Impact test

Impact testing data are summarized in table 3. Three different configurations have been tested: the as-casted plus tempered material, and two different HIP'ed material (1 hour and 10 hours at 950°C under 100 MPa). It can be seen that the HIP'ed materials reveal lower results than the casted one. However, the duration of the dwelling time has a major influence on the impact testing energy since the average value growth from 134 to 187 J/cm² when the duration increases from 1 hour to 10 hours at 950°C.

Table 3 : Impact testing data

materials	casted Eurofer quenched + tempered (J/cm²)	HIP'ed Eurofer 1 h 950°C + tempered (J/cm²)	HIP'ed Eurofer 10 h 950°C + tempered (J/cm²)
test results	294/284/314/ 299/320	153/132/126/ 125/132	190/173/193/ 189/191
mean value	**302**	**134**	**187**
standard deviation	**15**	**11**	**8**

Impact fracture surface on the 1 hour HIP'ed material shows few dimples and a rupture by decohesion at the PPB characteristic of a brittle behavior. After 10 hours, the fracture is almost ductile with much more dimples, as a result of a partial dissolution of the PPB. We can also notice in table 3 that impact energy results from HIP'ed material is significantly lower than the casted one.

Tensile test

Several tensile tests have been performed on samples HIP'ed at 950°C during 1h (t1-T950 n°1 and 2) and 10h (t10-T950 N°1 and 2). One other test have been performed on samples heated 20 additional hours at 950°C (t30-T950 + 20). It can be observed the effect of the dwelling time which increase greatly the Ultimate Strain from 16% to 21% from a dwelling time of 1h to 10h (figure 2). Moreover, an excessive dwelling time (30 hours) induces a decrease of the mechanical properties.

This result is related to the grain growth which occurs between 10 and 30 hours. In any case the mechanical properties are equivalent to the wrought Eurofer 97.

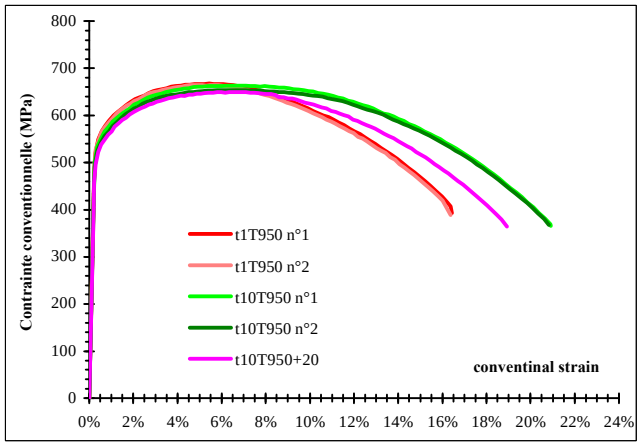

Figure 2 : Tensile results on powder HIP Eurofer

Based on these tensile test results, a HIP cycle of 10 hours at 950°C is recommended.

TRANSFORMATION TEMPERATURES

Transformation temperatures have been measured before and after atomisation : martensitic->ferrite (m->a), ferromagnetic-paramagnetic (ferro->para), Austenic start (As), Austenic finish (Af), Ferrite start (Fs), Ferrite finish (Ff) , Martensitic start (Ms), Martensitic finish (Mf). The results are compared and summarized in table 4.

Table 4 : Dilatometric measurements performed on Eurofer 97

Eurofer	Böhler ϕ10 mm	Böhler	Böhler	Osprey +45µm cold pressed	Osprey +45µm cold pressed	Böhler
heating rate	2°C/min	8°C/min	8°C/min	8°C/min	8°C/min	8°C/min
dwell	20 min at 1340°C	1h at 965°C	1h at 960°C	1h at 1345°C	10 min at 955°C	10 min at 955°C
cooling rate	2°C/ min	2.5°C/ min	38°C/min until 550°C then 20°C/min	90°C/ min	99°C/ min	99°C/ min
m->α	650	655		610	660	665
Ferro->para	760	760	770			760
As	850	855	850	830	845	850
Af	885	885	880	875	880	880
Fs		~780				
Ff		~660				
Ms	410	395	365	465	400	373
µs final	100% martens.	15% perlite	100% martens.	100% martens.	100% martens.	100% martens.
hardness	412 HV	332 HV	414 HV			

Dilatation coefficient

Based on the reference HIP cycle (950°C 10 hours under 100 Mpa), the determination of the evolution of the coefficient has been realized (figure 3). That determination is really important for the modeling of HIP process.

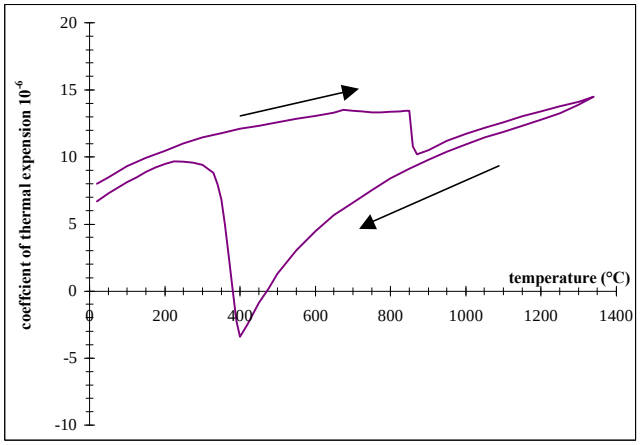

Figure 3 : Evolution of the thermal coefficient with the temperature

CONCLUSION

The use of HIP RAF steel material offers many advantages as simplification of the fabrication of complex design component, reduction of weldings and therefore risk of leaks, which is a major concern with this type of material.

The results of the work realized in 1999, can be summarized as follow :

- 2 different batches of Eurofer have been supplied and the morphology of the powder has been chemically analysed.

- Different HIP cycle have been tested and the HIP'ed material has ben analysed in terms of mecanichal properties (hardness, impact and tensile test), metallurgical properties (martensic transformation temperature).

- From the different results, a first reference HIP cycle has been defined. This HIP cycle correspond to 10 hours at 950°C under 100 MPa This cycle correspond to the best compromise between all the properties. However, this powder HIP material reveal only one weak point which correspond to the impact strength. This point could be improve by decreasing the O content within the powder induced during the atomisation.

- With the reference HIP cycle, measurement of dilatation coefficient has been realised on the powder HIP material.

REPORTS AND PUBLICATIONS

[1] G. Le Marois, L. Federzoni, P. Revirand : *Advanced ITER FW Fabrication Concept for cost reduction*, Note technique DEM N° DR 05/99.

[2] L. Federzoni : *Powder HIP development and characterization TASK SM4.1*, Note technique DEM N° DR 80/99.

TASK LEADER

L. FEDERZONI

DTA/DEM/SGM
CEA Grenoble
17, rue des martyrs
38054 Grenoble Cedex 9

Tél. : 33 4 76 88 57 26
Fax : 33 4 76 88 54 79

E-mail : federzoni@.cea.fr

SM 4-1.1

Task Title : SENSIBILITY TO WELD CRACKING / GENERAL WELDABILITY BEHAVIOUR
Assessment of EB and GTAW weldability of LAM steel

INTRODUCTION

The recently developed low activation martensitic (LAM) steels are the most viable as structural materials of DEMO reactor first wall. LAM steels compositions are based on replacement of molybdenum by tungsten in conventional CrMo heat resistant steel.

Prior to select one of these alloys, the evaluation of its weldability is required. The aim of this action was to evaluate the respective applicability of electron beam (EBW) and GTAW processes to the welding of LAM steels.

The last task report has been written by the end of 1999. It gathers the weldability data obtained by using the EB process on three experimental RAFM steel : F82H, JLF-1 and Optifer.

1999 ACTIVITIES

The report concerns the informations available about the origins of the plates that have been used for the weldability study for the three materials (F82H, JLF-1 and Optifer). The operating conditions applied by using a 30 kW EB gun are described. The weldability results are discussed on the base of external aspects, metallographic examinations and radiographic controls. Hardness profiles carried out in cross section allow to compare the process effects on the three materials.

CONCLUSIONS

The 1999 progress consisted in issuing the last task report. The task SM4-1 is now completed. The following task in the 1999-2002 programme is SM4-3.

REFERENCES

[1] A. Fontes, M. Barras, Soudabilité par procédé à faisceau d'électrons d'aciers martensitiques à faible activation (3ème partie) : résultats comparatifs obtenus sur F82H, JLF-1 et Optifer, CEA report n°DPSA/STA/LMS/RT 3918, January 2000

TASK LEADER

André FONTES

DTA/CEREM/DPSA/STA/LMS
CEA Saclay
91191 Gif-sur-Yvette Cedex

Tél. : 33 1 69 08 37 21
Fax : 33 1 69 08 75 97

E-mail : andre.fontes@cea.fr

SM 4-2

Task Title : MECHANICAL ALLOYING INCLUDING ODS

INTRODUCTION

Raising the operating temperature of fusion reactors is one of the keys to improving their efficiency. Present use of RAFM steels allows operation at temperatures around 550°C.

The use of Oxide Dispersion Strengthened RAFM steels offers the potential of temperatures up to 650° and may be up to 700°C.

Until now no ODS steels with Reduced Activation have been commercially available. The mechanical alloying laboratory of CEA/CEREM has important experience in the development of ODS alloys and especially in the field of ODS steels. This experience allows our laboratory to elaborate within a short delay new grades of ODS steels.

Our main objective in this task is to demonstrate the benefit of ODS RAFM steels for blanket design solutions. As powder Hot Isostatic Pressing is the principal and very interesting route to manufacture large net-shape or near net-shape-parts for structural applications, our work will be focused on this consolidation technique.

The study will mainly consist of the optimisation of the complete process of elaboration of consolidated ODS RAFM steels : raw materials supplying, mechanical alloying, Hot Isostatic Pressing and recrystallisation thermal treatments.

1999 ACTIVITIES

The work programme will include different steps. The first step done in 1999 is to produce different batches of ODS EUROFER steel powder and to obtain some consolidated samples.

MECHANICAL ALLOYING

Initial powders

The Eurofer steel which has been used is from Böhler. The Eurofer has been atomized under argon by Osprey.

In order to get better results after milling, only the powder with a size under 45 microns has been retained for milling.

Yttrium Oxide powder has been selected for the reinforcement because of its well known stability and its usual use for ODS materials (including commercial ones).

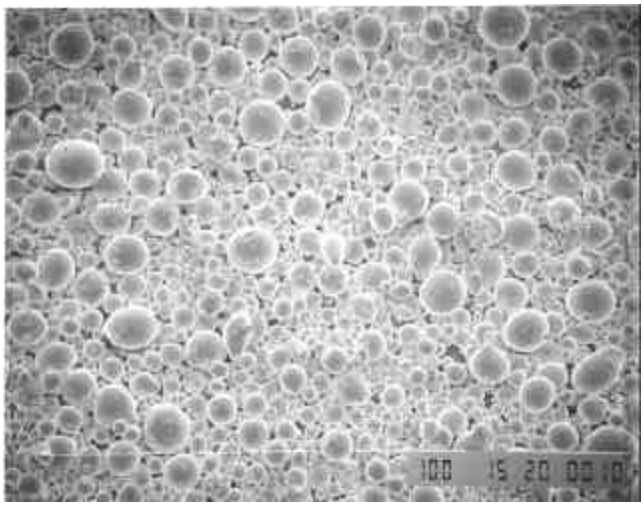

Morphology of the powder observed by S.E.M.

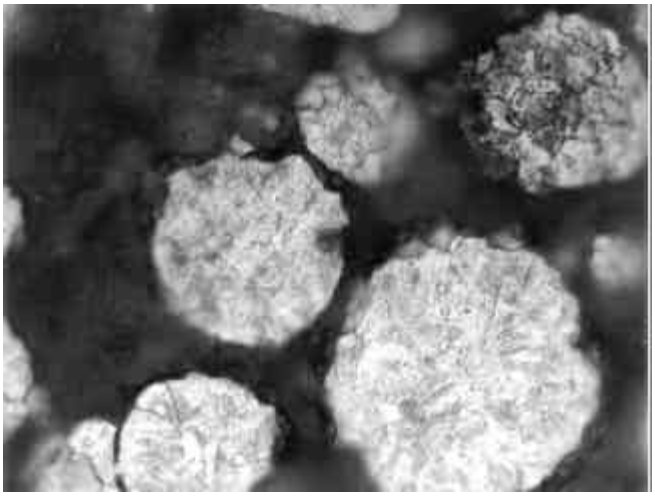

Microstructure of the powder

Processing

Reinforced Eurofer has been produced by mechanical alloying with different weights of yttrium oxide as reinforcement and in different kinds of mills.

The different kinds of mills used are attritors and ball mills which are the usual kinds of mills used in industry.

The attritor mills have capacities of 400 g per batch. The ball mills used have a 5 kg capacity.

One ball mill has been designed (based on our experience in this field) especially for the production of ODS steels and is dedicated for this application.

Complete control of milled powder has been done for each of these batches: the results are presented in the report [1].

- Morphologic characterization by M.E.B.
- Optical microstructural characterization.
- Sizing of the powder.
- Chemical analysis of the potential contaminations (O and C).

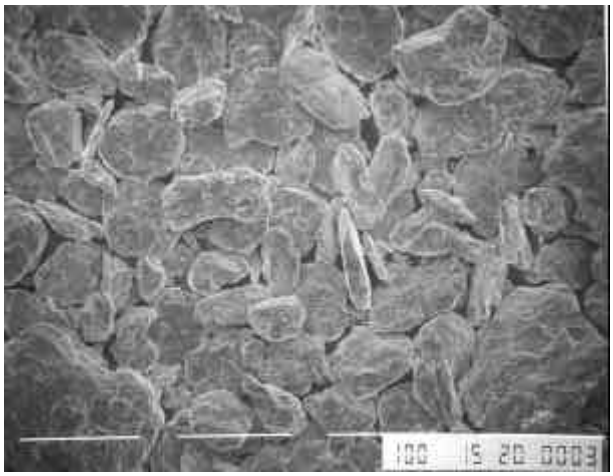

Example of the morphology of the powder milled by attritor

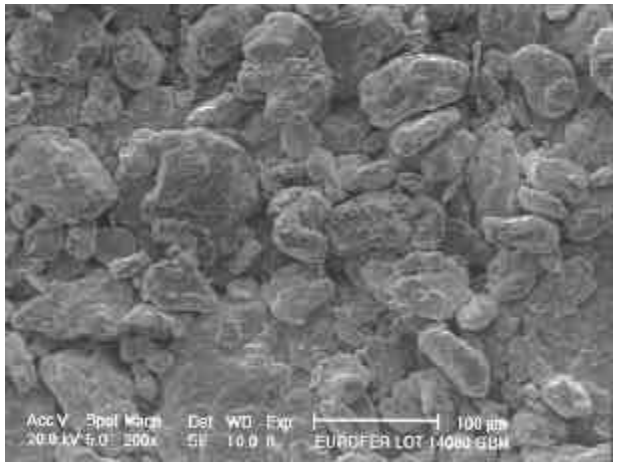

Example of the morphology of the powder milled by ball mill

In both cases the size, of more than 80%, of the powder is less than 100 microns.

The microstructure of the material is very fine and irresoluble by optical and SEM observations.

In the case of attritor and ball mill the chemical analysis done have not permit to show any pollution with carbon or oxygen.

CONSOLIDATION

The consolidation of the samples has been done by Hot Isostatic Pressing, following a cycle which has been selected for the Eurofer ODS.

Microstructure of milled powder by ball mill
Dimension of the powder around 100 microns

The cycle used is the following **1020°C/1000bar/2h.** Eurofer powder produced and consolidated in 1999 :

- By Attritor mill with 0.5% wt yttrium oxide.
- By Attrirtor mill with 1% wt yttrium oxide.
- By Ball mill with 0.5% wt yttrium oxide.
- By Ball mill with 1% wt yttrium oxide.

After this cycle the material is fully dense with the following microstructure :

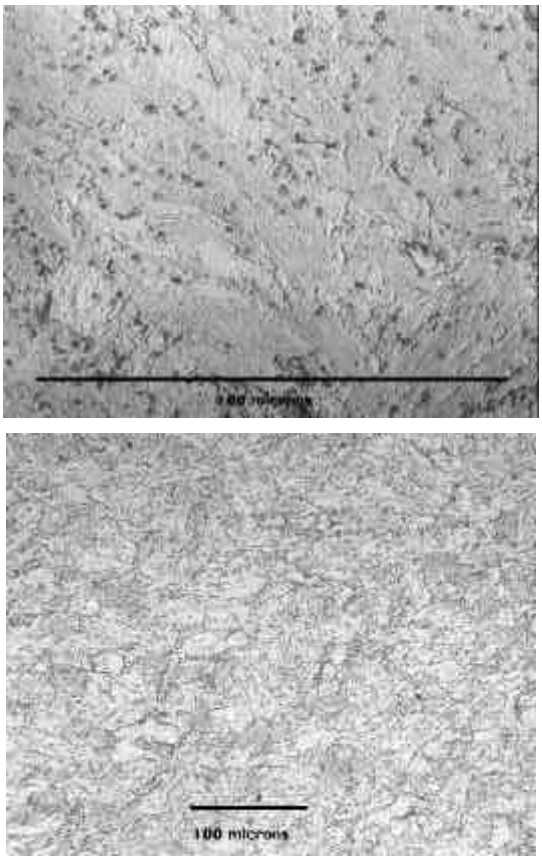

Optical observations of the microstructure

CONCLUSION

The work programme of this year 1999 was to produce different batches of ODS Eurofer powder and to obtain consolidated material. This programme has been fully accomplished as specimens of material consolidated by Hot Isostatic Pressing are available.

Regarding the first characterization, the microstructure is as expected and the material is fully dense.

The next steps will be to realize some fine charaterization and some mechanical testing on these available samples.
Some batches of ODS RAFM steels will also be produced in order to work on the influence of the composition of the steel on the mechanical alloying process and on the properties of the consolidated material.

REPORTS AND PUBLICATIONS

[1] Stéphane Revol, “Mechanical alloying including ODS, Task SM4.2”. Note Technique DEM n°71/99.

TASK LEADER

Stéphane REVOL

DTA/DEM/SGM
CEA Grenoble
17, rue des martyrs
38054 Grenoble Cedex 9

Tél. : 33 4 76 88 98 42
Fax : 33 4 76 88 54 79

E-mail : stephane.revol@cea.fr

SM 4-3

Task Title : EUROFER WELDABILITY AND FILLER METAL

INTRODUCTION

Concerning the innermost parts of DEMO reactor, the low activation martensitic (LAM) steels and reduced-activation ferritic/martensitic (RAFM) steels are primary candidate alloys as first wall and breeder blanket structural materials. Large structures consist of sub assemblies and components. In the case of breeder blanket, the bolting of structural materials is not a feasible solution.

Joining by fusion welding with or without filler metal will be used with the Tungsten Inert Gas welding (GTAW) and Electron Beam (EB) welding processes for the fabrication of structural parts of DEMO.

Thus, the weldability of RAFM steel needs to be studied in keeping with the application of the processes. The F82H TIG weldability will be studied in the case of various plate thicknesses, using matching filler metal.

The weldability of the Eurofer97 will be characterised taking into account both processes and several specimen shapes with butt joints in order to be compared to the F82H weldability. The weldments will follow radiographic controls and then metallographic examinations and microhardness measurements.

1999 ACTIVITIES

OPERATING CONDITIONS

During the year 1999, the experimental work has been dedicated to the TIG weldability of F82H using filler metal.

The test matrix has been settled in order to provide welded joints for both metallurgical weldability study and further characterization (mechanical testing...), knowing that only low quantities of F82H material were still available. The filler wire provided by JAERI has been chemically analysed.

The weldability samples have been designed as assemblies of plates. 3 plate thicknesses are taken into account : 5; 14 and 24 mm. The plates of 5 mm of thickness have been obtained by hot rolling of 25 mm plates at 1000°C. Samples made of 12%Cr martensitic steel have been considered first, for preliminary experiments.

Specific chamfer shapes have been designed for each assembly thickness. The characteristics of the assemblies are the following :

Material	Length (mm)	Width (mm)	Thickness (mm)	Chamfer	Quantities
Z12CN13 (12%Cr)	200	160	14	U shape	3
F82H	200	160	5	butt joint	4
F82H	200	160	5	V shape	2
F82H	200	160	14	U shape	7
F82H	200	160	24	U shape	7

In order to simulate the mechanical tightening of a large structural part during welding, the test assemblies are either clamped by an hydraulic press (up to 800 bar) or directly welded around upon a rigid support (a steel plate of 40 mm of thickness).

Thus, only very low transversal strains and displacements are allowed during the weldability experiments. However, the transversal strains are measured by means of engraved grids at the sample surfaces.

Each weldabilty test specimen has been instrumented with thermocouples in order to measure the cooling time between 800 and 500°C ($\Delta t_{800\text{-}500}$) and also in order to control the interpass temperature in the case of pre-heated specimen.

The 3 preliminary test assemblies have led to define suitable TIG welding conditions :

Voltage (V)	Current intensity (A)	Welding speed (cm/min)	Wire speed (m/min)	Wire scanning amplitude (mm)	Shielding gas (l/min)
10	100 - 230	4	0.5 - 1.5	4 - 11	10

Up to now 8 assemblies have been welded :

Material	Thickness (mm)	Pre-heating 200°C	Quantity	Number of paths	X-rays control	Control resuls
Z12CN13 (12%Cr)	14	no	3	6	yes	cavities, lack of penetration
F82H	14	no	3	6	yes	OK
F82H	14	yes	1	6	no	
F82H	24	yes	1	6	no	

RESULTS

The weldability study carried out on F82H 14 and 24 mm-thick plates has shown that the material may display internal flaws if the operating conditions are not optimised.

The possible flaws are essentially cavities, lack of fusion at the bottom of the chamfer or incomplete fusion at the interface with the chamfer.

These flaws have been eliminated by adjusting the operating conditions.

The major parameters to be considered are the filler wire speed, thus the quantity deposited in transversal section (mm^2), the associated intensity and the scan width (see figure 1).

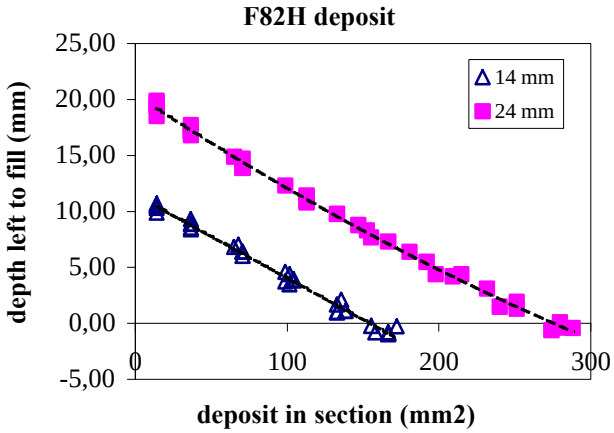

Figure 1

Selected operating conditions have led to the processing of sound weld as displayed by radiographic controls. Examples of defects and sound welds are displayed in figure 2.

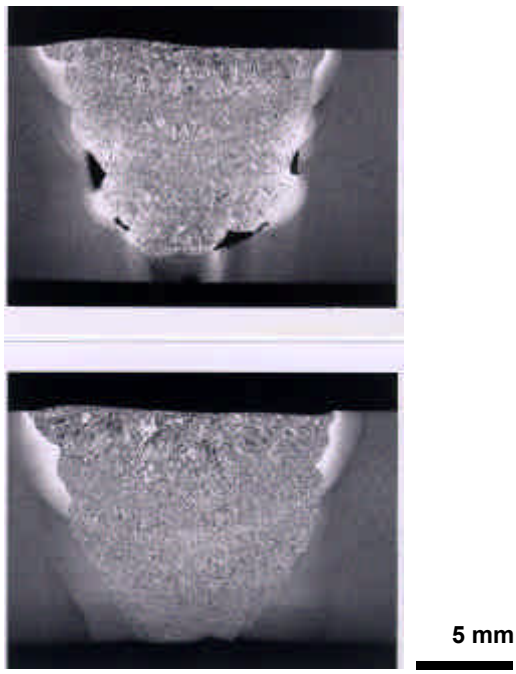

Figure 2 : Metallographic cross section of defects and sound welds, TIG welding of F82H 14 mm

The thermal instrumentation has shown so far that the $\Delta t_{800-500}$ can be adjusted in the range 10 to 30 s.

CONCLUSION

A F82H cut of 24 mm thick has been hot rolled down to 5 mm of thickness. F82H weldability test specimen of both 14 and 24 mm of thicknesses have been machined with a U-shape chamfer. The operating conditions have been roughly selected during preliminary welding experiments carried out on a 12%Cr steel of identical specimen shape, using the F82H filler wire with or without pre and/or post-heating. Several F82H 14-mm thick samples have been welded with matching filler metal following 6 paths and X-rayed. The radiographic controls display that the selected welding conditions lead to sound F82H welds.

The next step will concern the weldabity of Eurofer 97 using both GTAW and EB welding processes. The Eurofer97 has been delivered in January 2000.

TASK LEADER

André FONTES

DTA/DPSA/STA/LMS
CEA Saclay
91191 Gif-sur-Yvette Cedex

Tél. : 33 1 69 08 37 21
Fax : 33 1 69 08 75 97

E-mail : andre.fontes@cea.fr

SM 4-4

Task Title : DISSIMILAR WELDING, PWHT IMPROVEMENT

INTRODUCTION

Concerning the innermost parts of DEMO reactor, the low activation martensitic (LAM) steels and reduced-activation ferritic/martensitic (RAFM) steels are primary candidate alloys as first wall and breeder blanket structural materials. The blankets will have to be joined to secondary systems. These most probably will be built from austenitic SS 316LN. Thus, the weldability of RAFM steel with austenitic SS needs to be studied, by considering the possible use of filler metal, in keeping with the application of the processes. The task SM4.4 aims to deliver necessary data to produce dissimilar welds with PWHT as far as required.

1999 ACTIVITIES

During the year 1999, the experimental work has been dedicated to the EB welding of F82H/316LN joints.

A test matrix has been settled concerning the EB welding of F82H/316 transition weldments of 5 mm of thickness. Each assembly specimen was constituted by both 5-mm thick plates of F82H and 316LN of 160 mm of length and 45 mm of width, with a butt joint. Each plate has been hot rolled at 1000°C. In these conditions, the only low quantities of F82H still available allowed to weld 8 transition joints using previously defined operating conditions (SM4-4.1 1998).

High voltage (kV)	EB intensity (mA)	Welding speed (cm/min)	Position	Focus current (A)	Working distance (mm)
30	80	60	horizontal	2,16	160

First, a transition seam has been processed precisely at 0,3 mm from the joint axis, on the F82H side, in order to provide a welded zone nearly fully martensitic and to study the behaviour of such a microstructure when heat treated. Further, 7 transition joints have been processed following the identical idealistic conditions, *i.e.* with the seams centred on the joint axis. These 7 joints are now being heat treated. Then, they are planed to be sampled as an input for mechanical tests in the frame of the SM2-3 action.

Each assembly has been X-rayed. The radiographic controls have displayed that the selected welding conditions have led to sound F82H/316 transition welds.

CONCLUSION

F82H/316 EB welded joints of 5 mm of thickness have been processed according to previously defined operating conditions (SM4-4.1 1998). The welded joints have been X-rayed. The radiographic controls have shown that the weldments are free of flaws.

The next steps will concern the weldability of Eurofer97/316LN assemblies. The Eurofer97 has been delivered in January 2000.

TASK LEADER

André FONTES

DTA/CEREM/DPSA/STA/LMS
CEA Saclay
91191 Gif-sur-Yvette Cedex

Tél. : 33 1 69 08 37 21
Fax : 33 1 69 08 75 97

E-mail : andre.fontes@cea.fr

SM 4-5

Task Title : SOLID HIP PROCESS AND QUALIFICATION Development of martensitic steel / martensitic steel HIP joints with improved mechanical properties

INTRODUCTION

Diffusion welding is considered as a manufacturing technique for the fabrication of DEMO European blankets. The structural material is 9%Cr - 1%W martensitic steel. In the past years, good joint tensile properties have been easily achieved with F82H and Manet using hot isostatic pressing diffusion welding (HIP-DW). However the impact resistance of the joints is much more sensitive to joint defects and material heat treatment. Despite impact testing is not a design criteria for blanket conception, poor impact properties reveal that joints cannot be considered as equivalent to base metal.

It is thus necessary to optimise the HIP-DW process with the objective to obtain joints with properties as close as possible to the base metal. The main parameters of the process are the surface preparation technique and the HIP parameters (temperature, time and pressure).

The object of task SM4.5 is the optimisation of HIP parameters. Tensile and impact properties measurement are used as criteria. Full mechanical characterisation of the HIP-DW joints is made in the frame of task SM2.3.

1999 ACTIVITIES

GENERAL

The influence of the heat treatments of Eurofer (NET specifications 97/917) on the choice of HIP-DW parameters was studied from a theoretical point of view in order to define a priori a range of HIP parameters and post heat treatments. The HIP temperature should be high enough to obtain sound joints and low enough to avoid excessive grain growth. More precisely, it should be chosen between the specified normalisation temperature (950°C) and the temperature at which grain growth begins due to refractory carbides dissolution (~1050°C).

Sufficiently high cooling rates are achievable in industrial HIP devices to obtain a full martensitic transformation of the material from the austenitic phase. However, even if these conditions are respected, the HIP cycle may adversely affect base material properties. This is why it was chosen to apply systematically a complete post-HIP heat treatment consisting of a 2h normalisation at 950°C followed by water quench and tempering at 750°C. This post heat treatment allows restoring a fine grain size.

Previous studies on the diffusion welding of Manet and F82H steels showed that tensile properties similar to those of the base material were easily achieved. On the opposite, high impact properties were difficult to achieve.

This is because impact properties are very sensitive to the joint “cleanliness”, i.e. the presence of inclusions and oxide layers at the joint is extremely detrimental to the joint impact toughness.

These defect arise from improper surface preparation. More particularly, previous studies show that chemical pickling was not suitable.

Tensile and impact specimens were chosen as means of evaluation of joint properties. Many different impact specimen size and geometry have been used in the literature. The correlation between the overall results is very difficult even though normalisation factors have been proposed. In this study, the full size KCU specimens have been used because the larger notch compared to V notch specimens renders the result less sensitive to the joint position.

The surface preparation chosen in this study was based on polishing, degreasing and outgassing procedures.

EUROFER MECHANICAL PROPERTIES

A forged Eurofer bar dia. 107mm (heat 83344) was supplied from Böhler and drawn down to dia. 48mm bars. The material was then normalised at 950°C for 1h, quenched at 40°C/mn and tempered at 750°C for 30mn. The microstructure of the material is shown on figure 1.

Figure 1 : Bar diameter 48mm, quenched and tempered, longitudinal direction, x500

The mechanical properties of the material are given in table 1. They fulfil the requirements excepted hardness that is slightly too high.

Table 1 : Room temperature mechanical properties of quenched and tempered Eurofer bar dia. 48 mm

Property	Quenched and tempered Eurofer	NET specifications
Yield stress	523 / 521 MPa	-
0.2% Yield stress	612 / 611 MPa	> 500MPa
Maximum strength	720 / 717 MPa	> 600MPa
Total elongation	17 / 16%	> 15%
KCU	185 J/cm²	-
KCV	266 J/cm²	> 250J/cm²
Hardness	HV5=241	HV=200-240

DIFFUSION WELDING EXPERIMENTS

Samples 30mm high were cut from the bars for diffusion welding experiments. They were fitted into stainless steel canisters after having being submitted to the surface preparation procedure. The HIP cycle and post heat treatment were as shown on figure 2. The HIP pressure was 100MPa. The HIP temperature and time were varied.

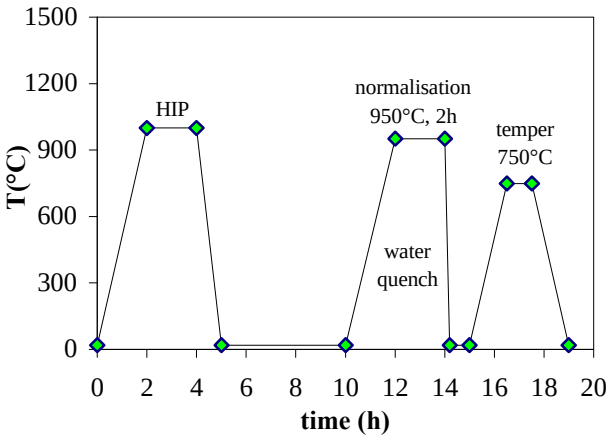

Figure 2 : HIP cycle and post heat treatment used for diffusion welding experiments (schematic)

After the whole process, tensile and KCU specimens were machined and tested at room temperature. The HIP conditions are given in table 2 and the results in table 3.

Table 2 : HIP diffusion welded samples

Sample	HIP temperature	HIP time	Temper duration	Remark
1	950°C	4h	1h	
2	1000°C	2h	1h	
3	1050°C	1h	1h	
4	1050°C	3h	2h	Sample no.3 re-HIPed
5	1100°C	2h	2h	Sample no. 2 re-HIPed

Samples 1-3 were manufactured in a first attempt. Tensile properties were excellent for all samples. The specifications were fulfilled in all cases.

The location of rupture was away from the joint in all cases. Unexpectedly, the hardness of the material increased with the HIP temperature despite the same post heat treatment was applied. It exceeds the specifications for specimen 3, and to a lesser extent, for specimen 2.

On the opposite, the impact properties were very low. As the joint microstructure did not show significant pollution, the low impact properties were attributed to a too short HIP time.

Table 3 : Mechanical properties of diffusion welded joints

Sample		1	2	3	4	5
Yield stress	MPa	471	549	710	467	439
0.2% Yield stress	MPa	510	605	769	513	488
Maximum strength	MPa	638	710	852	665	634
Total elongation	%	21	16.5	17.5	17.5	19
KCU	J/cm²	18	16	60	245	205
Hardness	HV5	216	243	286	211	189

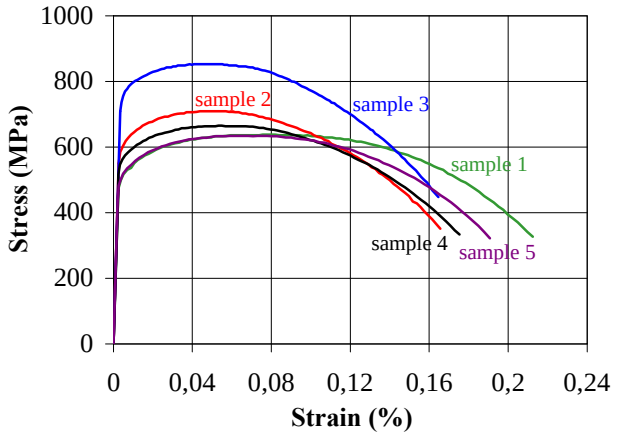

Figure 3 : Conventional stress-strain tensile curves for HIP DW joints.

Unbroken specimens of experiments 2 and 3 were then re-HIPed as shown in table 2.

The temper was prolonged to 2h in order to avoid excessive hardness. Again, the tensile properties were very good, except the yield stress of sample 5, which is lower than the required value (as well as hardness). Excellent high impact resistance was obtained.

For sample 4 it exceeds the base material value, the latter being harder due to a too short temper treatment.

CONCLUSION

The diffusion welding of Eurofer 97 steel was studied. Vacuum outgassing was used as surface preparation technique. Very good tensile properties are achieved even with short HIP times and low temperature. The impact resistance of the joints is very good only for high HIP temperature and long HIP time. Normalisation at 950°C for 2h followed by water quench is efficient to obtain a fine grain size. The mechanical properties of the joints strongly depend on the post-treatment. Tempering for more than 1h at 750°C is necessary to achieve reasonable hardness, more particularly when the HIP temperature is high.

The best conditions were HIP at 1050°C, 1000bars for 3h, cooling within 1h to room temperature, normalisation at 950°C, 2h and then tempering at 750°C, 2h.

The application of HIP diffusion welding for the fabrication of fusion components requires further work related to the influence of temperature and time parameters (HIP cooling rate, N and T parameters) because components are massive and water quench may not be acceptable due to thermal stresses and dimensional accuracy requirements.

Furthermore, it is necessary to investigate the creep and fatigue properties of the joints and how they vary with temperature.

REPORTS AND PUBLICATIONS

[1] L. Bedel, E. Rigal “Mechanical properties of a RAFM/RAFM HIP joint”, CEA report Note technique DEM 99/87 (Task SM2.3), 10 dec. 1999

[1] E. Rigal, L. Bedel “Development of martensitic steel – martensitic steel HIP joints with improved mechanical properties”, CEA report Note technique DEM 91/99 (Task SM4.5), 16 dec. 1999

TASK LEADER

Emmanuel RIGAL

DTA/DEM/SGM
CEA Grenoble
17, rue des martyrs
38054 Grenoble Cedex 9

Tél. : 33 4 76 88 97 22
Fax : 33 4 76 88 95 38

E-mail : rigal@chartreuse.cea.fr

SM 4-5.1

Task Title : INVESTIGATION ON COMMERCIAL FILLER METAL FOR GTAW OF LAM STEELS

INTRODUCTION

The recently developed low activation martensitic (LAM) steels are the most viable as structural materials of DEMO reactor first wall. LAM steels compositions are based on replacement of molybdenum by tungsten in conventional CrMo heat resistant steel.

Prior to select one of these alloys, the evaluation of its weldability is required. The task SM 4-5 of the SM (Structural Material) Fusion program has been initiated in 1998. The aim of this task was to provide filler metal as an input for TIG weldability tasks planned for the next Structural Material program (1999-2002). Informations concerning filler metal for the TIG welding of low activation martensitic steel has been gathered focusing on F82H steel proposed by JAERI. Further, commercial product suppliers have been contacted with a view to select suitable filler wire or electrode. The task report has been written by the end of 1999.

1999 ACTIVITIES

The report content is globally the following :

A literature review concerning the filler metal for RAFM steels has been carried out over the year 1998. It has shown that only low quantities of data are available at the moment concerning this type of material. Some complementary data come from the literature about conventional 9%Cr steels. The great majority of the papers that have been selected come from Japanese research units. They have shown that matching filler metal of optimised composition can be used to process sound welds by using the TIG process. In particular, filler metal specified for JLF-1 and F82H RAFM steels respectively can lead to weld metals of better mechanical characteristics than the base metal. Both the tantalum and carbon content have to be particularly optimised as regards the tensile strength and the toughness.

In parallel, several filler metal suppliers or manufacturers have been contacted internationally with a view to supply some commercial filler product adapted to the welding of RAFM steels. The enquiry has shown that no specific commercial product was available at the moment. However some industrial development was in progress. However, two F82H filler wires have been supplied from JAERI in order to carry out further weldability tests at CEA in the frame of the Fusion Structural Material Program over the period 1999-2002.

CONCLUSIONS

The 1999 progress consisted in issuing the last task report. The task SM4-5.1 is now completed. The results and conclusions will input the tasks SM4-3 and SM4-4 of the 1999-2002 programme.

REFERENCES

[1] A. Fontes, Filler metal for the TIG welding of 8Cr-2W RAFM steel (mod. F82H), CEA report n° DPSA/STA/LMS/98-RT3782 rev.0, March 2000

TASK LEADER

André FONTES

DTA/CEREM/DPSA/STA/LMS
CEA Saclay
91191 Gif-sur-Yvette Cedex

Tél. : 33 1 69 08 37 21
Fax : 33 1 69 08 75 97

E-mail : andre.fontes@cea.fr

SM 5-1

Task Title : RULES FOR DESIGN AND INSPECTION DESIGN CODE ASSESSMENT AND DEVELOPMENT

INTRODUCTION

The main objective of this task is to write the Appendix A, " Materials Data and Analyses" for interim design rules of ITER Test Blanket Modules and DEMO components (DISDC). The work to be done is similar to the one done for ITER, where designers use IISDC (ITER Interim Structural Design Rules) and IMPH (Iter Materials Properties Handbook) as guidelines for design of ITER components and systems.

ITER documents do not include rules and data for RAFM (Reduced Activation Ferritic/Martensitic) steels, i.e. the major structural materials used for the ITER Test Modules (ITM) and DEMO. The behaviour of RAFM steels is very different from those of the austenitic steels employed in ITER and hence ITER rules cannot be fully extended to them. In addition, the operating conditions of ITM and DEMO components differ from those of ITER (higher service temperature, higher irradiation doses) provoking damage mechanisms not considered in IISDC.

However, in order to write the Appendix A for RAFM steels one needs code qualified materials data. That work is done under task SM 5.4, where materials properties data are collected. However, the association in charge of SM 5.4 has since withdrawn from the fusion program. In addition, RAFM steels are new and only a limited materials properties data are available so far.

Despite the above difficulties, SM 5.1 has fulfilled its 1999 goals: a) definition of general rules for RAFM steels, b) definition of design rules for the conventional 9Cr steel.

1999 ACTIVITIES

PART 1: DISDC/A. GEN: GENERAL

Appendix A3 of RCC-MR is used as a model for organizing the material design properties in Appendix A of the ITER Interim Structural Design Criteria (IISDC). The same procedures are used here for DEMO Interim Structural Design Criteria (DISDC).

Three materials are retained at this stage. The first is a commercial grade developed for the steam generators of Fast Breeder Reactors (Mod 9Cr-1Mo). The second is an IEA low activation steel produced in Japan (F82H). The third is a Reduced Activation Ferritic/martensitic steel produced in Europe (Eurofer).

Appendix A begins with the section A.GEN, which contains the definitions of the physical and mechanical properties used in the ISDC together with the formulae used in calculating the various design limits provided in subsequent sections of Appendix A. Each subsequent section of this Appendix contains design data for materials defined in the reference specifications and indicated by numbers and a letter (e.g, S: structural material, S1: Type 316 L(N)-IG stainless steel, S18: Mod. 9Cr1Mo (Z10 CDVNB 9.1), B: bolting, etc.).

The low activation grades of 9Cr steels do not have a reference number in the RCC-MR. In this report F82H steel is identified by a letter F (S18F) and Eurofer steel by a letter E (S18E). Furthermore, different classes of materials are being discussed for DEMO plasma facing components and vacuum vessel. The methodology and organization to be used for each class of material is to be approved case by case, especially for those materials exhibiting different stress-strain, fatigue hardening, and creep behaviours and irradiation effects.

Presently, the interim DISDC A. GEN report covers the following topics:

- A.GEN.1 How to use Appendix A
- A.GEN.2 Determination of properties
- A.GEN.2.1 Introduction
- A.GEN.2.2 Physical properties
- A.GEN.2.3 Tensile strength properties
  - A.GEN.2.3.1 Monotonic stress-strain curves
  - A.GEN.2.3.2 Yield strength at 0.2% offset: (S_y, $S_{y,\,min}$)
  - A.GEN.2.3.3 Ultimate tensile strength (S_u, $S_{u,\,min}$)
  - A.GEN.2.3.4 Uniform elongation (ε_u, $\varepsilon_{u,\,min}$)
  - A.GEN.2.3.5 True Strain at Rupture (ε_{tr}, $\varepsilon_{tr,\,min}$)
- A.GEN.2.4 Determination of the negligible creep laws
  - A.GEN.2.4.1 Determination if nonlinear (finite deformation) analysis is needed
  - A.GEN.2.4.2 Determination of the negligible swelling curve
  - A.GEN.2.4.3 Determination of the negligible thermal creep curve
- A.GEN.2.5 Determination of the values of S_m
  - A.GEN.2.5.1 Determination of the bending shape factor $K_{eff,rect}$
- A.GEN.2.6 Determination of S_e
- A.GEN.2.7 Determination of S_d
- A.GEN.2.8 Fatigue curves for unirradiated and irradiated materials

A.GEN.2.8.1 Continuous Fatigue
A.GEN.2.8.2 Creep - Fatigue

A.GEN.2.9 Cyclic curves

A.GEN.2.9.1 Determination of K_ε
A.GEN.2.9.2 Determination of K_ν

GEN.2.10 Fracture toughness
GEN.2.11 Determination of ε_{tr} Rappels des principaux résultats
GEN.2.12 Determination of the swelling law

PART 2 : APPENDIX A: A3S18: MODIFIED 9CR-1MO STEEL

Contents of this report are summarised below. It is important to note that this report goes beyond the present RCC-MR documents and deals with properties yet to be added to future editions of RCC-MR.

A3.S18.1 Introduction
A3.S18.1.1 Compositions
A3.S18.1.2 Quality Safe Guarding Data

A3.S18.2 Physical Properties
A3.S18.2.1 Coefficient of Thermal Expansion : α_m and α_i
A3.S18.2.2 Young's Modulus : E
A3.S18.2.3 POISSON's Ratio : ν
A3.S18.2.4 Density : ρ
A3.S18.2.5 Specific Heat, Thermal Conductivity, Thermal Diffusivity : C_p, λ, and a
A3.S18.2.6 Electrical Resistivity : Ω
A3.S18.2.7 Magnetic Properties

A3.S18.3 Tensile Strength Properties
A3.S18.3.1 Minimum and average yield strength at 0.2% offset : S_y
A3.S18.3.2 Minimum and average ultimate tensile strength : S_u
A3.S18.3.3 Minimum uniform elongation : ε_u
A3.S18.3.4 Minimum true strain at rupture: ε_{tr}
A3.S18.3.5 Minimum time to stress rupture : t_r
A3.S18.3.6 Minimum creep ductility : ε_c
A3.S18.3.7 Minimum true strain at rupture for creep : ε_{ctr}

A3.S18.4 Curves for tests on creep and swelling
A3.S18.4.1 Negligible thermal creep curve
A3.S18.4.2 Swelling curve ϕt_{s1} for the test to determine if nonlinear analysis is needed
A3.S18.4.3 Negligible swelling curve
A3.S18.4.4 Irradiation induced creep
A3.S18.4.5 Irradiation induced creep curve (ϕt_{s1}) for the test to determine if nonlinear analysis is needed
A3.S18.4.6 Negligible irradiation induced creep curve

A3.S18.5 Analysis Data
A3.S18.5.1 Values of S_m
A3.S18.5.2 Values of S_t
A3.S18.5.3 Values of S_r
A3.S18.5.4 Fatigue curves at saturation
A3.S18.5.5 Isochronus and creep deformation curves
A3.S18.5.6 Values of S_{Rh} and S_{Rc}
A3.S18.5.7 Symetrisation factor, K_s
A3.S18.5.8 Creep-Fatigue interaction diagram
A3.S18.5.9 Cyclic curves, values of K_ε and K_ν

A3.S18.6 Additional Analyses
A3.S18.6.1 Monotonic hardening curve in tension
A3.S18.6.2 Bilinear curves
A3.S18.6.3 Creep deformation curve
A3.S18.6.4 Fatigue curves
A3.S18.6.5 Maximum allowable deformation: D_{max}

CONCLUSIONS

Despite lack of materials properties data on RAFM steels, the work performed in 1999 has achieved its projected goals. Two interim reports are issued:

- Appendix A. General Rules
- Appendix A. Rules for a conventional 9Cr steel

That allow designers to proceed with preliminary calculations.

REPORTS AND PUBLICATIONS

DEMO Interim Structural Design Criteria, DISDC:

1. Appendix A Material Design Limit Data, AGEN: General, Interim SM 5.1 & 5.4 Reports

2. Appendix A Material Design Limit Data, A3.S18 Modified 9Cr-1Mo Steel, Interim SM 5.1 & 5.4 Reports

TASK LEADER

Farhad TAVASSOLI

DTA/DECM
CEA Saclay
91191 Gif-sur-Yvette Cedex

Tél. : 33 1 69 08 60 21
Fax : 33 1 69 08 71 31

E-mail : tavassoli@cea.fr

SM 5-2

Task Title : FRACTURE MECHANICS CONCEPT

INTRODUCTION

Ferritic / martensitic steels have the characteristics of a ductile-brittle- transition-behaviour with a brittle fracture in the lower temperature regime. Fast crack propagation in the brittle regime depends on the loading condition, the stress state, the strain rate, the material, geometry and also the environment.

The 9 Cr 1 Mo materials exhibit less cyclic strain - hardening than the austenitic steels. This could have a strong effect on crack initiation and propagation under fatigue loading.

In fusion reactor components, rupture conditions can be achieved under large thermal shocks. A particular simplified rule must be developed to take into account such loading by calculations relying only on elastic stress and handbook solutions for limit load and KI.

This complex situation needs concern in each project especially for those of RAFM steels. The development of a concept for fracture mechanics needs significant effort and time. The concept must be developed with theoretical and experimental aspects.

1999 ACTIVITIES

EXPERIMENTAL DETERMINATION OF d DISTANCE WITH CT SPECIMENS OF 9% 1 CR STEEL

The results achieved correspond to the step 5.2.1 of the task. The σd method is proposed in the RCC-MR and ISDC. This method consist in calculating the real stresses and strains at a certain distance d, a material dependant characteristic, close to the diameter of a grain of the material. The stress or strain is then used with the usual design fatigue curve to define the number of cycles necessary to induce the initiation of the crack.

Inversely, the determination of the material distance d is to be made with experimental data concerning initiation conditions and by optimisation calculations (4), analysing the experimental scattering.

FATIGUE TESTS

These tests were performed at CEA Saclay under load controlled conditions with R ratio (minimum load / maximum load) = 0.1. The test temperature is 550°C and the specimen are CT (compact tension) ones. The dimensions are according the ASTM standard (ASTM E 399-90) : B = 19 mm, a = 27,5 mm (initial crack), W = 50 mm, R < 0.1 mm (notch end radius of the machined crack).

The number of cycles at initiation is obtained by an electric potential drop method. The evolution of this recording during a test follows the general shape illustrated on the following drawing :

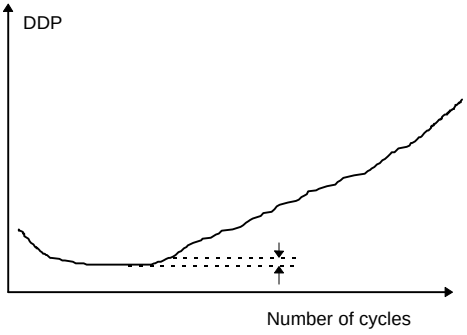

First the electric potential drop decreases, reaches a minimum and then increases.

The length of the final crack is measured after breaking the specimen in two parts. This quantity is used to draw a calibration curve that gives the evolution of crack length versus electric potential drop measured at that time. In this curve, the increment of electric potential drop is the variation between the minimum value and the final one.

Using this curve, initiation is defined here as an existing crack of 0,1mm. It corresponds to a variation of electric potential drop of 8 mV.

Finally, the following table contains all the experimental results obtained from the 9 tests performed. This results are necessary to adjust the « d » parameter for the σd method.
9 tests are performed.

Specimens	ΔF (kN)	N (0.1 mm)
2	7.4	560
3	7.4	2000
4	6.3	1736
6	8.1	1061
7	7	1108
9	4.5	5543
11	5.3	201
12	5.7	1951
13	6.1	1561

ΔF refers to the load variation and N refers to the number of cycles of initiation.

MATERIAL CHARACTERISTICS

To define the d value, the material characteristics are taken from a document established for the design of the European Fast Reactor (EFR) (5).

In particular the cyclic curve and fatigue curve are given at 550 °C.

- Young modulus : E = 163 000 Mpa

- Cyclic curve :

$$\Delta e = \frac{2(1+n)}{3}\frac{100\Delta s}{E} + \left(\frac{\Delta s}{Kp}\right)^{\frac{1}{mp}}$$

Kp=587.1

mp=0.0984

- Design fatigue curve, defined by the following points :

Δε(%)	N
2.78	400
1.53	800
0.86	$2\ 10^3$
0.643	$4\ 10^3$
0.519	8.10^3
0.421	$2\ 10^4$
0.362	$4\ 10^4$
0.318	10^5
0.292	$2\ 10^5$
0.270	$4\ 10^5$
0.248	10^6
0.218	$5\ 10^6$
0.208	10^7

For the GA plate we determine that the size of the grain of the material has an average value of 10µm.

EVALUATION OF FATIGUE

The variation of ΔK is a key parameter for the application of σd method. It characterizes the effect of loading during one cycle.

For usual CT specimen, handbook solution for this parameter are available in the ASTM E 399 - 81 standards. The formula used is :

$$K_I = \frac{F}{B\sqrt{W}} f\left(\frac{a}{W}\right)$$

where F is the applied load, B is the thickness, W is the width, a is the crack depth.

$$f(x) := (2+x)\cdot\frac{0.886 + 4.64x - 13.32x^2 + 14.72x^3 - 5.6x^4}{(1-x)^{1.5}}$$

with x=a/W

Once ΔK variation is calculated, the next step is to evaluate the elastic stress at a distance d of the crack tip. This value is labeled σ_{de}.

Creager (6) found simplified expressions giving the different stress components in the crack tip region as a functions of distance d, stress intensity factor, crack tip radius ρ, and θ angle defined according the following drawing :

In the case of plane crack and pure mode I, these expressions are :

$$\sigma_{xx} = \frac{K_1}{\sqrt{2\pi r}}\left[\cos\frac{\theta}{2}\left(1-\sin\frac{\theta}{2}\sin\frac{3\theta}{2}\right) - \frac{\rho}{2r}\cos\frac{3\theta}{2}\right],$$

$$\sigma_{yy} = \frac{K_1}{\sqrt{2\pi r}}\left[\cos\frac{\theta}{2}\left(1+\sin\frac{\theta}{2}\sin\frac{3\theta}{2}\right) + \frac{\rho}{2r}\cos\frac{3\theta}{2}\right]$$

$$\sigma_{xy} = \frac{K_1}{\sqrt{2\pi r}}\left[\cos\frac{\theta}{2}\sin\frac{\theta}{2}\cos\frac{3\theta}{2} - \frac{\rho}{2r}\sin\frac{3\theta}{2}\right]$$

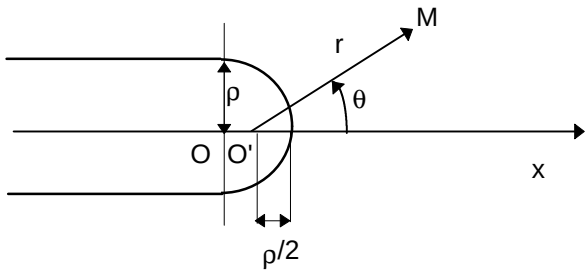

Note that r = d + ρ/2

According to A16 guide (7), it is proposed to choose the largest principal stress to define the equivalent stress. One can find :

$$\sigma_1 = \frac{K_1}{\sqrt{2\pi r}}\left[1+\frac{\rho}{2r}\right]$$

One can notice that for ρ values approaching zero, the ratio $\sigma_1 \Big/ \frac{K_1}{\sqrt{2\pi d}}$ is larger than one.

Therefore, for a small non null radius, the estimated stress is larger than the one calculated for a ρ = 0 crack.

In order to avoid this abnormal situation where this ratio is larger than one, it is proposed here to use for a very small ρ value the expression corresponding to ρ = 0 :

$$\sigma_{de} = \frac{\Delta K}{\sqrt{2\pi d}}.$$

The elastoplastic strain variation $\Delta\varepsilon_{elpl}$ is calculated with the ΔK variation and taking into account the cyclic plastic behaviour. This last effect is characterised by the material cyclic curve.

According to σd rule, $\Delta\varepsilon_{elpl}$ is the sum of 4 terms : $\Delta\varepsilon_1$, $\Delta\varepsilon_2$, $\Delta\varepsilon_3$ and $\Delta\varepsilon_4$.

- $\Delta\varepsilon_1$is the elastic strain variation obtained by the formula :

$$\Delta\varepsilon_1 = \frac{2(1+\nu)\Delta\sigma}{3E}$$

- Δε2 is the plastic increment due to the primary stress variation,

- Δε3 is the increment due to plastic behaviour and is evaluated according to Neuber's rule and the material cyclic curve,

- Δε4 is the plastic increment due to the triaxiality of stresses:

$$\Delta\varepsilon_4=(K_v-1).\Delta\varepsilon_1$$

The K_v magnification factor is calculated according the RCC.MR (A 3.593) method applied to the cyclic curve.

The different step are illustrated graphically on the following drawing.

At the end of calculation the value $\Delta\varepsilon^*$ is defined. It corresponds to the $\Delta\sigma^*_d$ that can be read on the cyclic curve. Knowing the strain variation, it is easy to calculate the fatigue usage factor V.

$$V = \frac{N\exp}{N(\Delta\varepsilon^*)}$$

where N ($\Delta\varepsilon^*$) is the number of cycles defined by the best fit fatigue curve for $\Delta\varepsilon^*$ value.

Initiation is assumed when V reaches unity.

DETERMINATION OF DISTANCE d

The problem is here to reduce the scattering of the calculated points of coordinates ($\Delta\varepsilon^*$, N_{exp}) by comparison to the fatigue curve. The variation of a correlation paramater is evaluated according different d values.

The "standard deviation" is a measurement of the scattering of the points. It has the following expression :

$$\frac{1}{k\max}\left[\sum_k\left[\ln(\Delta\varepsilon\_fat(N\exp_k)) - \ln(\Delta\varepsilon^*_k)\right]^2\right]^{0.5}$$

Δε_fat() represent the best fit fatigue curve
$\Delta\varepsilon^*_k$ is the strain variation calculated according σ_d method.

The optimal d distance is thus obtained when the standard deviation is minimal.

The appendix gives the details of the calculation sheets obtained with Mathcad software of Mathsoft.

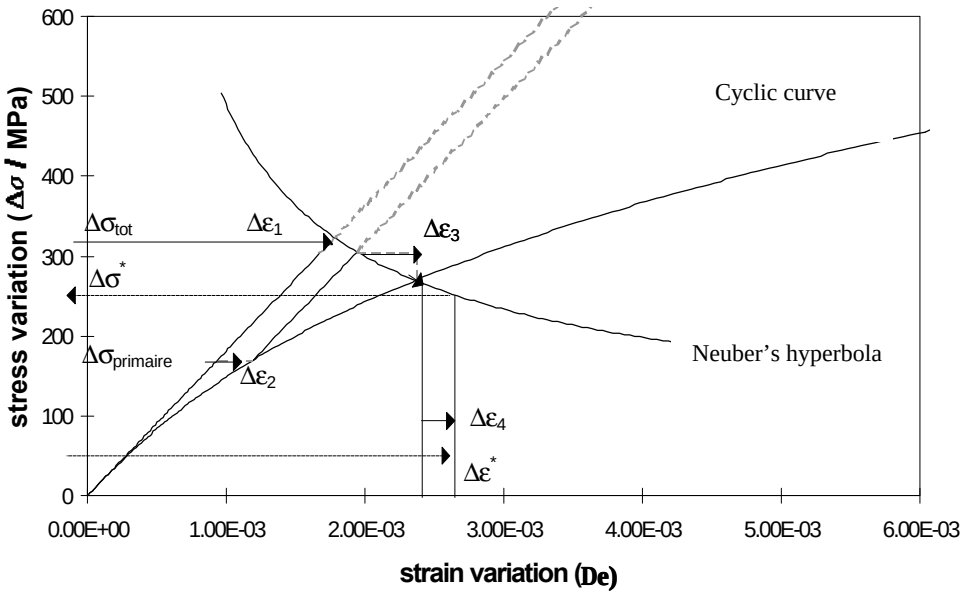

Depending on the 2 different ρ values (0 or 0.1 mm) in the Creager's formula, two characteristic distances are available :

ρ (mm)	0.1	0
d (µm)	36	38

The difference between the 2 values is rather small. The prudent value proposed here is d = 36 µm. Worth nothing is that this value is equal to 3 times the grain size of the material.

CONCLUSIONS

σ_d method is available now to evaluate fatigue initiation of crack in structures containing cracks-like defect and made of 9 Cr 1 Mo steel.

Nine experimental tests are presented. The data are obtained with CT specimens made of 9 Cr 1Mo steel. The material characteristics necessary to develop this method are gathered.

These tests were analysed according to σ_d rules proposed for evaluation of initiation of incracked components. The distance d necessary to apply σ_d rule is calculated with an optimisation algorithm evaluating the scatterband of calculated points versus the best fit fatigue curve.

A value of **36 µm** is proposed for this material at 550°C temperature.

Next step in the validation of this method could concern an other situation, close to the areas interesting fusion cases : cyclic stresses produced by thermal fluctuation for example.

REFERERENCES

[1] A.S.M.E.
American Society of Mechanical Engineers, Boiler and Pressure Vessel code, 1990

[2] RCC-MR
Règles de conception et de construction des matériels mécaniques des îlots nucléaires RNR ; AFCEN - Edition mai 1993.

[3] Structural design criteria for ITER.
Transaction of 13th SMIRT Conference, Volume I, page 551, 1995, Porto Alegre, RS, Brazil

[4] Mécanique de la rupture
Détermination de la distance caractéristique pour quelques aciers austénitiques, Méthode de la moindre dispersion, Lucien LAIARINANDRASANA
Rapport DMT/97-077

[5] Compendium of DCRD recommendation for EFR
European Fast Reactor Associates, RIOU - Fifth edition up to October 98

[6] The elastic stress field near tip of blunt crack
Thesis Lehigh University
M. CREAGER - 1966

[7] A16 - Guide pour l'analyse de la nocivité des défauts et la fuite avant rupture
B. DRUBAY, S. CHAPULIOT, M.H. LACIRE
Rapport DMT/98-063/A

REPORTS AND PUBLICATIONS

MATHERON P. and MOULIN D. - "Evaluation for the application of mechanical design codes for fusion reactor Fracture mechanics concept « sigma d » method - Determination of the distance « d » for the 9 Cr 1 Mo ", CEA Saclay, France, Report SEMT/LISN/RT/99-107/A

TASK LEADER

Didier MOULIN

DRN/DMT/SEMT/LISN
CEA Saclay
91191 Gif-sur-Yvette Cedex

Tél. : 33 1 69 08 66 54
Fax : 33 1 69 08 87 84

E-mail : didier.moulin@cea.fr

SM 5-4

Task Title : RULES FOR DESIGN AND INSPECTION DATA COLLECTION AND DATA BASE MAINTENANCE

INTRODUCTION

A limited database is available on RAFM steel mainly consisting of F82H data. This is, however, insufficient for design code generation.

There are also some results available on laboratory heats, but these are of little use considering their mass, compositions and lack of important test parameters.

The amount of data on F82H has grown during 1999, but EUROFER 97 and 2000 data are yet to be produced. As a result, the body of RAFM data will not be available before 2005.

1999 ACTIVITIES

Initially, JRC-ISPRA was in charge of this task. In 1999, CEA was allocated a small fund only to supervise the work. Unfortunately, JRC-ISPRA withdrew from this task, and practically discontinued their contribution.

CEA has had, therefore, to rely on its own internal resources to proceed.

Materials properties data for conventional 9Cr steel grade and some for low activation grade have been collected.

An example of materials property data collected for the Mod. 9Cr-1Mo steel is presented in figure 1. In this figure the data collected are used to propose a tentative lower bound for creep ductility.

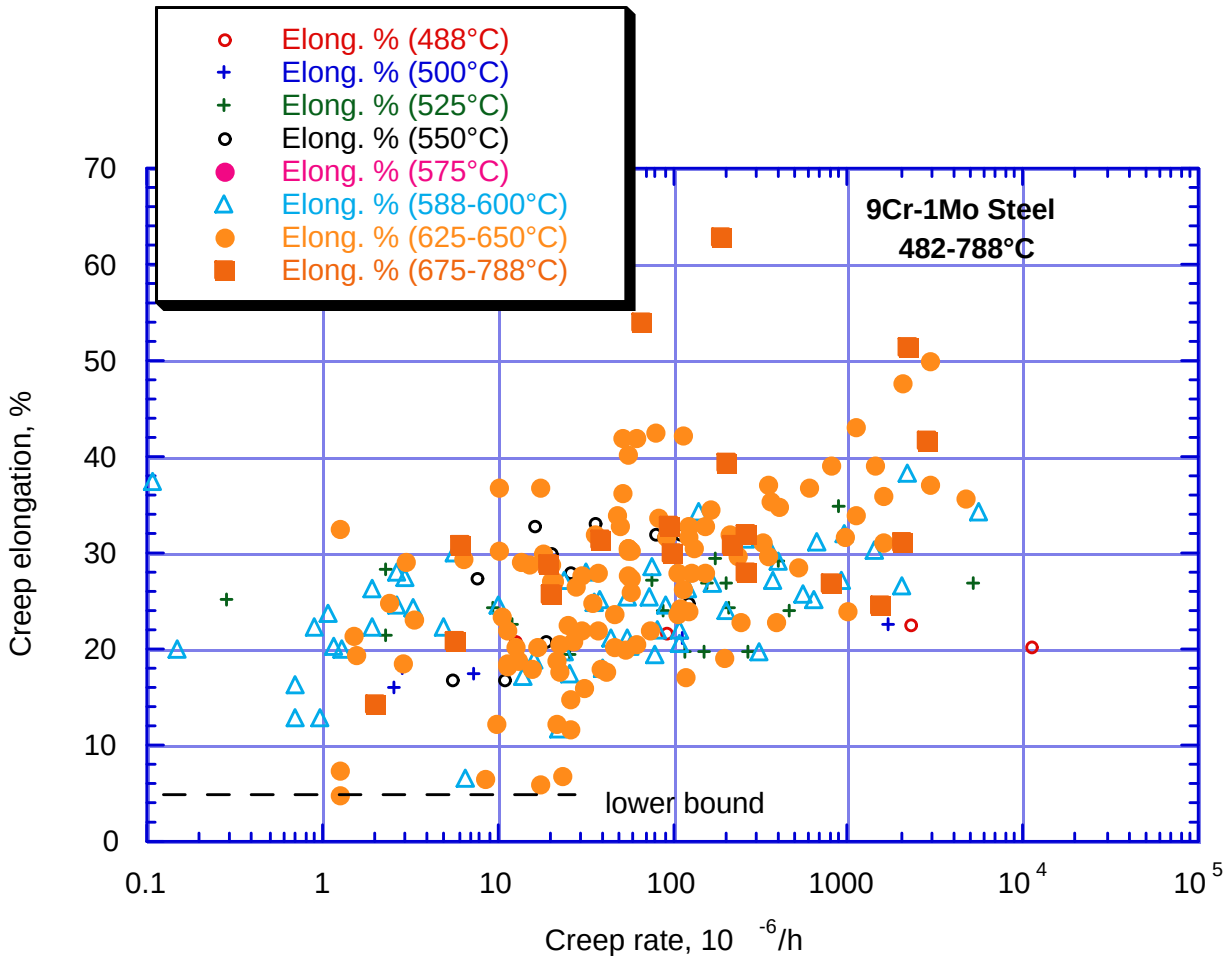

Figure 1 : Experimental data used to derive minimum creep ductility

CONCLUSIONS

Despite the withdrawal of principal investigator (JRC ISPRA) and small funding allocated to CEA, some progress

has been achieved. Materials properties data have been provided on conventional 9Cr steel for use in definition of design rules (SM 5.4)

REPORTS AND PUBLICATIONS

DEMO Interim Structural Design Criteria, DISDC:

1. Appendix A Material Design Limit Data, AGEN: General, Interim SM 5.1 & 5.4 Reports

2. Appendix A Material Design Limit Data, A3.S18 Modified 9Cr-1Mo Steel, Interim SM 5.1 & 5.4 Reports

TASK LEADER

Farhad TAVASSOLI

DTA/DECM
CEA Saclay
91191 Gif-sur-Yvette Cedex

Tél. : 33 1 69 08 60 21
Fax : 33 1 69 08 71 31

E-mail : tavassoli@cea.fr

SM 5-7

Task Title : SMALL SIZE SPECIMEN TECHNOLOGY

INTRODUCTION

Using testing volumes in neutron irradiation devices such as: ion beams, spallation-, 14 MeV neutron sources and material test reactors, requires large fractions of R&D budgets. There is a continuous push for irradiation of smaller test specimens to reduce exposure expenditure. With decreasing volume the representativity of the specimens for bulk properties might decrease. This is certainly the case for shape sensitive samples such as those with artificial defects (toughness and crack propagation testing), and discontinuities; cyclindrical fatigue specimens with weldments also cause problems.

The decrease in size results in non-standard specimens, usually with a near standard shape but a considerably smaller scale. The validity of non-standard specimens must be proven.

The development of smaller specimen is now aiming for sizes benificial for neutron sources. The results will also be valuable for other irradiation programmes.

1999 ACTIVITIES

The year 1999 was devoted to the feasibility of small tensile specimen testing. Two sizes of specimen were considered. The largest one has a section of 2 x 1 mm and the smallest one has a section of 1 x 0.4 mm (Figure 1).

For the largest specimen, it appears that no special device in needed to test this type of specimen. For the smallest, a special device has been designed in order to prevent the bending of the specimen during the preparation of the tests. The test for the qualification of the tests rigs are under progress and will be achieved in march 2000.

The second half of 99 has been devoted to study the possibilities of reduction of the fracture toughness specimens. Pre-cracked Charpy specimens and small cracked round bars tests results were analysed. Pre-cracked Charpy specimens give fracture toughness evaluation close to CT specimens measurements. Small cracked round bars results over-estimate the fracture toughness derived from CT testing.

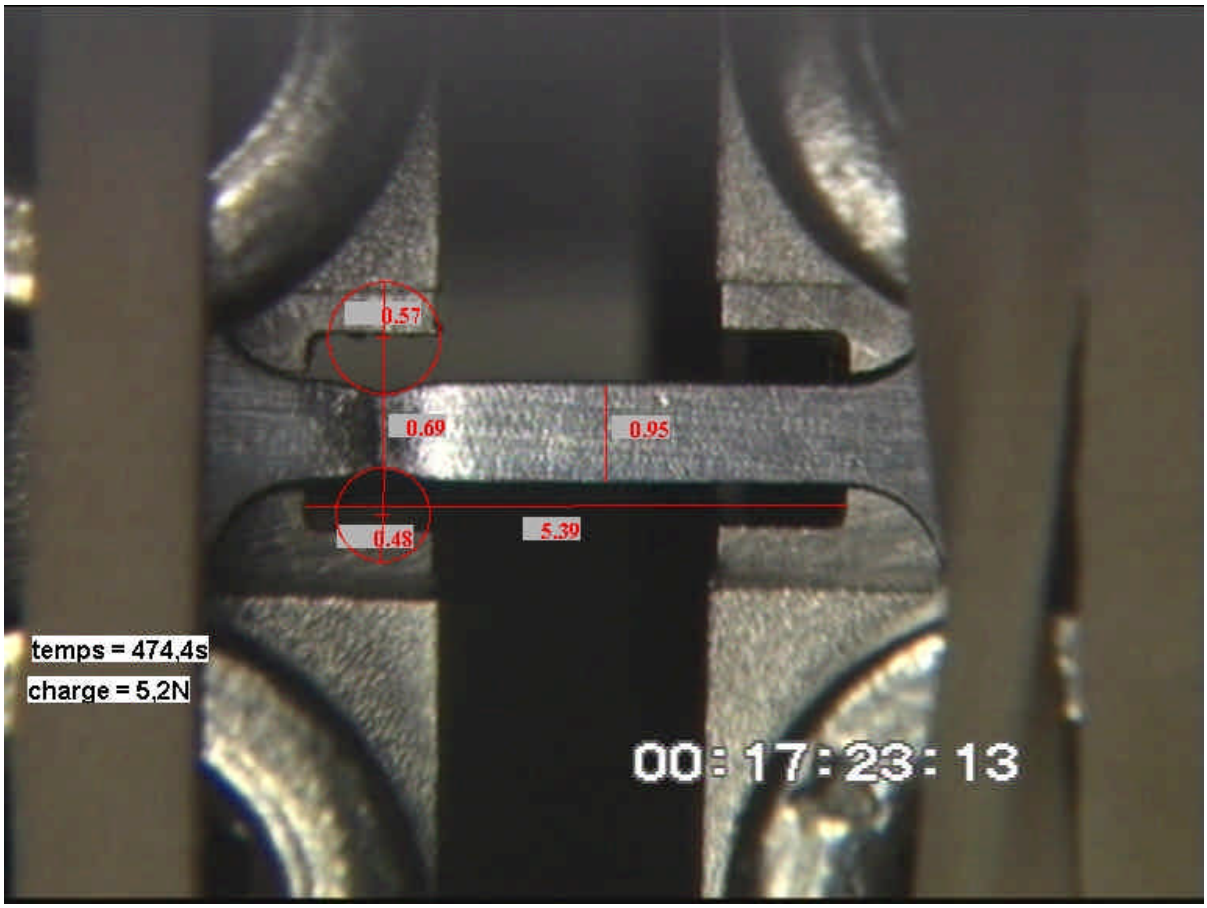

Figure 1 : Necking during the micro-tensile specimen testing
The specimen size is 5 by 1 by 0.4 mm at the beginning of the test. Measures are given in mm on the figure

REFERENCES

[1] “SM5.7 : SMALL SIZE SPECIMEN TECHNOLOGY. 1999 PROGRESS REPORT”, B. Marini, P. Lamagnère, P. Wident, NT SRMA, to be issued

TASK LEADER

B. MARINI

DTA/CEREM/DECM/SRMA
CEA Saclay
91191 Gif-sur-Yvette Cedex

Tél. : 33 1 69 08 85 99
Fax : 33 1 69 08 85 99

E-mail : bernard.marini@cea.fr

SM 6-1

Task Title : DEVELOPMENT OF HIGH DOSE HIGH TEMPERATURE LOW TEMPERATURE, HIGH DOSE IRRADIATION TEST WITH ISTC

INTRODUCTION

In fusion reactor blankets damage levels over 100 dpa are anticipated. Present day beam devices and Material Test Reactors cannot produce such displacement levels in a reasonable time. Liquid Metal cooled Fast Breeder Reactors are, in contrast, capable of providing high dose levels in acceptable times, but at temperatures 45O°C and above. While such temperatures are pertinent to most fusion components, there are segments that would be exposed to lower temperatures. As a result, the effects of high dose neutron irradiation have to be investigated at both low and high temperatures.

1999 ACTIVITIES

This task has two small objectives for the year ending Dec. 99. One of these is to contribute to the general discussion of an action carried out by FZK (irradiation in RF reactors at high temperature). The other one is to maintain contact with the progress of ELXIR irradiation experiment in Phénix (irradiation at low temperature). Both of these objectives have been followed during the second half.

The main RF irradiation experiment planning is proceeding and will be implemented next year. Also in the frame of the French material program, contacts (including a meeting in Russia) have taken place with RIAR staff of Dimitrovgrad Center. It has been concluded that irradiation of a material capsule in BOR 60 reactor with the following main parameters is feasible:

- Material capsule with a very low longitudinal temperature gradient and loading / unloading capability at intermediate exposure levels. An example of possible specimen loading is: 12 pressurized tubes, 66 tensile specimens of different sizes, and 80 subsize Charpy specimens.

- Irradiation temperature at around 320-330°C (can be adjusted to other ranges) and a dose rate of about 20 dpa/year

- All post irradiation experiments can be done at Dimitrovgrad. Cost of irradiation and PIE appears very attractive. The quality of the results has been already checked in a previous analogous irradiation experiment implemented in the frame of another material program.

The ELEXIR irradiation experiment in Phénix began at the start of the 50th reactor cycle, on 24th of May 1998 with an anticipated 120 EFPD per cycle. The 50th reactor cycle was, however, interrupted in September 1998 when Phénix was shutdown for repair. Until then, the capsule had cumulated 77.34 running days (EFPD) corresponding to 7 dpa max. Restarting of Phénix was further delayed in 1999. The 51st cycle is now scheduled for July 2000.

CONCLUSIONS

Contributions to irradiation experiments in RF reactors and Phénix reactor have been made despite problems beyond our control.

TASK LEADER

Farhad TAVASSOLI

DTA/DECM
CEA Saclay
91191 Gif-sur-Yvette Cedex

Tél. : 33 1 69 08 60 21
Fax : 33 1 69 08 71 31

E-mail : tavassoli@cea.fr

ADV 1.1.2

Task Title : SiC-SiC CERAMIC COMPOSITE Definition of material grade and mechanical test

INTRODUCTION

Recent years have shown increasing interest for the characterization of silicon carbide (SiC) based ceramic matrix composites (CMCs), envisaging their application in future power reactors. Interest for SiC CMCs in fusion power applications is based on their excellent thermo mechanical properties, their low neutron activation, as well as their dimensional stability under irradiation for temperatures up to 1273 K The most important matters to be addressed in SiC-SiC CMCs are :

- the thermal conductivity,
- the radiation effect on dimensional stability and strength,
- the anisotropy of properties,
- the strength of joints.

In this Task, the mechanical properties of 3D SiC/SiC composites are tested before irradiation (CEA) and after irradiation (NRG) [R1]. The mechanical properties will be determined at RT and up to 950°C , for two composite grades.

1999 ACTIVITIES

In year 1999, the following milestones were planned :

- Definition of material grade.
- Material procurement.
- Definition of a mechanical test and specimen geometry.
- Preliminary testing and report.

MATERIAL GRADE AND PROCUREMENT

Two different grades from SNECMA-Division SEP were ordered for the mechanical tests :

- CERASEP N3-1 is based on a three directional preform (multilayer) based on standard (medium oxygen content) Nicalon fibers. Densification is obtained by Chemical Vapour Infiltration (CVI). 25 samples were ordered, size 50*5*3 mm^3.
- CERASEP N4-1 is produced by using improved purity SiC fibers (Hi-Nicalon, oxygen free), enabling a better irradiation behaviour. Moreover, the weaving texture is improved, improving the thermal conductivity in the Z direction. 25 samples were ordered, size 50*5*3 mm^3.

DEFINITION OF A MECHANICAL TEST

The specifications for the choice of a proper mechanical test are as following :

- The test has to fit to the existing facilities, in terms of load cells (10, 20, 50 and 100 kN) and heating furnaces ($\varnothing_{max}$ = 100 mm, T_{max} = 1000°C).
- Variation in specimen geometry is limited, since the composite is produced by Chemical Vapour Infiltration (CVI) from a multilayer 3D texture. Parts with relatively complex shapes can be manufactured, but with a thickness of 0.8 to 6 mm.
- For direct comparison with the results after irradiation, we need to define a common test matrix between CEA and NRG for testing.

For composite strength determination, the most widely used mechanical tests are bending tests. Three or four points bending tests have been performed in several studies concerning Ceramic Composites [1, 2, 3].

These tests are well suited for the testing of small specimens with simple geometry (square or rectangular section bars). The 4 point fixture offers 2 major advantages in the case of ceramics :

- The maximum tensile stress is constant within the inner span. Therefore a large volume of material is tested, and the influence of surface defects is limited.
- In the case of shear strength testing of an interface, 4 point device allows to keep the stress concentration zones (under the loading rollers) apart from the interface.

Figure 1 outlines the denotations of the system. The tests are conducted under displacement control with a constant crosshead movement rate. The flexural strength σ_b is determined by $\acute{o}_b = 3F(L - l)/(2bd^2)$ according to the simple beam theory. For easier handling with small specimens, the inner span can be reduced to 1/3 of the outer span length, instead of 1/2 as in ASTM specifications. A look at the table in annex 1 shows that 1/2 is often taken for SiC/SiC composite testing (L = 40 mm, l = 20 mm).

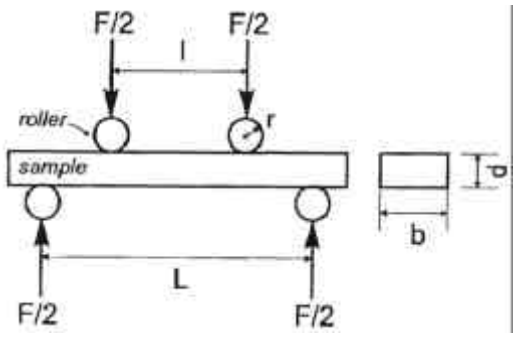

Figure 1 : Schematic diagram of 4 point bending fixture. [4]

When testing ceramic composites, orientation of the load with respect to fiber orientation is an important parameter. In this work, we will test pseudo 3D composites, with two major orientations in the braided structure.

Miriyala has performed mechanical test on 2D SiC/SiC composites, and the two possible specimen orientations are shown in figure 2 [2].

The inter-laminar bending strength is measured with the orientation given in figure 2a (edge-on geometry) and the trans-laminar strength is measured with the orientation given in figure 2b (transverse geometry).

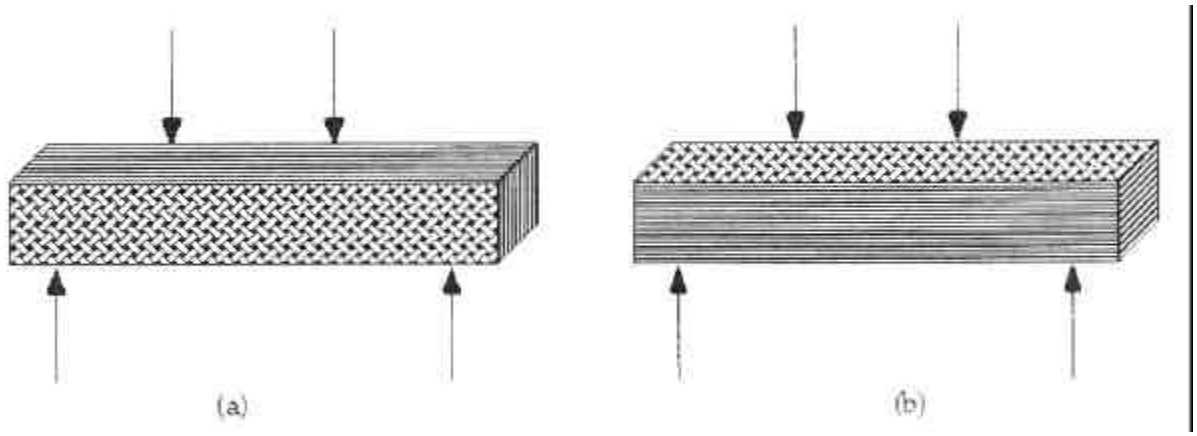

Figure 2 : Geometries for flexure-testing laminate composites : (a) edge-on and (b) transverse. [2]

Recently, Lube studied the properties, limitations and errors associated with these flexural tests [4, 5]. A typical problem originates in the defect controlled failure which is common for ceramic materials. Ceramic specimen often break due to inherent defects.

The tensile surface of the specimen has to be prepared in such a way that no defects are introduced that may cause fracture. An other limit of this test is the contact pressure between rollers and specimen. Lube shows that the contact pressure should not exceed the yield strength of the fixture material or the compressive strength of the tested material.

In this project, surface preparation of SiC/SiC composites appears rather difficult. Test samples will be manufactured with rough tolerances on geometries :

- +/- 0.3 mm on length and width
- +/- 0.5 mm on the thickness

Concerning the contact pressure, we will use rollers made of αSiC and therefore we will have to check if the compressive strength of the composite is not exceeded during the test.

For structural ceramics, a decrease of characteristic strength with increasing specimen volume is observed. This volume dependence of strength can be explained with fracture statistics concepts. In most cases, Weibull statistics describe this effect satisfactory.

CONCLUSION

In year 1999, a sample geometry and associated mechanical testing conditions have been chosen. 50 specimens have been ordered to evaluate the mechanical properties of SiC/SiC composite before irradiation, at room temperature and up to 950°C.

We have decided to test the composite with a 4 point bending fixture. This test is similar to NRG test and thus direct comparison between properties before and after irradiation will be possible.

In year 2000, the bending test fixture will be used to obtain the first mechanical results on the CERASEP composites. Scanning Electron Microscope imaging will be performed to analyse composite failure mode on broken specimens.

REPORTS AND PUBLICATIONS

[1] Takeda M., Kagawa Y., Mitsuno S., Imai Y., Ichikawa H. *Strength of a Hi-Nicalon / Silicon carbide matrix composite fabricated by the multiple polymer infiltration pyrolysis process.* Journal of american ceramic society, vol. 82, n°6, pp. 1579-1581. 1999.

[2] Miriyala N., Liaw P.K., McHargue C.J., Snead L.L. *The mechanical behaviour of a Nicalon/SiC composite at room temperature and 1000°C.* Journal of nuclear materials vol 253, pp. 1-9. 1998.

[3] Zhu S., Mizuno M., Kagawa Y., Mutoh Y. *Monotonic tension, fatigue and creep behavior of SiC-fiber reinforced SiC matrix composites : a review.* Composites Science and Technology vol 59, pp. 833-851. 1999.

[4] Lube T, Manner M. *Development of a bending test device for small samples.* Key engineering materials, vol. 132-136, pp. 488-491. 1997.

[5] Lube T, Manner M, Danzer R. *The miniaturisation of the 4-point bend test.* Fatigue fracture of engineering materials and structures, vol 20, n°11, pp. 1605-1616. 1997.

[R1] R. Couturier, A. Gasse
SiC-SiC ceramic composite : Definition of material grade and mechanical test.
Advancement Report M1-M3, Subtask ADV 1.1.2.
Note technique DEM n° 99/84.

TASK LEADER

Raphaël COUTURIER

DTA/DEM/SGM/L3M
CEA Grenoble
17, rue des martyrs
38054 Grenoble Cedex 9

Tél. : 33 4 76 88 35 59
Fax : 33 4 76 88 58 91

E-mail : couturier@chartreuse.cea.fr

ADV 1.2.2

Task Title : SiC/SiC CERAMIC COMPOSITES
Brazing of SiC/SiC composites with thermo-mechanical testing

INTRODUCTION

In the frame of the European Fusion Technology Programme on Advanced Materials for fusion power reactors, SiC_f/SiC materials are good candidates as breeding blanket materials. In the different concepts that are nowadays envisaged, such as the TAURO Concept, the components to be produced are modular and require reliable joining techniques. Brazing has been recognized has one of the promising technique to produce such components with complex parts and large dimensions. In this way, the BraSiC® process originally developed for the high temperature brazing of bulk SiC has demonstrated its ability to the joining of such joints.

The guidelines for the implementation of the Basic® process for the joining of SiC_f/SiC composites has to take into account specifications directly related to the working conditions (activation, working temperature ...) and some directly related to the intrinsic nature of this material (roughness, porosity ....). Within the previous years, the feasibility has been demonstrated using BraSiC® V grades, showing the ability to control infiltration within the porous composite. The specifications have recently changed with in particular a rise of the expected working temperature, 900 to 1100°C approximately. In this progress document are presented the results of the preliminary brazing trials using other BraSiC® alloys. Both BraSiC® RE and H grades have been selected regarding to the requirements. Preliminary joints have been obtained using bulk SiC parts due to delays in the delivery of SiC/SiC composites. In the same time, the definition of a suitable mechanical test at temperatures as high as 800°C has been done for the assessment of SiC_f/SiC composite brazed joints.

1999 ACTIVITIES

The melting point of the BraSiC® RE and H grades are roughly 1200°C and 1300°C respectively. They are compatible with the maximum working and brazing temperatures (1100 and 1400°C respectively). The brazing process has been optimised to achieve the best performances of the joint in terms of microstructure homogeneity, to avoid the damaging presence of pores etc. Good results have been obtained with both BraSiC® grades and sound joints have been obtained. We note that using the BraSiC® RE grade, a difference in thermal expansion coefficient leads to some small cracks at the edges of the joint. In the future, experiments will be conducted to adapt the thermal cycle or the braze composition to adapt the thermal expansion mismatch.

In order to simulate the behaviour of the porous composite, brazing trials have been carried out using porous SiC parts (porosity of about 12 volume %). We have shown that it is possible to control the infiltration within the porous composite using specific parameters of the brazing process. This alternative allows in some circumstances the brazing of porous composites.

We have reproduced the brazing trials carried out previously with the BraSiC® H2 grade. Brazing was carried out either under high vacuum or under a dynamic argon atmosphere. The temperature was maintained at about 1350°C during 5 minutes. A micrograph of the cross section shows the good filling of the joint, the microstructural homogeneity with no pores nor cracks (figure 1).

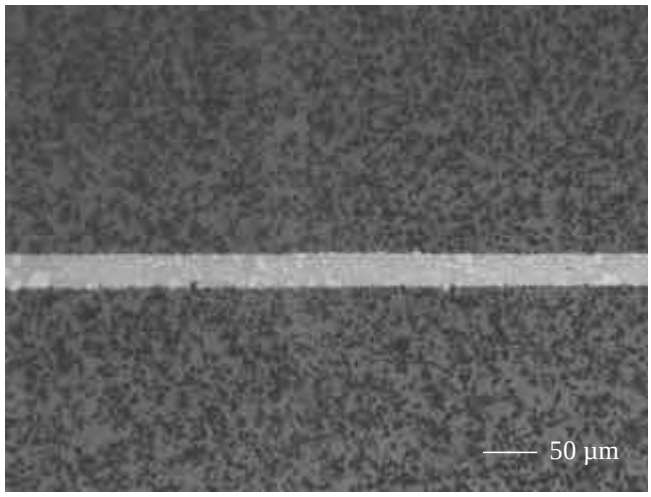

Figure 1 : Bulk SiC/SiC joint with a BraSiC® H2 alloy

MECHANICAL TESTING

The objective is to define a mechanical test for determining the strength of the joints at RT and up to 800°C. In addition, the shear strength will be derived from the test. A bibliographic analysis has been performed to evaluate the possible mechanical tests adapted to the SiC_f/SiC joints. The most widely used mechanical tests for composites are bending tests. Three or four points bending tests can be carried out on small specimens with simple geometry. The 4 points fixture offers 2 major advantages : a maximum tensile stress constant within the inner span and a stress concentration zones (under the loading rollers) far from the joint. For composite shear strength evaluation, several techniques have been developed and tested (shear lap, guillotine test, asymmetrical four point bending (AFPB), Iosipescu etc). All these tests have advantages and drawbacks but the asymmetrical four point bending seems the most appropriate in our case.

Sketch 1 shows the force diagrams associated with the AFPB

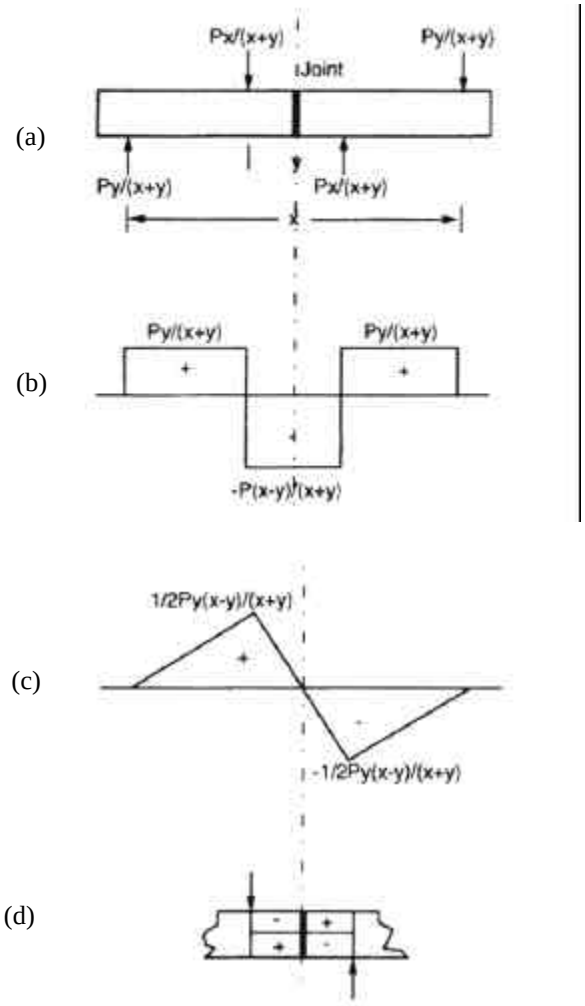

Sketch 1 : (a) Force, (b) shear, (c) moment diagrams associated with the AFPB test and (d) stress state in the specimen within the inner loading points

There are two force couple acting opposite to each other, the inner one being counter clockwise and the outer one being clockwise. The specimen has four distinct regions where the tensile and compressive stresses are illustrated by (+) and (-) respectively. An important characteristic of this fixture is that the shear force within the inner span is constant. In the middle of the inner span (main axis of the testing machine), the bending moment is zero, thus a pure shear stress condition is applied to this plane. The bending fixture that will be used is made of α-SiC and is therefore suitable for high temperatures (at least 1000°C). The use of such a device for bending and shear strength determination of SiC/SiC junctions is possible with the appropriate geometry. The most appropriate geometry (and also the most widely used) is a bar, with rectangular or square cross section. The joint is of a butt joint geometry as displayed in sketch 2 :

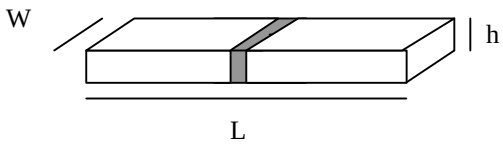

Sketch 2 : Joint test specimen

Taking into account the cost and the manufacturing capability of the composite supplier, the specimens dimensions could be : L = 50 mm, W = 5 mm, h = 3 mm.
The joint thickness is critically dependent on the following features : flatness of the surface of the composite and alignment of both composite parts during joining. One possibility is also to chamfer the joint area in order to concentrate the shear stress within the joint area.

CONCLUSION

BraSiC® H an RE alloys have been selected regarding the requirements of TAURO concept, with an estimated maximum working temperature of about 1100°C. Preliminary brazing experiments have been carried out on bulk SiC. Both BraSiC® grades give promising results and successful brazed joints have been obtained. In the case of the BraSiC® RE grade, some improvement is necessary to adapt the thermal expansion mismatch between SiC and the braze.

We have shown that it is possible to control the infiltration of the braze through porous SiC. So, the next step is to confirm these preliminary results on porous SiC/SiC composites. In the same time, we have defined a proper test for assessing the mechanical strength of the junctions. The test and specimen dimensions have been determined taking into account the features of the composite and the test capabilities.

Once the optimisation of the brazing is done, the mechanical strength (bending strength and shear stress) of the junctions will be determined at temperatures up to 800°C. Scanning Electron Microscope imaging will be performed to analyse composite failure mode on broken specimens.

REPORTS AND PUBLICATIONS

NOTE TECHNIQUE D.E.M. DR N° 30/99, A. Gasse, R. Hostache, R. Couturier, 1999.

TASK LEADER

A. GASSE

DTA/DEM/SGM/LTP
CEA Grenoble
17, rue des martyrs
38054 Grenoble Cedex 9

Tél. : 33 4 76 88 57 44
Fax : 33 4 76 88 95 38

E-mail : gasse@chartreuse.cea.fr

UT-SM&C-LAM/W

Task Title : PULSED AND CW YAG LASER-WELDING OF F82H REDUCED ACTIVATION STEEL

INTRODUCTION

The laser weldability of F82H ferritic martensitic steel was investigated with the use of various laser sources (pulsed and cw YAG, cw CO_2) and welding positions (flat, roof, vertical…) on 6 mm to 15 mm thick plates, with application to define optimal welding conditions and to characterize the metallurgical changes occurring in the weldments.

1999 ACTIVITIES

OPTIMIZATION OF WELDING CONDITIONS

1.2 kW pulsed YAG position welding of 6 mm plates

First of all, the influence of welding position was assessed for a 1.2 kW pulsed YAG welding.

Optimal conditions frequency and pulse durations were shown to be nearly 30 Hz – 4 to 5 ms, whatever the welding position.

This corresponds to a 8-9 kW peak power focused on a 1.5 mm spot with a 120 mm focus distance.

Above 10 kW peak power (below 4 ms pulse duration), metal ejection occurs on both sides due to a drilling-like effect.

With these conditions, a 0.06 +/- 0.01 m/min maximum welding speed was found, irrespective of the position, driving to a 4 mm width on the front face.

This indicates a rather narrow weldability with 1.2 kW YAG.

Thus, no specificity was evidenced concerning the welding position and possible gravity effects occurring during welding (particularly with a roof configuration which favorizes the drop-down of the liquid metal).

Surface aspects of the weldments have been shown to be acceptable : no surface oxydation with 30 l/min front and rear Argon shielding (fluid velocity : 3 m/s), and the absence of external defects.

Cross sections (Fig 1) exhibit a classical nail-head aspect of the beads. Lastly, X-ray radiographies did not evidence any macroflaw (>0.5 mm) in the weldments.

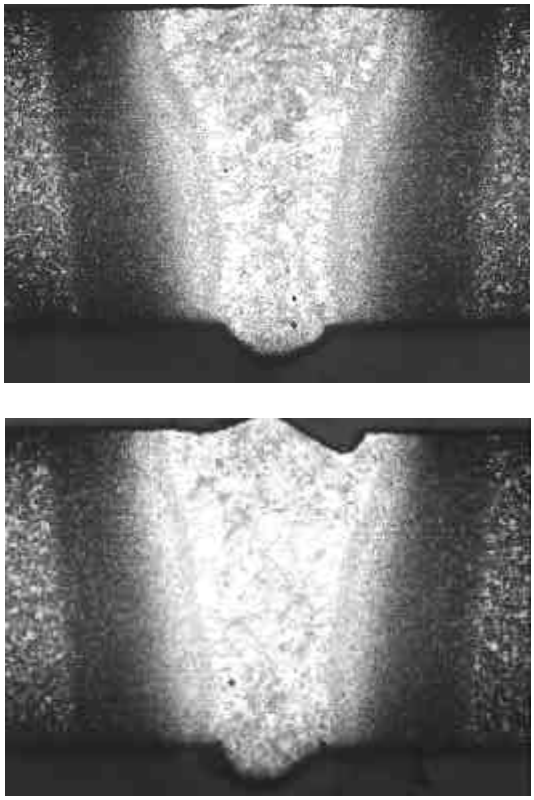

Figure 1 : Cross section of a 6 mm thick joint welded with 1.2 kW YAG at 0.065 m/min (a) and 0.055 m/min (b) in a roof position (x 8 magnification)

Weldability on 7.5 and 15 mm-thick plates with continuous wave (cw) 4 kW YAG and 22 kW CO_2

Fusion lines have been carried out on 7.5 mm (cw 4 kW YAG) and 15 mm thick (22 kW CO_2) plates in flat position to evaluate the weldability domain in full penetration condition.

Fully penetrated welded lines could be displayed with 4 kW cw YAG and a 150 mm focus lens (0.45 mm spot) below 0.25 m/min welding speed in a flat welding position. However, with such conditions, weldments are very large (more than 5 mm) and many macro and microporosities are evidenced, due to the low welding speed as compared with usual cw YAG conditions (more than 1 m/min). Higher powers (2 + 4 kW with a bifocal system for instance) and welding speeds seem to be necessary for achieving full penetration without flaws by limiting turbulent flows in the melting pool.

CO_2 fusion lines were performed with 12 to 18 kW mean powers and 0.7 and 1.1 m/min.

Many (laser power-speed) couples were shown to generate fully penetrated welds but most of them include porosities (0.2 to 1 mm), especially when the initial 50-100 µm oxyde layer has not been removed before welding. At welding speeds above 1 m /min, cracking occurs due to the mechanical restreint during solidification and the thickness of the plates (15 mm) which emphasizes the tensile stresses during cooling. Pre- and post-heating could be a possible solution to avoid cracking by reducing thermal gradients during solidification.

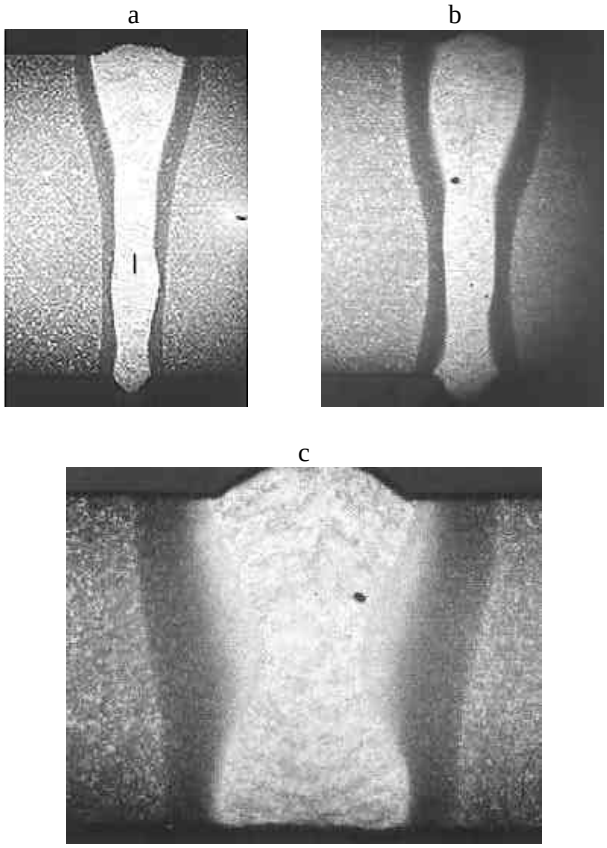

Figure 2 : CO_2 bead on plate welding of 15 mm with
a) 16 kW - 1.1 m/min,
b) 15 kW - 0.7 m/min,
c) cw YAG welding of 7.5 mm plates with 4 kW – 0.25 m/min

METALLURGICAL ANALYSIS OF WELDMENTS

A metallurgical analysis of welded beads obtained with optimal welding conditions (speed and gas protection) has been performed through microstructural observations and hardness measurements. These investigations have evidenced 3 microstructures : a coarse martensitic structure in the weld zone (WZ), a γ-recrystallized structure in the first heat affected zone and a precipitation zone in the second HAZ close to the base material, whatever the welding conditions. In the case of CO_2 welding, due to higher welding speeds (factor 10 as compared with YAG, the 2 HAZ are thinner.

High hardness increases (210 to 400 HV_{1kg}) are evidenced in the WZ and the first HAZ. These HV levels are associated with a weakening of assemblies. In consequence, tempering treatment after welding have to be envisaged so that F82H recovers plasticity.

TASK LEADER

P. AUBERT

DTA/DPSA/CLFA
CEA Fontenay aux Roses
Boîte Postale 6
92265 Fontenay aux Roses Cedex

Tél. : 33 1 42 31 87 09
Fax : 33 1 42 53 97 47

E-mail : paubert@clfa.fr

UT-SM&C-LAM2

Task Title : IRRADIATED BEHAVIOUR OF REDUCED ACTIVATION (RA) MARTENSITIC STEELS AFTER NEUTRON IRRADIATION AT 325°C

INTRODUCTION

The objective of this task is to study the metallurgical and mechanical behaviour of FeCrW Reduced Activation (RA) compared to the conventional FeCrMo martensitic steels during neutron irradiation at 325°C, relevant temperature for fusion reactor applications.

Irradiated specimens of each material are available for 5 levels of radiation damage ranging from 1 to 9 dpa. These doses appear as enough to investigate the first step of irradiation-induced embrittlement and hardening of such materials.

Post-irradiation examinations (PIE) involve tensile tests, measurements of reduction in area to rupture, fractographic examinations and microstructural studies by transmission electron microscopy (TEM) of irradiated specimens. PIE also include dose decay rate and spectrometric measurements of activated elements after irradiation.

1999 ACTIVITIES

The irradiation experiment performed in Osiris reactor finished on November 1999. Specimens with doses of 5dpa and about 9 dpa were unloaded respectively on July 99 and November 99. The first ones were transferred to the hot-cells and the corresponding tensile tests are in progress.

During this period, the activities were mainly focused to the fractographic examinations of tensile specimens tested at room temperature and at 325°C and irradiated to 3.4 dpa.

On the other hand, measurements of dose decay rate as a function of the cooling time have been continued for specimens irradiated with a dose of 0.8-1 dpa. Thus, data are available now up to 39 months after unloading.

IRRADIATION CONDITIONS

Irradiation in Osiris reactor started on January 96 and finished on the second semester 1999. Because of partial unloadings, irradiated samples are available with 5 different dose levels, that is, 1, 2 , 3.4, 5 and 9 dpa.

Materials were irradiated at 325°C (+5°C, -10°C) in pressurised water at 155 bars as tensile specimens and plate samples intended for different post-irradiation examinations.

Irradiation was carried out in a mixed neutron spectrum. The maximal neutron flux was about 2.10^{14} n/cm^{2}s (E > 1 Mev) and the fast to thermal flux ratio is about 1.1.

MATERIALS

Two types of relevant martensitic materials for fusion applications were irradiated in the present experiment, that is, 7/11CrW RA-steels and 9/12CrMo conventional martensitic steels for comparison (see Task SM1.1 for chemical compositions and metallurgical conditions).

The following nuances of RA martensitic steels were irradiated :

- F82H is a 7.5CrWTaV RA-steel developed by JAERI (Japan).
- LA12LC, LA4Ta and LA13Ta are RA experimental alloys of 9/11CrWTaV type with different contents of Cr, W, Ta.

Conventional martensitic steels are commercial alloys which present different contents of Cr (9 to 12%), Mo and stabilising elements (V, Nb).

FRACTOGRAPHIC EXAMINATIONS

The objective was to study the failure mode of martensitic steels after irradiation. For this purpose, several materials have been investigated : F82H and LA12LC RA-steels, 9Cr-1Mo and HT9 conventional steels and two ODS alloys, all of them irradiated up to 3.4 dpa. Examinations of the rupture surface were performed by SEM on broken specimens after tensile tests at 20°C and 325°C [1].

In the case of RA-steels, the failure mode is mainly a transgranular ductile rupture characterised by small dimples as shown in figure 1. A low density of smooth regions, without dimples, are also observed in particular for LA12LC steel. Some secondary cracks occur in the neighbour of these regions. No indications of cleavage failure mode were detected for these steels.

Rupture of 9Cr-1Mo specimens display the same characteristics described for RA-alloys, that is transgranular ductile failure with some smooth zones, sometimes with ledge aspect, as shown in figure 2. In contrast, very different features are observed on the rupture surface of HT9 irradiated samples. An important proportion of intergranular fracture and cleavage failure mode is observed besides some ductile regions with dimples. The typical aspect is illustrated in figure 3 where intergranular facets are clearly detected.

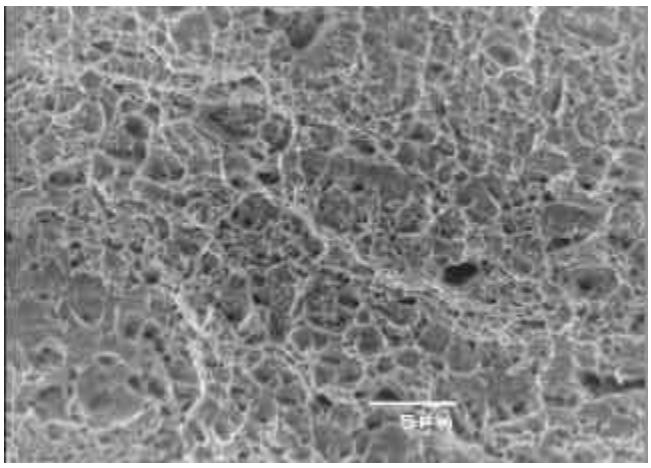

Figure 1 : Fracture surface of F82H specimen tested at 20°C

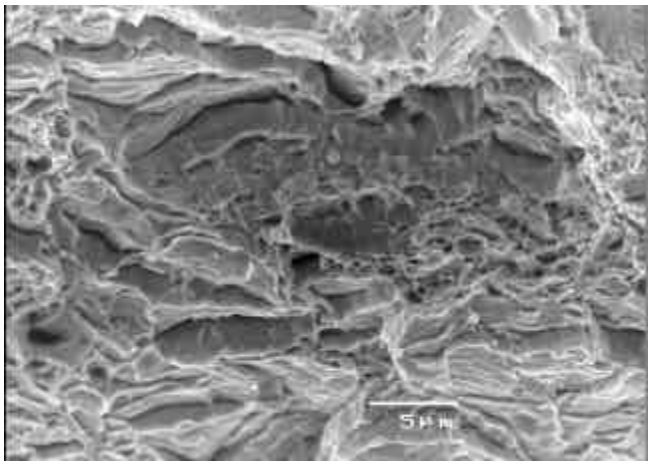

Figure 2 : Fracture surface of 9Cr-1Mo specimen tested at 20°C

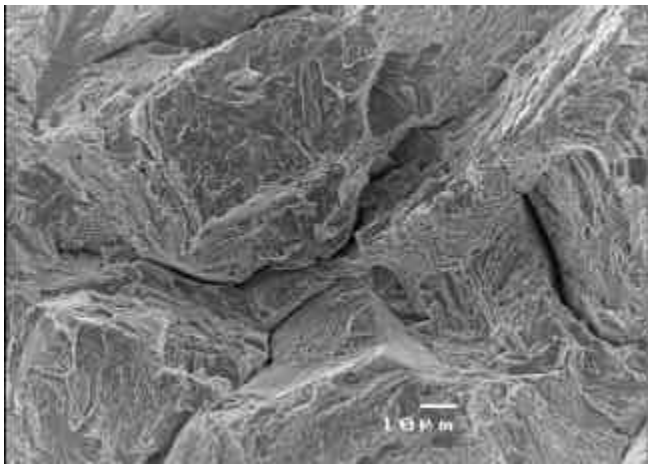

Figure 3 : Fracture surface of HT9 specimen tested at 20°C showing the intergranular failure mode.

Table 1 summarises the tensile strength and reduction in area values determined at 20°C for the initial condition and after irradiation up to 3.4 dpa [2]. For all materials, an important increase of tensile strength with the fluence, which ranges from 190 to 520 Mpa, was observed.

Table 1. Tensile strength and reduction in area values of martensitic steels before and after irradiation for 3.4 dpa, measured at 20°C

Material	0.2% Yield Stress (MPa)		Hardening (MPa)	Reduction in area (%)	
	0 dpa	3.4 dpa	3.4 dpa	0 dpa	3.4 dpa
F82H (7.5Cr-2W)	535	847	312	73-75	71
LA12LC (9Cr-0.7W)	675	865	190	71-74	65
LA4Ta (11Cr-0.7W)	739	1006	267	69-71	61
9Cr-1Mo	539	888	349	72-78	63
HT9 (12Cr-Mo/W)	581	1106	525	49-54	31

The most important irradiation-induced hardening, measured as the increase of yield strength at 20°C, is obtained for HT9 steel (520 Mpa), which associates a strong degradation of ductility. The low values of reduction in area obtained for this material (at 20°C and also at 325°C) imply poor impact properties according to the correlation that was established between reduction in area and the upper shelf energy (see Task SM2.1 /SM2.2). The fractographic examinations confirm this point, an important embrittlement is detected related to the major contribution of the intergranular and cleavage failure mode.

On the other hand, materials which exhibited the highest values of reduction in area (> 60%) after irradiation up to 3.4 dpa, like F82H, LA12LC and 9Cr-1Mo, display a transgranular ductile fracture at both test temperatures.

Next time, fractographic examinations will be conducted on control specimens to separate the typical features due to the evolution under irradiation. Moreover, the present observations will be compared with specimens with the maximal dose (about 9 dpa) reached in this experiment to study the eventual evolution of fracture surface with the dose.

DOSE RATE DECAY MEASUREMENTS

To check the concept of « reduced activation », the dose rate measurements are performed on several types of steels, including stainless steels, conventional and reduced activation martensitic alloys, all of them irradiated in the same conditions. Measurements have been conducted on specimens of the first unloading (0.8-1 dpa), which was obtained on March 1996.

The dose rate is measured with a Geiger-Müller counter for different distances between the samples and the counter, that is, 50, 100 and 185 mm. The first measurements have been performed 9 months after unloading, the following ones at 15, 27 and 39 months and it is planned to go on them each 12 months.

After 9 months of cooling (see Annual Report CEA/Euratom Association, 1998), the group of stainless steels (type 304 and 316) present the highest residual activity (30-58mGy/h) and both types of martensitic steels are characterised by dose rates in the range 8-20mGy/h).

Measurements performed after different cooling-times show a decrease of the residual activity for all materials. Figure 4 compares the dose rate values measured after 39 months [3] for a distance sample-counter of 100 mm. After this period of time, the activity of stainless steels is always the highest one and ranges from 15 to 33 mGy/h, the conventional martensitic steels CrMo from 3 to 10 mGy/h and in the case of the reduced activation CrW martensitic steels the dose rate is $\leq$ 2.0 mGy/h. In figure 4, experimental data are compared with decreasing activity calculated with the Microshield code. A quite good agreement is obtained, except for 9/12CrMo conventional martensitic steels where some scattering between experimental and calculated activity was found.

On the other hand, it is worthwhile to point out that the relative rate of the decreasing activity is different for each class of steels as shown in figure 5. Compared to the first measurements (9 months), 304 and 316 steels exhibit a reduction of the dose rate of 28-38%, 42-78% in the case of conventional martensitic alloys, and 80-90% for the reduced activation steels during a period of 2.5 years.

These experimental data assess the good performance of « reduced activation steels » from the point of view of radiological effects and environmental considerations. Consequently, reduced activation materials are very encouraging for applications as structural materials for fusion reactors and other projects where components are submitted to in-service high doses.

CONCLUSIONS

The irradiation experiment performed in Osiris reactor at 325°C finished on November 1999. Several Cr-W low activation and Cr-Mo conventional martensitic steels have been irradiated for five dose levels : 1, 2, 3.4, 5 and 9 dpa. PIE corresponding to last doses are in progress. Fractographic examinations of martensitic steels irradiated up to 3.4 dpa were performed. The analysis of the fracture surfaces have shown that : material that exhibited the higher hardening :

- Reduced activation steels display a ductile fracture mode at 20 and 325°C as well as the conventional 9Cr-1Mo. These materials present the lower sensitivity to the irradiation-induced hardening and ductility degradation.
- In contrast, intergranular and cleavage modes operate in the case of HT9 (12%Cr) conventional steel, which exhibit the stronger hardening and the more severe ductility degradation.

Measurements of the dose rate have been performed after several cooling-times up to 39 months to validate the concept of « reduced activation materials ». For this purpose, specimens of different types of steels have been examined : austenitic steels, conventional martensitic and reduced activation martensitic alloys, after irradiation for a dose of 0.8-1 dpa. Compared to the conventional martensitic and the austenitic steels, experimental data show that the reduced activation steels exhibit :

- the lower residual activity (< 2 mGy/h).
- the higher rate of decreasing activaty.

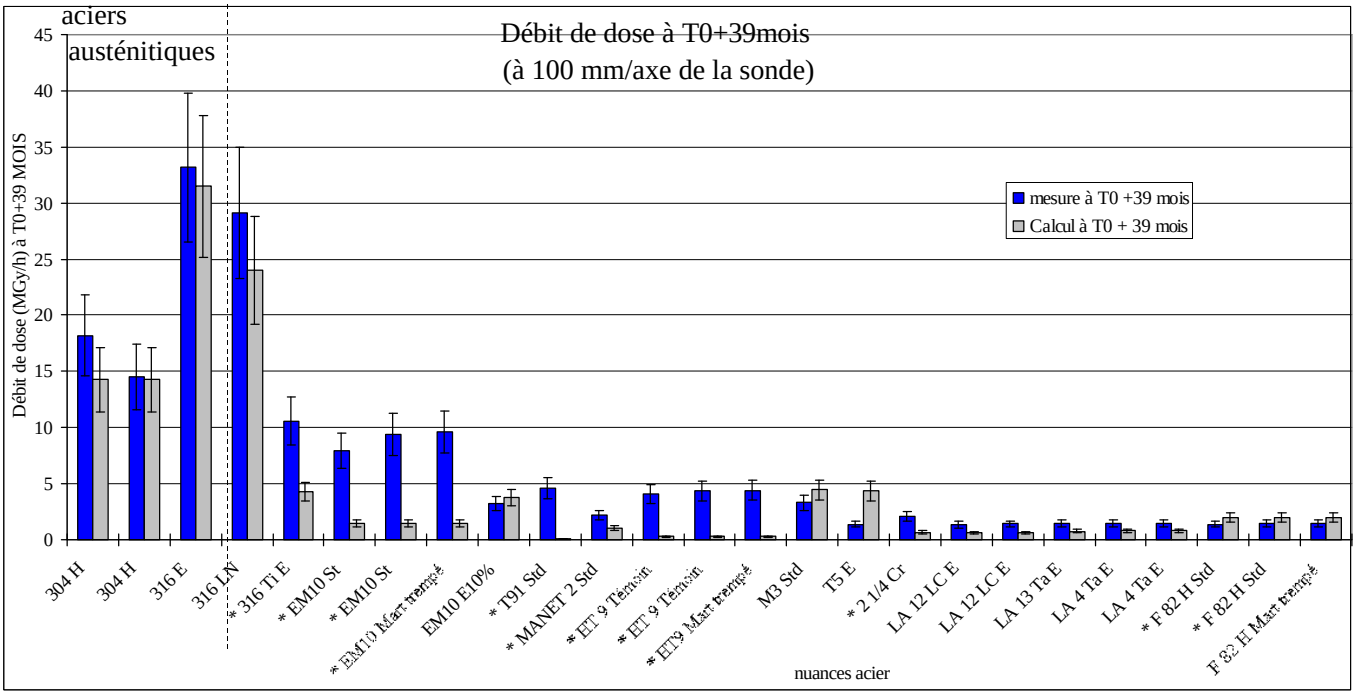

Figure 4 : Dose rate measured after 39 months of unloading for different classes of steels irradiated at 0.8-1dpa in the Osiris reactor

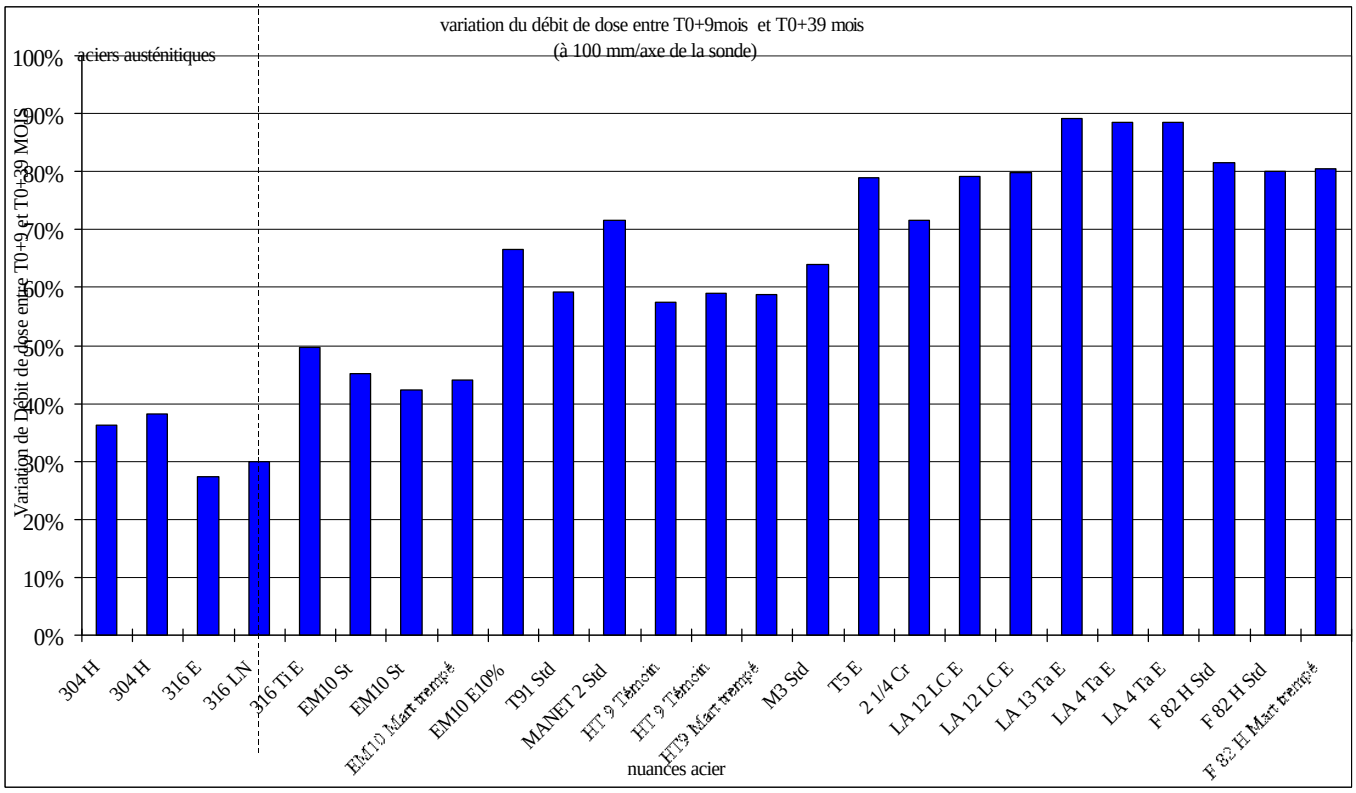

Figure 5 : Relative decrease of the dose rate measured after 39 months of unloading for different classes of steels irradiated at 0.8-1dpa in the Osiris reactor

REPORTS AND PUBLICATIONS

[1] J.J. Espinas, O. Rabouille, J.C. Brachet, « Fractographies au MEB après essais de traction sur éprouvettes de l'expérience Alexandre », CEA Report SEMI/LU2M/RT/99/001/A, 1999.

[2] A. Alamo, X. Averty, " Status of post-irradiation examinations performed on RA and conventional martensitic steels irradiated at 325°C in Osiris reactor », Progress Report UT-SM&C-LAM2, CEA report, NT SRMA 99-2316, April 1999.

[3] X. Averty, A. Garro, P. Coffre, "Irradiation Alexandre – Débit de dose pour le panier n°1 à 39 mois", CEA Report SEMI/LCMI/RT/99/018/A, 1999.

TASK LEADER

A. ALAMO

DTA/DECM/SRMA
CEA Saclay
91191 Gif-sur-Yvette Cedex

Tél. : 33 1 69 08 67 26
Fax : 33 1 69 08 71 30

E-mail : ana.alamo@cea.fr

UT-SM&C-LAM3

Task Title : MICROSTRUCTURAL INVESTIGATION OF REDUCED ACTIVATION FERRITIC-MARTENSITIC (RAFM) STEELS BY SMALL ANGLE NEUTRON SCATTERING (SANS)

INTRODUCTION

Small Angle Neutron Scattering (SANS) allows to characterise heterogeneities in alloys (precipitates, pores, cavities, …) where the size ranged between 10 and 1000 Å. Indeed, from the scattered intensity analysis, microstructural information can be deduced, such as mean size, shape, number density and in some cases, chemical composition of the particles. In this task, this technique is used to characterize RAFM steels, after thermal ageing but also after neutron irradiation.

SANS technique is complementary to Transmission Electron Microscopy (TEM) and in many cases, the microstructural evolutions detected by SANS can be correlated to mechanical behaviour and specially to explain the embrittlement of the material.

1999 ACTIVITIES

During 1999, SANS was used to complete the characterisation of RAFM steels after thermal aging in the range 250°C to 550°C and to perform some preliminary examinations on neutron irradiated materials for a dose of 0.8 dpa. Significant SANS data on RAFM steels are now available to explain, in several cases, the modifications of tensile and impact properties observed after thermal ageing.

MATERIALS AND EXPERIMENTAL PROCEDURES

Several RAFM steels (about 8 heats), and also conventional steels for comparison, were characterised by SANS, after thermal ageing, during the last years [1, 2, 3].

This work complete the data already obtained on thermal aged materials by adding the characterisation carried out on the LA4Ta, LA12Ta and LA13Ta steels. The other objective of this work is the presentation of the first results concerning the F82H and LA4Ta steels irradiated 0.8 dpa at 325°C. Chemical composition, prior austenite grain size, metallurgical conditions and aged conditions of the steels are given in Table 1. The fabrication route is described in the tasks SM 2.1 and SM 2.2 (Metallurgical and mechanical characterisation of RAFM steels).

Thermal ageing of LA12Ta, LA13Ta and LA4Ta steels was performed in the range 250-550°C. F82H and LA4Ta steels were irradiated in Osiris reactor at 325°C in the frame of Alexandre experiment (see UT-SM&C-LAM 2 : Irradiated behaviour of Reduced Activation Martensitic steels after neutron irradiation at 325°C).

Table 1 : Chemical composition of RAM steels (wt%) and conditions of examined samples

Alloy	C	Si	Mn	Cr	V	W	N	Ta	Grain size (μm)	Initial Met. Cond.	Thermal ageing	Irradiation condition
LA12Ta	0.155	0.03	0.88	9.86	0.28	0.84	0.0430	0.10	20	N&T+CW	2000 h at 400 and 500 °C 10000 h at 350, 400, 550 °C 13400 h at 250°C	
LA13Ta	0.179	0.04	0.79	8.39	0.24	**2.79**	0.0480	0.09	25	N&T+CW	2000 h at 400 and 500 °C 10000 h at 350, 400, 550 °C 13400 h at 250°C	
LA4Ta	0.142	0.03	0.78	**11.08**	0.23	0.72	0.0410	0.07	7	N&T+CW	2000 h at 400 and 500 °C 10000 h at 350, 400, 550 °C 13400 h at 250°C	0.8 dpa at 325°C
F82H	0.087	0.10	0.21	**7.46**	0.15	**1.96**	**0.0066**	0.023	100	N&T		0.8 dpa at 325°C

The experimental set-up and the treatment of SANS data are described in [1].

The chemical composition of the examined steels allows to study the influence of the chromium content, which ranged from 9% for LA13Ta steel, 9.9 % for LA12Ta to 11.2 % for LA4Ta steel, and the influence of increasing W-content from 0.8 % for LA12Ta and LA4Ta steels to 3 % for LA13Ta steel.

THERMAL AGED MATERIALS

LA12Ta steel (Fe 9.9Cr 0.85W)

No effect after 2000 hours ageing whatever the temperature is and after 10000 hours at 550°C is observed. So, the precipitation condition does not significantly evolve. But, some effects are detected after thermal ageing at $T \leq 400°C$ for times of about $\geq$ 10000 hours. A slight increase of the scattered intensity is observed, in all the investigated domain of the scattering vector "q". This behaviour tends to indicate that there is a slight evolution, that could be attributed to occurrence of some small size particles, which are not yet identified.

No modifications of impact properties are observed after different conditions of ageing, except for LA12Ta samples aged at 400°C during 10000 hours which exhibit a decrease of the Upper Shelf Energy (USE) of 35 Jcm^{-2} without an increase of the Ductile to Brittle Transition Temperature (DBTT). This evolution could be related to the microstructural evolution detected by SANS consisting in a precipitation of Cr-rich small size particles.

LA4Ta steel (Fe 11.2Cr 0.85W)

SANS data obtained for this steel, which presents the higher Cr-content, are quite different compared to the other RAFM steels and to the conventional steels. In fact, whatever the time and the ageing temperature, the scattered intensities of the aged materials, in all the q domain, are always clearly increased compared to the reference (unaged) material.

It means that whatever the aged sample considered, there is a modification of the precipitation condition compared to the reference material. This behaviour could be partially explained by the dissolution of M_2X precipitates which could enhance the precipitation of M_4X_3 V-rich particles, as observed by TEM [3].

On the other hand, aging at 400°C show a further increase of the scattered intensity with the aging time for the high q values (q >0.08 $angström^{-1}$), that is from 2000 hours to 10000 hours as shown in figure 1. These patterns have been interpreted by the precipitation (between 2000 hours and 10000 hours) of Cr-rich alpha prime particles with a mean radius of 1.5 nm and a volume fraction close to 0.16%.

This result could explain the mechanical behaviour that we reported on this material, which shows at this ageing temperature (400°C), an increase of the DBTT simultaneously to a decrease of the USE [1].

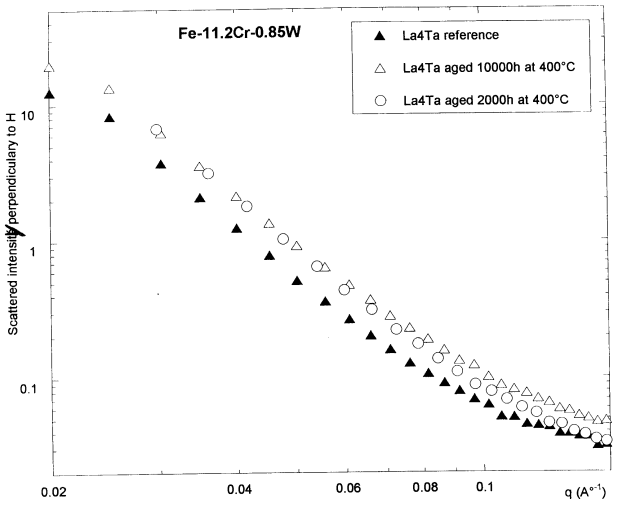

Figure 1 : Scattered intensities measured on LA4Ta samples (reference, aged 2000h and 10000h at 400°C)

LA13Ta steel (Fe 9Cr 3W)

This steel has the highest W content among all the studied steels.

The comparison between the scattered intensities of aged samples and controls shows that thermal ageing does not induces significant differences in the range from 250°C to 450°C.

This should indicate that the precipitation state does not vary at these ageing temperatures.

This is not the case for thermal ageing performed at 550°C. Indeed, on all the "q" domain, the scattered intensities of samples aged during 10000 hours, but also for shorter time (2000 hours), are significantly higher compared to the reference sample ones (see figure 2).

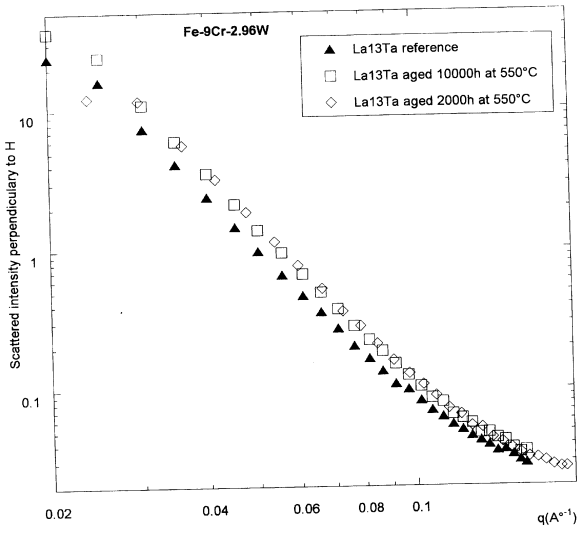

Figure 2 : Scattered intensities measured on LA13Ta samples (reference, aged 2000h and 10000h at 550°C)

The A ratio (ratio on the scattered intensities measured perpendicularly and parallel to the magnetic field), that gives information about the chemical composition of the phase, is constant for all the "q" domain and is close to 5. TEM observations performed on LA13Ta steel aged at 550°C during 10000 hours show that the precipitation of Laves phase (Fe_2W type) occurs as a very thin film on grain and lath boundaries [3]. The chemical composition of precipitates is close to 49Fe-25Cr-2V-25W in at % and is in agreement with the value of the A ratio. This precipitation could explain the signal obtained by SANS.

The SANS intensities obtained with the materials aged at 550°C after 2000 hours and 10000 hours are quite similar. That seems to indicate two things :

- Firstly, after 2000 hours the Laves phase is already present in the material. This point will be confirmed by TEM examination but Thermoelectric Power measurements (TEP) available after 2000 hours appears to confirm this result [3].

- Secondly, it seems that the SANS signal related to Laves phase saturates from 2000h ageing. This saturation is probably not associated to a saturation of the Laves phase precipitation. Indeed, TEP values still decrease between 2000 hours and 10000 hours and, above all, impact properties, that are very sensitive to intergranular precipitation, shows an important degradation between 2000 and 10000 hours. That indicates that the maximum of the Laves phase precipitation, and the maximum of embrittlement, was not reached after 2000 hours.

The saturation of the SANS signal after 2000 h ageing can be explained by the fact that Laves phase precipitates as a very thin film on lath and grain boundaries. In this case, the SANS intensity is only sensitive to the shape of the precipitation (extended bi-dimensional objects with a large diameter > 100 nm) and not to the volume fraction. The shape of the Laves phase precipitation does not change between 2000 hours and 10000 hours as the precipitated fraction does. For this case, SANS is an appropriate technique to detect the precipitation of a new phase and to obtain some information on the chemical composition but do not allow to get the precipitated volume fraction.

Irradiated materials

SANS experiments, on irradiated specimens, were conducted with thinner samples compared to non active specimens. Thus, longer counting time was used for each materials. The data shown on figure 3 and 4 obtained on F82H and LA4Ta steels irradiated at 0.8 dpa at 325°C are just preliminary results. The pattern obtained from F82H steel irradiated and unirradiated are quite similar (see figure 3). No new phase seems to appear during the irradiation. In the case of the LA4Ta steel, at high values of "q" (q>0.05 angström^{-1}) an important increase of the scattered intensities is observed (see figure 4) . The data treatment is still in progress but the first analysis indicate that the behaviour could be due to the precipitation of Cr-rich alpha prime particles in the matrix. This is in agreement with the fact that the chromium content in this steel is higher compared to 9Cr steels and F82H steel.

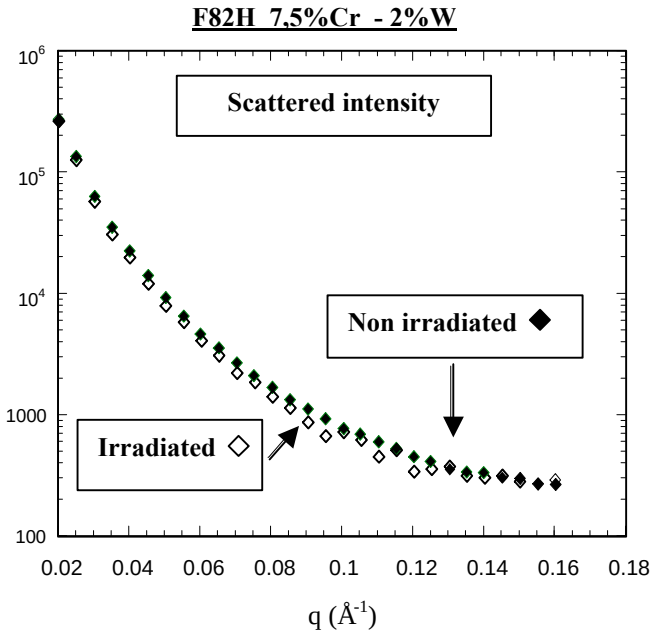

Figure 3 : Scattered intensities measured on F82H samples (non irradiated and irradiated 0.8 dpa at 325°C)

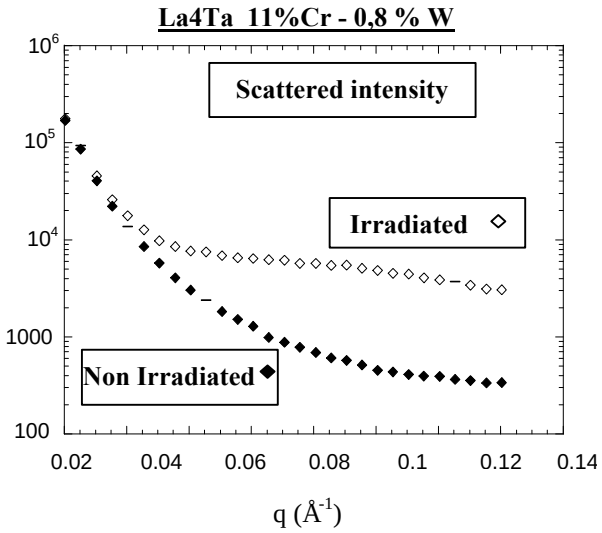

Figure 4 : Scattered intensities measured on LA4Ta samples (non irradiated and irradiated 0.8 dpa at 325°C)

CONCLUSION

RAFM steels were characterised by SANS after thermal ageing and after irradiation. After thermal ageing, results show that this technique is very useful to detect very fine features of microstructural evolutions that are responsible of the embrittlement of materials.

- It appears that for steels with a chromium content higher than 9 %, and after thermal ageing at 400°C, the formation of Cr-rich alpha prime particles of 1.5nm size is detected by SANS and can be correlated to the degradation of impact properties.

- Tungsten content of the material prones the formation of Laves phase after thermal ageing at 550°C. This Laves phase was detected by SANS in the LA13Ta steel with 3 % of tungsten after ageing 2000 hours and 10000 hours at 550°C.

- The preliminary results obtained on specimens irradiated at 325°C with a dose of 0.8 dpa indicate that there is no new precipitation in the F82H steel. On the other hand, significant modification of the scattered intensities on the LA4Ta steel is observed, which could be related to the occurrence of alpha prime particles.

REPORTS AND PUBLICATIONS

[1] M. H. MATHON, G. GEOFFROY, C. H. DE NOVION, Y. DE CARLAN, A. ALAMO « Microstructural characterisation of EM10, HT9, F82H and JLF-1 steels by small angle neutron scattering, intermediate report contract SM 6.4.2 », Note Technique LLB/97/170-LSI/98/01, December 1997.

[2] M.H. MATHON, G. GEOFFROY, A. ALAMO, C.H. DE NOVION, "Small Angle Neutron Scattering of secondary hardening phenomena in martensitic steels", Progress report fusion technology contract UT-M-CM4, Note Technique LLB/96/119, December 1996.

[3] Y. DE CARLAN, A. ALAMO, M. H. MATHON, G. GEOFFROY, A. CASTAING, « Effect of thermal ageing on the microstructure and mechanical properties of 7-11 Cr W steels », Note Technique SRMA 99-2345, December 1999.

- Y. DE CARLAN, C. FOUCHER, M.H. MATHON, G. GEOFFROY, A. ALAMO, « Study of secondary hardening phenomenon in F82H steels by SANS », CEA report N.T. SRMA 99-2398, April 1999.

- M.H. MATHON, G. GEOFFROY, Y. DE CARLAN, A. ALAMO, C.H. DE NOVION "Microstructural characterisation of LA4Ta, LA12Ta, LA13Ta and F82H steels by small angle neutron scattering" Intermediate report UT-SM&C-LAM 3, N.T. SRMA 2000-2359, Mars 2000.

TASK LEADER

A. ALAMO

DTA/DECM/SRMA
CEA Saclay
91191 Gif-sur-Yvette Cedex

Tél. : 33 1 69 08 67 26
Fax : 33 1 69 08 61 75

Email : ana.alamo@cea.fr

UT-SM&C-ODS

Task Title : DEVELOPMENT OF FORMING AND JOINING TECHNOLOGIES FOR ODS STEELS

INTRODUCTION

In this task, the workprogramme has been focused on the joining of the ODS material.

The joining of ODS steels is a very important topic, that has to be taken into consideration in order to develop the use of this kind of material for use as structural material in fusion reactors. Different joining techniques can be considered, in a first step, like brazing or friction welding. But regarding the potential needs, joining by diffusion welding seems to be the best solution because of the ability of this technique to join parts of large dimensions with complex shapes.

The work related in this report consists of a bibliographic study on the diffusion welding of ODS steel, the supplying and production of different kinds of ODS steels and some preliminary trials of joining of ODS steels.

A bibliographic study has been focused on the work already done on the joining of Oxyde Dispersion Strenghthened Materials by diffusion welding. We can note that there are few publications on this topic and that the conditions of joining are strongly linked to the recrystallisation state of the material.

1999 ACTIVITIES

BIBLIOGRAPHICAL STUDY ON DIFFUSION WELDING OF ODS STEELS

Réf. 1 to 3 as examples.

Different important elements have been reviewed by the bibliographical study. These elements are detailed in the report [4]. The mains elements concern the following parametrers of the joining process :

- **Base Material structure.**
- **Surface preparation.**
- **Hot Isostatic Pressing cycle.**
- **Interlayers.**

PRELIMINARY TRIALS OF JOINING ODS STEELS

Specimen preparation

- Surface preparation : The mechanical properties of the joint are correlated to the cleanliness of the interface. The presence of oxides on the initial surfaces that could not be dissolved during the HIP cycle act as diffusion barriers and weaken the joint.

  The preparation of the surfaces has consisted after grinding in a chemical cleaning and drying. Just before the mounting of the part in the canister a slight mechanical etching followed by a second chemical cleaning and then drying.

- Geometry of the specimens : cylinders of 30 mm in diameter and thickness.

Realization of the joints

Joints done have been made by using different ODS steel
A bar from MA 956 has been supplied from Inco. This bar is a special product with a small grain size. The bar has been delivered directly after the extrusion without any thermal treatments of recrystallisation.

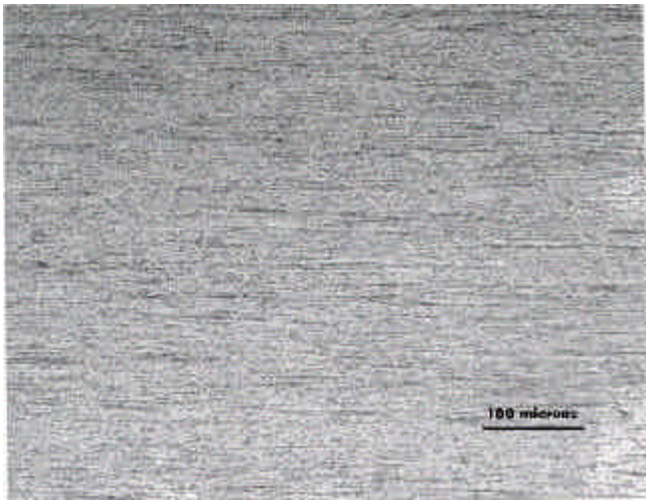

Microstructure of MA 956
Longitudinal direction

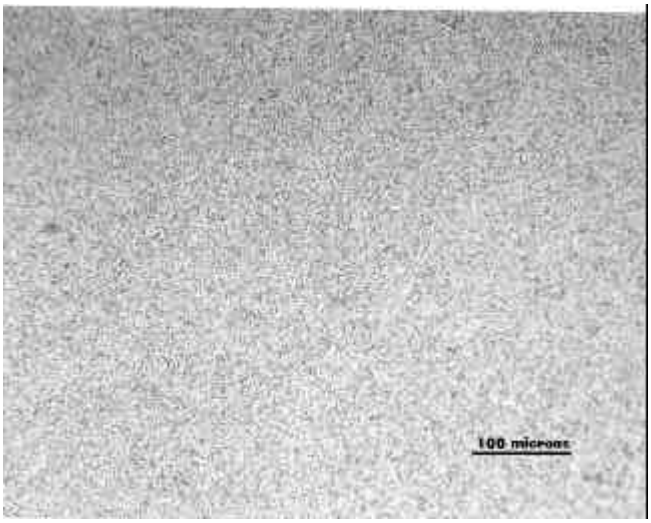

Microstructure of MA 956
Transverse direction

Four grades of ODS Eurofer has been used . These grade has been produced in our laboratory by mechanical alloying following the same procedure as the one defined for the task SM4.2. These ODS Eurofer steels used to prepare the sample have been consolidated by Hot Isostatic Pressing. No thermal treatments of recrystallization have been applied before the joining.

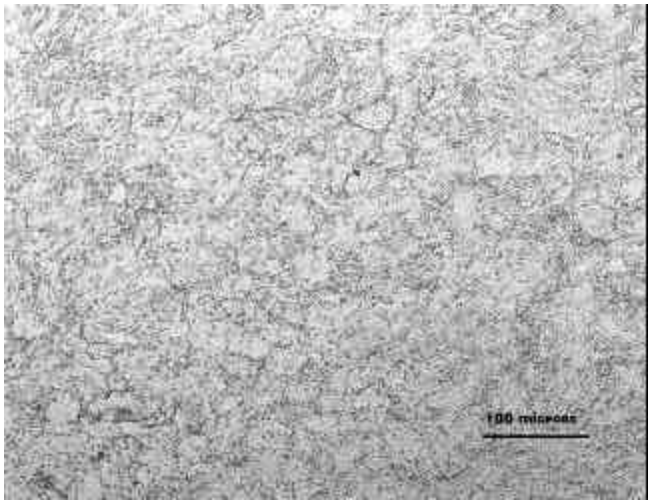

Microstructure of Eurofer ODS

The different joints consist in extruded material (MA 956) to Hot Isostatic Pressed material :

- MA 956 / MA956,
- MA 956/ Eurofer ODS 1% (wt) Y_2O_3 prepared by ball mill,
- MA 956 / Eurofer ODS 1% (wt) Y_2O_3 prepared by attritor,
- MA 956 / Eurofer ODS 0.5% (wt) Y_2O_3 prepared by ball mill,
- MA 956 / Eurofer ODS 0.5% (wt) Y_2O_3 prepared by attritor.

The applied HIP cycle is 1100°C under 1000 MPa for 1 h.

The following picture is an example of the microstructure of one of the joints :

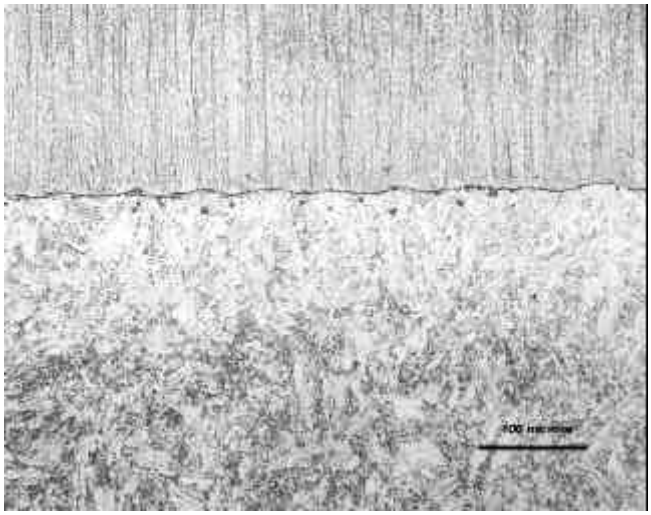

Joint MA 956 (up)/ Eurofer ODS

CONCLUSION

The workprogramme of this year has been focused on the supplying or production of different kinds of ODS steels followed by the realization of joints and preliminary characterizations.

Our knowledge in the field of elaboration of ODS materials have allowed our laboratory to go from the elaboration of ODS steel by a powder metallurgy route to the production of the joints with various grades of ODS steels. The different steps of the process have been accomplished as planned.

The workprogramme for the next year will be more oriented toward the characterization and understanding of the process of joining of our ODS steels. Some fine microstructural characterization will be done on the available joints sample and some preliminary mechanical testing will be defined and realized.

REPORTS AND PUBLICATIONS

[1] The Metallurgical and Mechanical Properties of ODS Alloy MA 956 Friction Welds. Welding Research Supplement August 1997. K.Shinozaki, C.Y. Kang, Y.C. Kim, M. Aristoshi, T.H. North and Y. Nakao.

[2] HIP-Diffusion Bonding of ODS MA 6000. « 3rd International Conference/Exhibition on Isostatic Pressing », London, November 10-12, 1986. C. Verpoort, M .Nazmy, C.P. Jongenburger.

[3] Joining of ODS superalloys. Proceeding conference, Liège, Belgium, 24-27 Sept 1990. H.D. Hedrich Daimler-Benz AG Stuttgart, FRG, H.G. Mayer, G. Haufler, M. Kopf IKE-University of Stuttgart, FRG, N. Reheis Metallwerk Plansee Gmbh Reutte, Austria.

[4] Stéphane Revol, « UT-SM&C-ODS Development of forming and joining technologies for ODS steels ». Note technique DEM n° 79/99.

TASK LEADER

Stéphane REVOL

DTA/DEM/SGM
CEA Grenoble
17, rue des martyrs
38054 Grenoble Cedex 9

Tél. : 33 4 76 88 98 42
Fax : 33 4 76 88 54 79

E-mail : stephane.revol@cea.fr